ENCAPSULATION OF COBALT COMPLEXES IN ZEOLITE Y FOR USE AS HYDROFORMYLATION CATALYSTS

By

Paul Joseph Victor Galatolo
BSc (Chem. Eng.) (Cape Town)

Submitted to the University of Cape Town in fulfilment of the requirements
for the degree of
MASTER OF SCIENCE IN ENGINEERING

Departments of Chemical Engineering and Chemistry
University of Cape Town
Rondebosch
Cape Town
South Africa

November 1997

ACKNOWLEDGEMENTS

I would like to thank the following:

Both of my supervisors for all their help and guidance throughout my time at UCT: Professor John Moss of the Organometallic Research Group in the Department of Chemistry and Professor Mark Dry of the Catalysis Research Unit in the Department of Chemical Engineering.

Professor Cyril O'Connor, the Head of Chemical Engineering as well as the Catalysis Research Unit, for making the Catalysis Research Unit as dynamic as it is.

Dr Alan Hutton, Dr Klaus Möller and Dr Eric van Steen for all their help and very constructive criticisms that they gave me about my project.

Leslie Petrik for allowing me to exclusively borrow one of her autoclaves for the entire duration of my project. Suzana Vasic for her important atomic absorption analyses as well as allowing me to use the BET machine for some of my zeolite dehydrations. Noel Hendricks for the NMR analyses and Mr. G.P. Benin-Casa for the elemental analyses. Pam Linck and Denise Wederburn for the ordering of my chemicals.

The FRD and UCT, without whose funding this research could not have been carried out.

Granville, Peter and Joachim for their great helpfulness. Maria, Jackie, Nellie, Martin and James for ensuring that our lives in the department were always clean and comfortable.

All the postgraduates of the Chemical Engineering and Chemistry Departments; a really stimulating bunch.

My parents and my brother, for all their help and support throughout my project.

SYNOPSIS

In industry, the hydroformylation reaction is predominantly homogeneously catalysed using carbonyl complexes of cobalt and rhodium (*1-3,45*). The main disadvantage of homogeneous catalysts is that, especially for the longer chain hydrocarbon systems, very energy-intensive methods (such as distillation) are required to remove them from the reaction products. These separation techniques usually lead to losses of the catalyst. From an economic viewpoint, this is highly undesirable since the catalysts (especially rhodium) are expensive. Research has been carried out on encapsulating the catalysts within the cages of a zeolite, maintaining the activity of the catalyst while allowing it to be easily removed from the reaction medium (eg. by filtration). However, all research reported so far has only considered rhodium catalysts (*1,66-71,87*). Furthermore, in most cases, leaching of the rhodium from the zeolite was significant enough to be undesirable. No successful research has been reported on encapsulating cobalt in zeolites for use as a hydroformylation catalyst.

In this study, the synthesis of cobalt complexes encapsulated in the supercages of zeolite Y was attempted. The species initially present on the zeolites were analysed by Fourier-Transform Infrared Spectroscopy (FT-IR) and identified by comparison with the IR spectra of pure cobalt complexes synthesised independently in the laboratory. The impregnated catalysts were washed with various solvents to see if the cobalt complex remained in the zeolite. The impregnated zeolites were also tested as hydroformylation catalysts and compared with homogeneous catalysts.

Five cobalt carbonyl complexes were synthesised in the laboratory by reaction with either PPh_2Et or 1,2-bis(diphenylphosphino)ethane (DPPE): $[Co(CO)_3(PPh_2Et)_2]^+[Co(CO)_4]^-$, $[Co(CO)_3(PPh_2Et)]_2$, $Co_2(CO)_7(PPh_2Et)$, $[Co_2(CO)_4(DPPE)_3]^{2+}\{[Co(CO)_4]^-\}_2$ and $[Co(CO)_2(DPPE)]_2$. These compounds were characterised using IR, ^{31}P NMR, melting point, colour and elemental analysis.

The encapsulation methodology followed was the "ship-in-a-bottle" approach. The general approach involves impregnating zeolite Y with two compounds, each small enough to

move through the pores of zeolite Y, which react with each other within the cages of the zeolite (diameter 13Å) to form molecules too large to exit the cages of the zeolite via the pores (diameter 7.5Å). The two components, a metal carbonyl and a tertiary phosphine, were impregnated into zeolite Y using solution impregnation to form a metal carbonyl complex encapsulated within the cages. The metal carbonyl used in this project was dicobalt octacarbonyl, $Co_2(CO)_8$. Two different phosphines were used: a monodentate, tertiary phosphine, ethyldiphenylphosphine (PPh_2Et) and a bidentate, phenyl phosphine, 1,2-bis(diphenylphosphino)ethane (DPPE).

Five batches of impregnated zeolite Y were synthesized. Three batches were impregnated with PPh_2Et and $Co_2(CO)_8$; one of the batches was loaded with ~4.5% cobalt while the other two were loaded with ~0.2% cobalt. The remaining two batches of zeolite were impregnated with DPPE and $Co_2(CO)_8$, one batch with ~4.5% cobalt and the other batch with ~0.2% cobalt. Four of the five batches were impregnated with the tertiary or bidentate phosphine first, followed by $Co_2(CO)_8$. The fifth batch was impregnated with $Co_2(CO)_8$ first (~0.2% cobalt), followed by PPh_2Et.

The mass percent loading of cobalt on the zeolite support affected the species formed in the zeolite. The species formed with ~4.5% cobalt loading were the ionic species, $[Co_2(CO)_4(DPPE)_3]^{2+}\{[Co(CO)_4]^-\}_2$ and $[Co(CO)_3(PPh_2Et)_2]^+[Co(CO)_4]^-$. The species formed with ~0.2% cobalt loading were $Co_2(CO)_7(PPh_2Et)$ (unaffected by the order of impregnation) and the cation, $[Co_2(CO)_4(DPPE)_3]^{2+}$ (the anion was not detected on the zeolite).

Small portions of all five batches of impregnated zeolites were washed with a variety of solvents. The 4.5% cobalt-loaded zeolites were washed with hexane, 1-decene, 1-decanol and dichloromethane. Dichloromethane washed off most of the cobalt complex from both batches, indicating that the cobalt species in the zeolites were probably situated predominantly on the surface of the zeolites rather than encapsulated. The 0.2% cobalt-loaded zeolites were washed with hexane, 1-decene and dichloromethane. None of the cobalt complexes were washed off any of the batches by any of the solvents. This suggested that, in these cases, the cobalt complexes were successfully encapsulated in the

zeolite cages.

Reactions with zeolite loaded with 4.5% cobalt and PPh_2Et showed product selectivities characteristic of homogeneous catalysis (with cobalt carbonyl and PPh_2Et). Recycling the zeolite catalyst showed sharp decreases in activity and the product selectivities were characteristic of homogeneous catalysis with $Co_2(CO)_8$ alone. Addition of PPh_2Et to the reaction system for some of the reactions showed similar trends. Whether extra phosphine was added or not, the reaction solution after one reaction showed strong bands in the infrared spectra in the carbonyl region. This indicated that the cobalt carbonyl complex had leached out of the zeolite and into solution and was probably carrying out catalysis in the solution rather than within the cages of the zeolite. Recycling of the zeolite catalysts did not result in carbonyl bands being observed in the IR of the solution.

Reactions with zeolite loaded with 4.5% cobalt and DPPE showed a similar trend to that observed using the zeolite loaded with 4.5% cobalt and PPh_2Et. However, addition of extra DPPE to the system resulted in anomalous results which could not be explained.

Reactions with zeolite loaded with 0.2% cobalt and PPh_2Et showed product selectivities characteristic of homogeneous catalysis with cobalt carbonyl and PPh_2Et. Recycling of the zeolite catalyst showed sharp decreases in activity and showed product selectivities characteristic of homogeneous catalysis with $Co_2(CO)_8$ alone. Cobalt carbonyl complexes were not detected in solution after any of the reactions and about 90% of the cobalt was retained on the zeolite after the zeolite was recycled twice. Addition of extra phosphine to reactions in which the zeolite catalyst was recycled showed a constant conversion for each reaction together with product selectivities similar to homogeneous catalysis with $Co_2(CO)_8$ and PPh_2Et. Cobalt carbonyl species were detected in solution after all reactions, indicating that the cobalt carbonyl complexes in the zeolite were leaching out of the zeolite and carrying out catalysis in solution rather than within the cages of the zeolite.

Reverse-impregnation of the zeolite ($Co_2(CO)_8$ and PPh_2Et) showed similar trends but with a few important differences. Single reactions showed almost no conversion together with no carbonyl complexes in solution; recycling of the zeolite catalyst gave results similar to

the previous batch of 0.2% cobalt-loaded zeolite. This suggested an initial "lag phase" for the cobalt to diffuse to the surface of the zeolite to carry out catalysis (assuming that catalysis was mainly homogeneous).

Reactions with zeolite loaded with 0.2% cobalt and DPPE showed product selectivities characteristic of homogeneous catalysis with cobalt carbonyl and DPPE. Recycling of the zeolite catalyst showed sharp decreases in activity and showed product selectivities characteristic of homogeneous catalysis with $Co_2(CO)_8$ alone. Cobalt carbonyl species were not detected in solution and 100% of the cobalt was retained on the zeolite after three consecutive reactions. It was suspected that catalysis was still occurring in solution but that the cobalt carbonyl species decomposed and returned to the zeolite. Addition of extra DPPE to the reaction system resulted in retention of 100% of the cobalt on the zeolite in the form of a carbonyl complex. However, there was almost a total elimination of activity of the catalyst. This suggested that the cobalt complex had been immobilised within the cages of the zeolite and was not in solution to carry out catalysis.

It was concluded that the use of $Co_2(CO)_8$ and PPh_2Et or DPPE to form encapsulated cobalt complexes within the cages of zeolite Y for use as hydroformylation catalysts was not successful. Significant amounts of cobalt leached out of the zeolite and carried out catalysis in solution. The zeolite loaded with 0.2% cobalt did appear to have encapsulated the cobalt. However, it was speculated that use of the zeolite under hydroformylation conditions led to conversion of $Co_2(CO)_7(PPh_2Et)$ to cobalt carbonyl species small enough to exit the cages of the zeolite. This resulted in significant leaching of the cobalt from the zeolite into solution.

The most promising result was obtained, surprisingly, with Na-Y loaded with 0.2% cobalt using $Co_2(CO)_8$ and DPPE. The catalyst produced was inactive for hydroformylation but retained 100% of the cobalt in the form of a cobalt carbonyl complex. Qualitative washing experiments suggested encapsulation of the cobalt complex.

TABLE OF CONTENTS

LIST OF FIGURES

LIST OF TABLES

ABBREVIATIONS

AA	Atomic absorption
alc:ald	Alcohol to aldehyde ratio
CoNa-Y	Faujasite Y zeolite containing both sodium and cobalt ions
dec	decomposed
DPPE	1,2-bis(diphenylphosphino)ethane
DPPM	1,2-bis(diphenylphosphino)methane
GC	Gas chromatography/Gas chromatograph
FT-IR	Fourier Transform Infrared Spectroscopy (shortened to IR) (vs = very strong, s = strong, m = medium, w = weak, vw = very weak, sh = shoulder)
NMR	Nuclear magnetic resonance
Na-Y	Sodium form of the faujasite Y zeolite
n:iso	Normal to branched (isomer) ratio
ppm	parts per million
PR_3	Tertiary phosphine in which "R" represents an alkyl or phenyl group
Si:Al	Silicon to aluminium ratio
THF	Tetrahydrofuran
vs	versus

CHAPTER 1

Introduction

1. INTRODUCTION

1.1. INTRODUCTION TO HYDROFORMYLATION AND "SHIP-IN-A-BOTTLE" CATALYSIS

Hydroformylation of alkenes to alcohols and aldehydes is one of the processes performed in industry which utilises homogeneous catalysts (*1,2,3*). Unfortunately, homogeneous catalysts are frequently difficult to separate from the liquid products and may require energy-intensive procedures such as distillation to effect the separation. If the hydroformylation product stream is low-boiling (ie. C_6 and lower), then the conditions required to isolate products (eg. fractional distillation) are not economically prohibitive in terms of energy requirements and thermal decomposition of catalysts. However, in the production of detergent-range alcohols (C_{10} and higher), the boiling points of the products are high and complicate the separation procedure. The catalyst must be separated from products because of product purity requirements and because the catalysts are very expensive (consisting of cobalt or rhodium complexes); this makes alternative methods of catalyst separation desirable.

The separation problem is common to all homogeneous catalysts, thus it might appear strange that such catalysts are still utilised in industry. The reason is that homogeneous catalysts are very active and, more importantly, very selective. High selectivity means minimal by-products (ie. waste) which has to be processed. Ideas followed so far to overcome the separation problem involve heterogenizing homogeneous catalysts on a support in some way to simplify the separation procedure to one of filtration or decantation (*4*). One such idea involves encapsulating the catalyst inside the pore structure of a zeolite and is frequently referred to as **"ship-in-a-bottle"** synthesis (*5,6,7*).

The term "ship-in-a-bottle" appears to have first been used to describe $Ni(CO)_{n-4}L_n$ complexes entrapped in zeolite X (*5*). The analogy is drawn from the procedure of placing a model ship inside a glass bottle and then, once inside, raising the mast of the ship so that it can't exit through the mouth of the bottle. In chemistry, this concept refers to immobilising molecules within some semi-rigid or rigid substrate and can occur in two basic ways. The first way involves synthesising a molecule inside some molecular cage (eg. cages found in the faujasite

zeolite family), the precursors of the molecule being small enough to enter the cage individually via access pores but the resultant product being too large to exit. The second way involves some interaction between the molecule and the substrate resulting in immobilisation of the molecule, even if the molecule is actually physically small enough to exit the encaging structure. The main application of this idea is the immobilisation of homogeneous catalysts on heterogeneous supports to retain the selectivity of the homogeneous catalysts while simplifying separation of the catalysts from the reaction media.

1.2. A COMPARISON OF HOMOGENEOUS, HETEROGENEOUS AND HYBRID CATALYSTS

Heterogeneous and homogeneous catalyst systems each have certain advantages and disadvantages. The main reason for ship-in-a-bottle syntheses is to try and produce catalysts which combine favourable characteristics of both and in the process eliminate the unwanted characteristics. One point which should be noted is that the term "homogeneous catalysis" is generally accepted to refer to catalysis by transition-metal complexes in solution (*8*) and this will be the implied meaning in any further use of the term unless otherwise specified; note that this does not preclude transition-metal catalysts as heterogeneous catalysts.

1.2.1. Homogeneous catalysts (*4*)

Advantages

1. High activity (reaction conditions usually 20°-200°C).
2. High selectivity.
3. Usually well characterized.
4. Relatively easy control of steric and electronic properties.

Disadvantages

1. Separation of catalyst from products is usually very difficult and costly.
2. Catalysts are usually very expensive.

The advantages are due to the fact that the active sites in homogeneous catalytic systems are metal atoms of discrete molecules. This means that there is (theoretically) only one type of active site and also that every site can take part catalytically, which explains the high selectivity and activity respectively. Furthermore, it is relatively easy to do *in situ* analysis of such systems which allows extensive characterisation. Finally, the active sites can be easily modified to tailor the catalyst to specific needs.

The consequence of having the catalyst and reactants/products in the same phase is that the methods required to separate out the catalyst are usually energy intensive (eg. distillation) unlike the simpler methods possible with heterogeneous catalysts (eg. filtration). The low thermal stability of some homogeneous catalysts can complicate the procedure even further and a number of techniques which can be used instead of distillation are listed in **Table 1.1** (these techniques have been used for recovering rhodium catalysts from hydroformylation processes) (*8*).

Nevertheless, the characteristic of greatest importance in industrial reaction processes is selectivity (*9*), mainly because of the emphasis on waste minimisation, and this has led to adaptation of homogeneous catalysis by industry (*1*).

1.2.2. Heterogeneous catalysts (*4*)

Advantages

1. High mechanical and thermal stability.
2. Separation from reaction system usually very easy.

Disadvantages

1. Severe reaction conditions are often required.
2. Selectivity to desired products is frequently poor.
3. Active sites are frequently ill-defined.
4. Limited accessibility and effectiveness of catalytic sites due to mass transfer limitations.

Table 1.1 : Methods for recovery of homogeneous catalysts (*8*)

PROCESS	DESCRIPTION
Reverse osmosis	Use of silicon latex membranes
Adsorption	Adsorption on solid followed by regeneration
Precipitation	Self-explanatory
Cation exchange	Oxidation of catalyst into an aqueous phase and then isolation with cation exchanger
Two-phase extraction	Treatment of system to make catalyst soluble in aqueous media
In situ regeneration	Reduction to metal, then react with CO and phosphine

The high activity of these types of catalysts is due mainly to the fact that the reaction conditions are severe.

Unlike the homogeneous catalysts, heterogeneous catalysts usually do not consist of only one type of active site and furthermore the active sites are usually clusters of molecules rather than single molecules, reducing the selectivity as well as the effectiveness of the catalysts. Thus, severe reaction conditions are often required to obtain economically viable yields of desired products. This gives rise to another problem; most heterogeneously catalysed reactions cannot be studied *in situ* which makes it very difficult to characterise the catalyst under reaction conditions and to elucidate the mechanisms involved.

1.2.3. Hybrid catalysts

In general, the hybrid catalysts consist of active "homogeneous" catalyst molecules dispersed

on some porous solid support. Organic supports are typically styrene polymers, poly(amino acids), acrylic polymers and cross-linked dextrans. Inorganic supports range from glass, silica and alumina to zeolites and clays (*4,10*). Obviously, an appropriate support must be used in any given reaction system; it should be inert, resistant to the reaction conditions and have a suitably large surface area.

Besides the advantage of obtaining high selectivity (characteristic of homogeneous catalysts) together with easy removal of the catalyst from the reaction system (characteristic of heterogeneous catalysts), there are a few other desirable characteristics as well as some undesirable characteristics sometimes encountered (*4,10*).

Advantages

1. Stabilisation of catalytically active species which are normally unstable.
2. Possibility of a change in equilibrium between metal atoms and their ligands.
3. Stereochemistry around metal atoms are altered.
4. Metal complexes supported in preferred orientations.

Disadvantages

1. Decrease in apparent activity of catalyst due to mass transport resistances.
2. Leaching of active catalyst from solid support under reaction conditions.

Stabilisation of catalytically active species by the support can lead to increased activity of the catalyst. This is mainly due to site isolation of the catalytically active species which prevents deactivation by interactions between more than one active species. An example is the prevention of dimerisation to stable, inactive species in rhodium(I) systems by site separation (*10*). The metal complex can also be activated to lose or exchange ligands due to the interaction with the support; this can be an advantage or a disadvantage, depending on what is desired. An example is the evolution of CO when $Co_2(CO)_8$ is mixed with Na-Y zeolite (*11*). Both the orientation of and the stereochemistry around the metal complex due to the support can affect the selectivity of the reaction. An example of this is the shape selectivity

which is exerted by Rh-zeolite catalysts in the hydrogenation of olefins (*12*).

1.3. SUPPORTS USED FOR ENCAPSULATION

As mentioned in Section 1.2., both organic and inorganic supports can be used to immobilise catalysts and each of these types of supports has certain properties which can be either advantageous or disadvantageous, depending on the application.

1.3.1. Organic Supports (*4,10*)

Advantages

1. Easily functionalised.
2. Usually chemically inert.
3. Wide range of physical properties can be engineered by changing extent of cross-linking of the polymer structure (porosity, surface area, flexibility).

Disadvantages

1. Poor heat transfer abilities.
2. Usually have poor mechanical properties (easily pulverised in stirred systems).
3. Can have unknown, incorporated impurities.
4. Flexibility of organic supports can lead to deactivation of the supported catalyst by intermolecular condensation reactions.
5. The thermal stability of the hybrid catalyst is usually a function of the thermal stability of the support rather than that of the supported catalyst (upper limit of about 433K).
6. Swelling of organic supports under variable temperature and solution conditions makes practical control of diffusional variables difficult.

1.3.2. Inorganic supports (*4,10*)

Advantages

1. Reasonable heat transfer capability.
2. Mechanically very stable (very inflexible). This inflexibility also prevents the possibility of catalyst deactivation mentioned about organic supports.
3. Thermally very stable. The thermal stability of the hybrid catalyst is a function of the thermal stability of the supported catalyst (over 573K for some metal carbonyls).
4. Good control of diffusional factors. Zeolites in particular, with their well-defined pore structure, have stable diffusional characteristics.

Disadvantages

1. Supports which include hydroxyl or oxide surface species can lead to undesirable side-reactions with the supported catalyst and the reaction medium; such supports are common and include silica-alumina and zeolites.

The support used in this project was a zeolite, an inorganic support. Thus, in Section 1.4., zeolites are discussed in more detail.

1.4. ZEOLITES

1.4.1. Background

Zeolites are aluminosilicates, ie. their crystal structures incorporate Al, Si and O atoms in a variety of configurations. This gives the zeolites the unique characteristic of having channels, pores and cavities extending through their crystal lattices in one, two or three dimensions (*13,14*). Catalytic sites are distributed throughout the lattice as well. Since the cavities of zeolites are on the molecular scale (10-100 Angstroms), zeolites as catalysts are comparable to enzymes, which also have catalytic sites embedded within molecular-scale clefts (*13*).

1.4.2. General structure of zeolites

The aluminosilicate structure is ionic and incorporates Si^{4+}, Al^{3+} and O^{2-} ions. The building block of the structure is the SiO_4 unit with the oxygens in a tetrahedral arrangement around the Si. The zeolite is built up by sharing of O-atoms between tetrahedra and the way in which they are assembled defines the crystalline structure and properties of the zeolite. Some of the Si-atoms are usually replaced by Al-atoms during the synthesis of zeolites; since the formal valency of Si is 4+ and of Al is 3+ in the zeolite lattice, an excessive negative charge is generated throughout the zeolite lattice. The charge is compensated for by extraframework cations which are distributed throughout the zeolite, eg. H^+, Na^+. The negative charge is dispersed throughout the zeolite lattice and although the cations present are found at discrete positions in the zeolite, they are still fairly mobile and can "hop" from site to site (*15*).
Figure 1.1 shows a secondary building block (called a sodalite cage) which is built up by a certain configuration of SiO_4 and/or AlO_4 tetrahedra; the points of intersection of the straight black lines represent Si or Al ions and the straight lines themselves represent an oxygen ion bonding two Si ions or a Si ion and an Al ion.

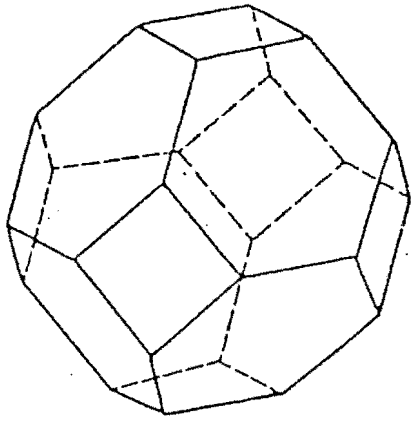

Figure 1.1 : A sodalite cage, building block of faujasite zeolites

Notice that the cage has six square faces and eight hexagonal faces. A number of cages can be linked via these faces, with or without bridging oxygens to form a variety of zeolites. This structure is just an example of the way in which the tetrahedra can be assembled to form zeolites and is by no means a common configuration to all zeolites. However, the sodalite

cages are the characteristic secondary building blocks of zeolite A and the faujasite zeolites X and Y and the structure of zeolite A is shown in **Figure 1.2** as a visual illustration. This figure clearly shows the pores formed which access the larger enclosed cavity or "supercage". The unit cell in **Figure 1.2** is made up of eight sodalite cages, each cage joined to four others via their square faces; each connecting unit is a set of four bridging oxygens.

1.4.3. Zeolites as ion-exchangers

As mentioned previously, a number of extraframework cations are present in zeolites to balance out the net negative charge of the lattice. The ion usually present after synthesis is Na^+ but is easily exchanged for other cations under mild conditions (temperatures up to 100°C and atmospheric pressures). For example, a large number of transition metal cations can be ion-exchanged into zeolite Y at room temperature (*16*).

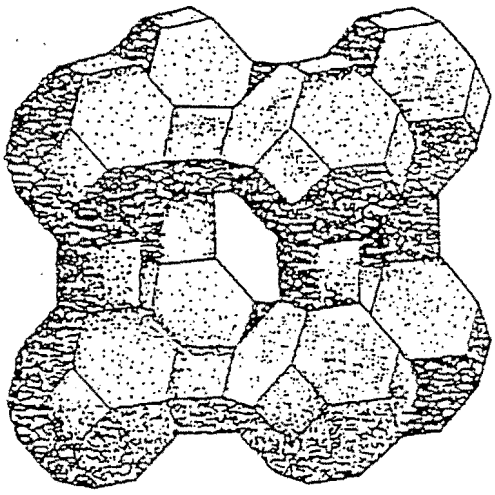

Figure 1.2 : Unit cell of Zeolite A

1.4.4. Zeolites as molecular sieves

The term "molecular sieve" refers to the fact that zeolites can physically restrict the movement of substances through their structures on the molecular scale. The pore/channel diameters of zeolites, being in the 3-10 Å range, can separate a mixture of compounds from each other purely on the basis of size differences. For example, isoparaffins are too large to move

through the pores of zeolite A whereas the n-paraffins are able to do so (*13*). This imparts to zeolites a characteristic which is highly desirable in catalysis: viz. shape selectivity.

Although zeolite lattices are generally considered inflexible, the atoms of the zeolite structure undergo normal atomic vibrations and, together with vibrations of molecules (allowing the molecules to enter openings smaller than their kinetic diameter), molecules of diameters 0.5-1 Å larger than the diameter of the zeolite pores can move through the pores (*13,17,18*).

On the other hand, the cations present in zeolites can occupy positions which partially block the pores, thereby reducing the size of the pore (*17*).

1.4.5. Zeolites as solvents

Zeolites can behave in a similar way to solvents because their ionic character gives them electrolytic properties varying from weak to strong, depending on the Si/Al ratio; the lower the ratio, the more "ionic" is the zeolite. Zeolites with low Si/Al ratios are hydrophilic while high ratios equate to hydrophobicity. Thus, hydrophilic zeolites will selectively extract water and polar molecules from hydrocarbons and vice versa for hydrophobic zeolites. However, the more ionic zeolites can, in some cases, even affect nonpolar molecules in solvent-like ways; upon absorption, hydrocarbons can become slightly polarised and consequently concentrated in the zeolite (*13*). A striking example of the solvent character of the faujasites is in the production of acetaldehyde by direct oxidation of ethene (*19*).

1.4.6. Zeolites as catalysts

Although this thesis is concerned with zeolites as supports for transition metal catalysts, it should be noted that zeolites themselves can catalyse reactions. Zeolites can provide a large number of catalytic sites with stability at high temperatures and zeolites with H^+ counterions are used extensively in industry for acid catalysed reactions (*13*). The protons in acid zeolites are very acidic and hydrocarbons exposed to these zeolites form carbocations which are the intermediates in many important industrial reactions, eg. hydrocarbon cracking, isomerisation, alkylation and hydrogen-transfer reactions (*20,21,22*).

1.4.7. Zeolites as supports for catalysts

Besides being acid catalysts, zeolites are also used extensively as supports for other catalysts and these catalysts can range in form from ions (*13,23,24*) to metal clusters (*13,18,20,22,25*) to metal complexes (*6,15,25,26*). The mechanism whereby these complexes are retained on the zeolite crystal surface or within the zeolite structure also vary according to which type of complexes are being used. Ions are held by ionic interactions with the zeolite lattice. The clusters and complexes are retained by two possible mechanisms:

1. Interactions with the zeolite walls, either via lattice atoms or with the counterions.
2. Physical encapsulation; the cluster/complex is small enough to inhabit the spaces within the zeolite structure but too large to exit the spaces via the smaller pores which access the spaces. As previously mentioned, these species are frequently called "ship-in-a-bottle" compounds.

The ship-in-a-bottle approach is particularly appealing in terms of trying to discover a hybrid between homogeneous and heterogeneous catalytic systems; transition metal complexes might be encapsulated within zeolites without necessarily being bound to the oxide surface (*6*). The interest in this idea has led to most of the research being concentrated on the faujasite zeolite Y (*6,15,22,25,26*), although certain applications allow, even require, different zeolites to be used, eg. the AlPO's (*6*), VPI-5 (*18*) and the ZSM zeolites (*19*). Zeolite Y in particular has received the most attention in this regard because it consists of "supercages" (diameter ~13Å) extending in three dimensions, each cage accessed by a number of pores/windows (diameters of ~7.5Å). Furthermore, zeolite Y appears to be more suitable for encapsulation than zeolite X (with which it is isomorphous) because the charge density on zeolite Y is smaller than on zeolite X, allowing metal cations or centres to be more mobile and available to coordinate with ligands other than the zeolite lattice oxygens (*15*). The structure of a unit cell of zeolite Y is shown in **Figure 1.3**. Note the difference to the structure of zeolite A shown in **Figure 1.2**. In zeolite A, the sodalite cages are joined via their square faces whereas in zeolite Y they are joined by their hexagonal faces; each supercage in zeolite Y is not surrounded by only eight sodalite cages at eight corners as in zeolite A but rather by ten sodalite cages.

Of particular importance to this project is the encapsulation of transition metal complexes within zeolites and this is discussed more thoroughly in Section 1.4.9.

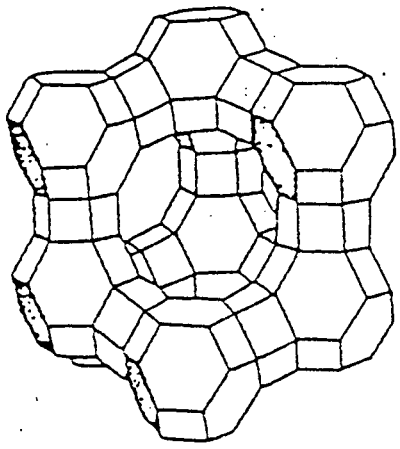

Figure 1.3 : Unit cell of Zeolite Y

1.4.8. Shape selectivity of zeolites

As previously mentioned, zeolites have the capability of imparting shape selectivity to reactions. This selectivity arises if all the active catalytic sites are situated within the zeolite structure rather than on the exterior surface of the zeolite crystals; this can be ensured by poisoning the exterior sites. The reaction is then controlled by the dimensions of the pores and/or the cages present in the zeolite structure. If the zeolite itself is the catalyst (ie. the acid sites are the catalytic sites) then the exterior sites need to be eliminated (frequently referred to as "poisoning"). If the zeolite is a support, then it must be ensured that all the active metal centres reside inside the zeolite and not on its surface to take advantage of the shape selective capability of the support; fortunately, this happens to be the same aim in the encapsulation of catalysts and results in the interesting (and useful) possibility of combining shape selectivity with ease of separation of the catalyst, both as a function of the zeolite support.

There are three types of shape selectivity which can be imposed by zeolites (*17*) (also illustrated in **Figure 1.4**):

1.4.8.1. Reactant selectivity

This is a function of the pore diameters of the zeolite. In a mixture of reactants, those with diameters the same size or smaller than that of the pores will be the only reactants to diffuse into the zeolite and reach the catalyst sites to react.

1.4.8.2. Product selectivity

This is a function of the pore diameters of the zeolite. Reaction products smaller than the pore diameter will diffuse out of the zeolite while those too bulky to do so can be converted to smaller molecules or can block up the pores (blocking of pores ultimately causes deactivation).

1.4.8.3. Transition-state selectivity

This is a function of the internal diameter of the cages of the zeolite. This occurs when certain reaction pathways are prevented because the transition states involved are too large to fit into the zeolite cage, even though reactants and potential products are able to pass through the pores.

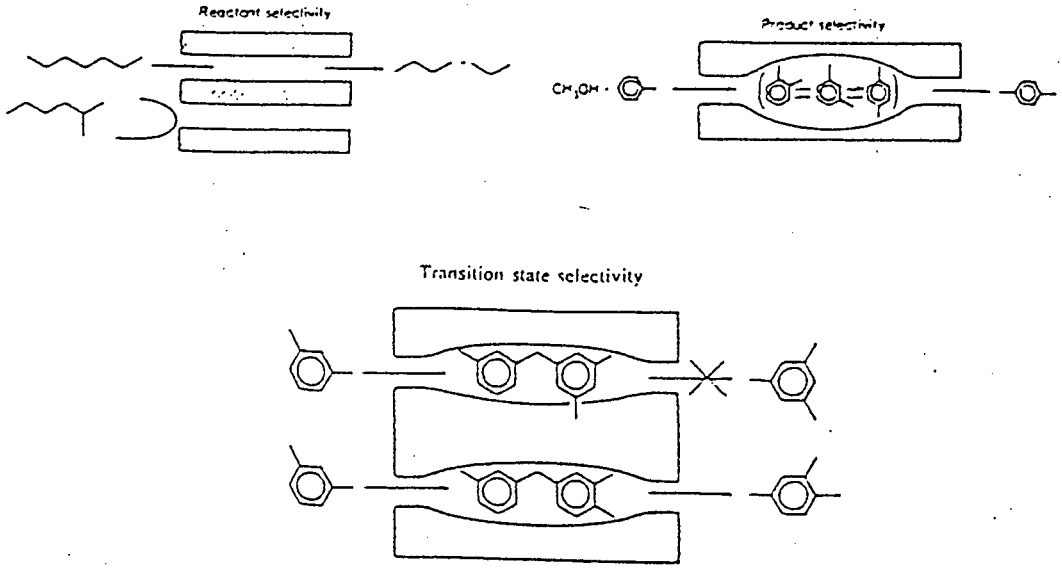

Figure 1.4 : Shape selective effects possible using Zeolite Y

1.4.9. Encapsulation of Transition Metal Complexes in zeolites

1.4.9.1. Encapsulation strategies

There are a number of general strategies that have been used to encapsulate transition metal complexes (TMC's) in zeolites:

(i) Impregnation with preformed complex

In this case, the complex to be encapsulated is formed outside the zeolite pores and then transported into the cages. Cationic complexes, such as the $Cp^*RhL_3^{2+}$ ion (L=ligand; in this particular case, the ligand is the solvent (*27*)) are ion-exchanged with the counterions in the zeolite while neutral organometallic complexes, such as titanocene dichloride (*24*), are absorbed in and then react with the zeolite surface to anchor the complex. Obviously, the complexes must be small enough to move through the pores of the zeolite.

(ii) Complex assembly inside zeolite

In this approach, the transition metal and its intended ligands are impregnated separately into the zeolite and react inside the zeolite to form complexes too big to exit the zeolite structure. The transition metal is impregnated either by ion exchange or as some neutral organometallic or carbonyl complex. Encapsulation is then achieved in a number of different ways:

1. Reaction of exchanged ions with CO and H_2 to form multinuclear metal carbonyl clusters, eg. $Ir(CO)_2(acac)$ to form $Ir_4(CO)_{12}$ or $Ir_6(CO)_{16}$ (*28*) and $Ru(CO)_5$ to form $Ru_3(CO)_{12}$ (*29*)

2. Reaction of exchanged ions with various ligands to form the encapsulated complexes. The ligands are usually bi- or polydentate ligands and are complexed with the metal ions in one of two ways:

   - the ligand is flexible and diffuses into the zeolite cages and chelates to the

ions to form complexes too large to exit the cages, eg. SALEN diffuses into zeolite X and Y and chelates with Pd^{2+} ions (*12*).

- the ligand is synthesised inside the cages from precursors using the metal ion as a template. For example, cobalt-exchanged Na-Y zeolite is impregnated with dicyanobenzene (DCB). The DCB forms pthalocyanine around the Co^{2+} ions using the ions as templates (*30*). Another example is the reaction of pyrrole and acetaldehyde around Co^{2+} ions in the cages of zeolite Y to form cobalt-tetramethylporphyrin (*31*).

3. Reaction of the neutral metal complex with a ligand inside the cages. An example of this is the reaction of $Ni(CO)_4$ with isopropyldiphenylphosphine to produce a "ship-in-a-bottle" complex, $Ni(CO)_3(Ph_2PCHMe_2)$ (*32*).

(iii) Template synthesis

In this method, the metal complex to be encapsulated is preformed and then the zeolite is crystallised around the complex, ie. building the bottle around the ship. Metal phthalocyanines and the dye, methylene blue, have been encapsulated in this way (*6*).

1.4.9.2. Methods of impregnation

Essentially, there are three methods for getting the metal centre and/or the ligands into the zeolite.

(i) Ion exchange

The zeolite is mixed with an aqueous solution of the metal ion for exchange with the cations already in the zeolite. The metal used is in the form of a water-soluble salt (eg. nitrate or acetate). A number of transition metal ions have been successfully exchanged into zeolite Y, including cobalt, manganese, chromium and copper (*16*).

(ii) Solution impregnation

The zeolite is mixed with a solution of the neutral metal compound and the ligand to distribute the compound and the ligand throughout the zeolite structure. The metal compound and the ligand are added separately and in consecutive steps and either the metal compound or the ligand can be added first. The solvent can be either aqueous or non-aqueous but this depends on the solubility of the compound to be impregnated, the pore architecture of the zeolite and the affinity of the solvent for the zeolite (*26*). Zeolite Y is very hydrophilic and the complexes impregnated using this method are normally insoluble in aqueous media, so hydrocarbon solvents (eg. hexane) are preferred for solubility reasons as well as to minimise the competition for adsorption between solvent molecules and the complex molecules. For example, in the encapsulation of $Ir_4(CO)_{12}$ and $Ir_6(CO)_{16}$, the $Ir(CO)_2(acac)$ precursor is dissolved in hexane after which zeolite Y is placed in the solution (*28*). CH_2Cl_2 was used to impregnate zeolite Y with $[Cp^*RhCl]_2(\mu\text{-}Cl)_2$ (*27*) while hexane was used to load isopropyldiphenylphosphine into zeolite Y for reaction with $Ni(CO)_4$ (*32*).

(iii) Chemical vapour deposition (CVD)

The zeolite (usually rigorously dehydrated) is placed in an evacuated container and then exposed to the vapour of the volatile metal compound. For example, $Ni(CO)_4$ (*32*), $Co_2(CO)_8$ (*33*), and $Zn(CH_3)_2$ and $Cd(CH_3)_2$ (*34*) have been loaded onto zeolite Y in this way. Ligands can also be introduced using CVD techniques; trimethylphosphine is a volatile tertiary alkyl phosphine which has been loaded onto zeolite Y in this manner (*35,36*).

1.4.10. Versatility of "Ship-in-a-bottle" catalysts

A wide variety of applications of ship-in-a-bottle catalysts have been and are being pursued, and some such examples follow.

1.4.10.1. Dioxygen-binding carriers

The cobalt SALEN complex encapsulated within zeolite Y has been found to be a very active

oxygen binder (*7*); the SALEN ligand (shown in **Figure 1.5**) loses its two hydroxyl protons and chelates to a divalent cobalt cation to form a ship-in-a-bottle species

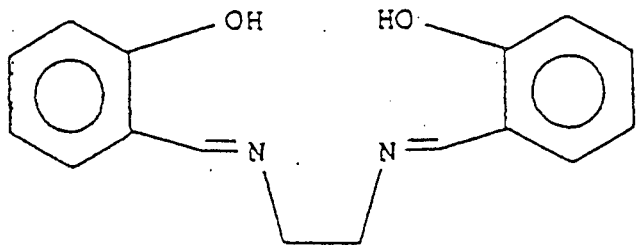

Figure 1.5 : The SALEN Ligand

Recently (1994), a cobalt tetramethylporphin complex was encapsulated within zeolite Y and is capable of undergoing reversible oxygenation (*31*); oxygen is adsorbed by the catalyst at 25°C and is desorbed at about 70°C.

1.4.10.2. Oxidation catalysts

Manganese pthalocyanine and manganese SALEN have been encapsulated in zeolite Y and are both reported to catalyse the oxidation of alkenes (*6*). Very recently (1997), a manganese salen complex was encapsulated within zeolite Y for use as a catalyst for epoxidation of alkenes at 5°C (*37*).

1.4.10.3. Hydrogenation catalysts

A palladium SALEN complex has been encapsulated in zeolite X and zeolite Y and reported to greatly enhance selectivity to hydrogenation of alkenes over the isomerisation reaction at 25°C (*12*). Iron pthalocyanine complexes encapsulated in zeolite Y have been reported for the effective hydrogenation of toluene to methylcyclohexane (*6*). $Ir_4(CO)_{12}$ encapsulated in zeolite Y has been reported for the hydrogenation of alkenes (*28*). Rhodium encapsulated in a variety of zeolites for the hydrogenation of cyclopentene and 3- or 4-methylcyclohexene

(60°C, 50 psi) have also received attention (*38*). Ruthenium carbonyls have been encapsulated in Na-Y and used successfully as catalysts for hydrogenation of CO and CO_2 at 21 bar pressure and temperatures ranging from 150-320°C (*29*).

1.4.10.4. Other reactions

Other reactions mentioned in the literature include:

- catalysis of the water-gas shift reaction by (zeolite Y)-encapsulated iron carbonyl at 60-160°C (*39*)
- dehydrogenation of cyclohexane by zeolite-encapsulated metal phthalocyanines (*6*)
- conversion of butylmercaptan to butylenes, dibutylsulphide and hydrogen sulphide over zeolite Y containing metal phthalocyanines (*6*)

1.5 THE HYDROFORMYLATION REACTION

1.5.1. Background

Hydroformylation entails the production of aldehydes and alcohols by reacting olefins with CO and H_2 (syngas) using a transition metal complex as a homogeneous catalyst. The process is called hydroformylation because it involves the formal addition of formaldehyde across an olefinic double bond, but the older name "oxo process" is still often used. Otto Roelen discovered cobalt to be a hydroformylation catalyst in 1937 while attempting to recycle olefins in a Fischer-Tropsch reaction (*40,41*) but it has since been found that many carbonyl-forming transition metals can act as catalysts (*1*). At present, the most extensively used catalysts in industry are rhodium and cobalt (rhodium is more active than cobalt) (*1,42*).

Hydroformylation is used to produce a range of aldehydes and alcohols from C_3 to C_{15} and the worldwide capacity for oxo chemicals as at 1990 was 7×10^6 metric tonnes. The largest volume of these products is by far the C_4 products (73%); n-butanal is converted mainly to n-butanol for production of butyl acrylate or methacrylate, or converted to 2-ethyl-1-hexanol as a precursor to PVC plasticizers (*1,42*).

1.5.2. Mechanism of hydroformylation

The mechanism of the hydroformylation reaction is essentially the same whether rhodium or cobalt carbonyl is used; cobalt is described here because it is the catalyst used in this project. The general mechanism, which is still accepted today (*42*), was formulated by Heck and Breslow in 1961 (*43*) and the catalytic cycle for the formation of aldehydes is shown in **Figure 1.6** and for the formation of alcohols in **Figure 1.7**.

The cobalt can be introduced in a variety of forms (from cobalt salts to cobalt carbonyl) but under hydroformylation conditions is always converted to the 18e$^-$ species, $HCo(CO)_4$ (which is in equilibrium with the coordinatively unsaturated species, $HCo(CO)_3$, the species involved in the catalytic cycle). This forms an alkylcobalt species with an olefin after which CO insertion, alkyl migration and hydrogenolysis steps lead to an aldehyde and the unsaturated cobalt species again (*2*).

In **Figure 1.6**, two interlinked cycles are shown; the lower one results in linear aldehydes while the upper one produces branched-chain aldehydes. Commercially, the linear products are more desirable and thus much research has gone into modifying hydroformylation catalysts to improve the normal-to-branched ("n:iso") product ratio (*2*).

1.5.3. Cobalt catalysts and their modification

Although $HCo(CO)_4$ is an active catalyst, it has some properties which are undesirable from an economic viewpoint:

- the catalyst is very unstable and requires high partial pressures of CO under operating temperatures, otherwise cobalt metal (inactive) precipitates out from solution, eg. at 200°C, p_{CO} required = 100 atm (*44*); this equates to 200-300 atm operating pressure in industry (H_2:CO of 1:1-2:1).
- the best ratio of n:iso which can be achieved is 4.4:1 (*3*)
- $HCo(CO)_4$ is very volatile which means that the cobalt can be lost with the lighter reaction products in a fractional distillation separation procedure. In industry, an aqueous-phase

catalyst separation step called decobalting is utilized and is a complicated procedure (*40*).

- $HCo(CO)_4$ is a very poor hydrogenation catalyst and a second reaction step is required if alcohols are desired (19:1 ratio aldehyde to alcohol) (*3,40*)

The catalyst can be modified by replacing a carbonyl ligand with a tertiary phosphine ligand, PR_3 (R = alkyl or phenyl) (*3*). This involves an equilibrium between the unsubstituted hydride and the substituted hydride under hydroformylation conditions, shown in equation (1):

$$HCo(CO)_4 + PR_3 \rightleftharpoons HCo(CO)_3(PR_3) + CO \qquad \text{.....(1)}$$

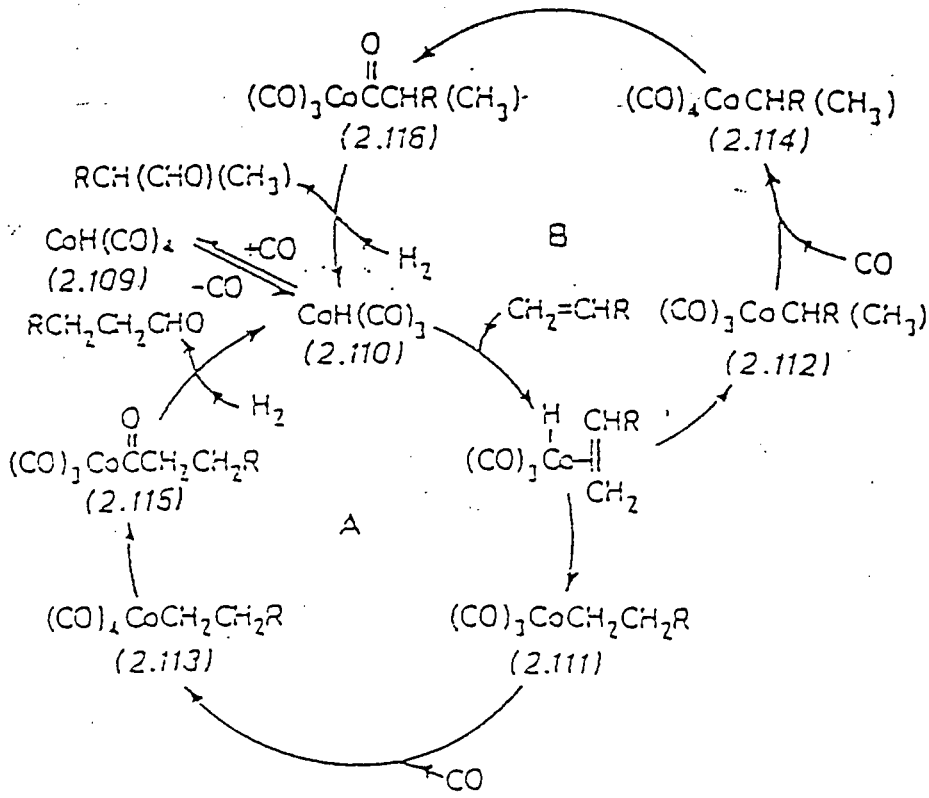

Figure 1.6 : Hydroformylation of olefin to aldehyde using cobalt carbonyl as catalyst

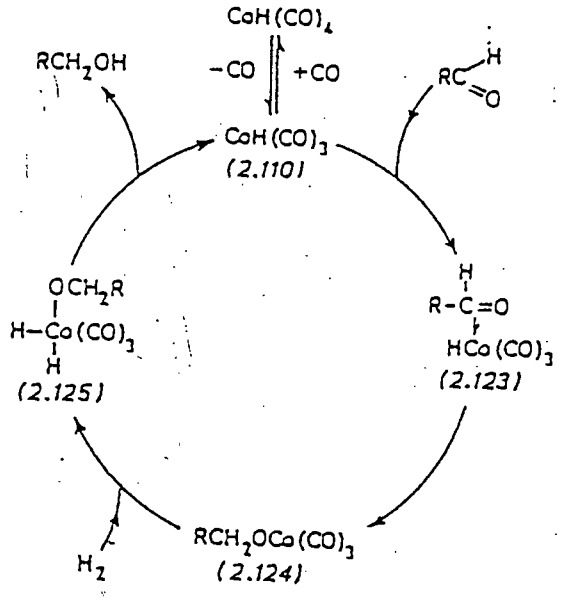

Figure 1.7 : Hydrogenation of aldehyde to alcohol using cobalt carbonyl under hydroformylation conditions

The benefits of doing this are considerable:

- required operating pressures are reduced to 20-100 atm because the active catalyst, $HCo(CO)_3(PR_3)$ is thermally more stable than $HCo(CO)_4$ (*2,42,45*)
- n:iso ratio can reach 9:1 (*3*)
- $HCo(CO)_3(PR_3)$ is thermally very stable and can be involved in distillation processes (for separation of products and catalyst) without decomposing.
- good hydrogenation catalyst (8:1 ratio alcohol to aldehyde, sometimes 90% selectivity to alcohols with no aldehydes, the other 10% being paraffins and esters) (*3*).

One disadvantage of the phosphine-substituted cobalt carbonyl catalyst is that the thermal stability of this complex requires that the reaction is run at higher temperatures to obtain satisfactory activity. This also results in a higher rate of olefin hydrogenation, which is undesirable. It should be noted that the cycles in **Figure 1.6** and **Figure 1.7** are analogous to the modified catalyst cycles as well. Rate equations which are generally accepted for the hydroformylation and hydrogenation reactions are as follows:

Aldehyde formation (*2*):

$$\frac{d\ [aldehyde]}{dt} = k_{obs}\ [alkene][cobalt]\ p(H_2)\ p(CO)^{-1} \qquad \text{..... (2)}$$

Alcohol formation (*2*):

$$\frac{d\ [alcohol]}{dt} = k_{obs}\ [aldehyde][cobalt]\ p(H_2)\ p(CO)^{-2} \qquad \text{..... (3)}$$

1.5.4. Rhodium catalysts

At present, modified rhodium-catalysed processes dominate the hydroformylation industry in terms of annual production. Most advances in technology over the past 15-25 years have occurred in rhodium catalysis whereas, cobalt technology has remained almost unchanged for about the last 15 years (*1*). This preference for rhodium catalysts occurred because rhodium is up to 1000 times more active than cobalt and it is very selective to aldehydes (almost 100% selectivity with >9:1 n:iso ratio) (*1*). The operating conditions and product distributions obtained using the various catalysts are compared in **Table 1.2.**

1.5.5. Cobalt vs rhodium as catalyst

Since rhodium is so much more active and selective than cobalt, a question might arise as to why cobalt is still used in industrial hydroformylation. Rhodium is preferred to cobalt for C_3 hydroformylation but the exact opposite is true for hydroformylation of C_6 and higher alkenes (*1*). The following is a list of the factors which have necessitated keeping cobalt as a catalyst.

1. Rhodium catalysts used at present are not as thermally stable as cobalt catalysts and are decomposed at the high temperatures required to distil high-boiling products (eg. heptanal boils at 154°C).

Table 1.2 : Operating conditions required for rhodium and cobalt hydroformylation catalysts (*1*)

	$HCo(CO)_4$	$HCo(CO)_3PR_3$	$HRh(CO)_2(PR_3)_2$
Temperature	>140°C	160-200°C	80-130°C
Pressure	>240 bar	50-100 bar	7-60 bar
Aldehydes:alcohols	19:1	90% selectivity to alcohols; no aldehydes	99:1
n:iso of all products	2-4:1	8:1	>9:1

2. Rhodium catalysts do not produce alcohols. Since the longer-chain alkenes are used to produce detergent alcohols, a two-stage reaction scheme would be required: rhodium is used to produce the aldehydes which are then hydrogenated with another catalyst in a second step.

3. Cobalt hydroformylation technology is well-established with a combined recovery and recycling system which can be applied to a wide range of olefins.

4. New developments in rhodium catalysts involve producing water-soluble complexes which can catalyse the reaction but are then removed from the hydrocarbon product by solvent-extraction with water. However, these "biphasic" catalysts are not highly soluble in the olefins (*1*) which limits the productivity. Admittedly, the newest water-soluble catalysts are "single-phase" (*46*), ie. soluble in hydrocarbons but can be induced to become polar for extraction with water by using water-solubilizing agents. However, no industrial-scale plant appears to be in operation yet (c.1996).

1.6. COBALT CARBONYL CHEMISTRY

Since the hydroformylation catalyst used in this project is cobalt-based, it is appropriate to mention some general transition metal chemistry (which applies to cobalt as well) and to then focus upon some chemistry of dicobalt octacarbonyl (the cobalt precursor used in this project).

1.6.1. Transition metal chemistry in general

Transition metal atoms have one *s*, three *p* and five *d* orbitals that are geometrically and energetically available for bonding. Furthermore, if all of these orbitals are filled with electrons due to bonding with ligands, their electron configuration resembles that of atoms of the noble element in the same period as the transition metal, ie. a very stable atom. In fact, this has led to the so-called "18 electron rule" used to predict the stability of transition metal complexes: the most stable transition metal complexes result when the outer nine orbitals of the transition metal centre are filled with electrons (*47,48*).

As catalysts, there are two main reasons for the usefulness of transition metals.

(i) Transition metal atoms are very versatile in forming bonds with ligands, either forming covalent bonds or coordinative bonds. Coordination induces changes in the electron distribution in a ligand (eg. CO) which modifies the reactivity of the ligand.

(ii) The nine outermost orbitals of the transition metals, as well as hybrids formed from them, can have a wide variety of shapes and orientations, both along and between atomic axes. The stability of coordinate bonds between ligands and transition metals are affected by the geometries of the interacting orbitals. An example of this is the bonding of carbon monoxide to transition metals. Carbon monoxide is usually inert but forms complexes with electron-rich transition metals and can result in the activation of the C-O bond. The geometries of the orbitals involved in the bonding lead to a carbon-metal bond which is stronger than expected; this is explained in more detail in Section 1.6.2. and is illustrated in **Figure 1.8**.

1.6.2. Carbon monoxide as a ligand for transition metals

Carbon monoxide is a π-acceptor ligand because it is capable of accepting π-electron density from transition metal atoms into empty π or π^* orbitals (*48*). It is one of the most extensively studied π-acceptor ligands because it is a ligand involved in many important applications of homogeneous catalysis (*47*).

Carbon monoxide is a fairly stable molecule, yet it nevertheless does react with metals and often forms very stable transition metal complexes. Electron density from a CO σ orbital is donated to a vacant metal *d* orbital; electron density is also donated from filled metal *d* orbitals or *dp* hybrid orbitals to vacant antibonding CO *p* orbitals (*47,48*). The interaction is shown in **Figure 1.8**; it is generally referred to as "back-bonding" and has a synergic effect, which can be explained as follows.

The σ-donation of electron density from the CO to the metal centre makes the CO more positive and thus increases its electron acceptor strength; the back-donation of electron density onto the CO from the electron-rich d-orbitals of the metal centre makes the CO more negative and thus a stronger electron donor to the metal centre. CO is known to stabilize low oxidation states of transition metal complexes such as mononuclear, binuclear, trinuclear, tetranuclear and polynuclear carbonyls because back-bonding allows the high electron density at the metal centres (a property of low oxidation state metal atoms) to be delocalised into the vacant CO *p* orbitals (*48*).

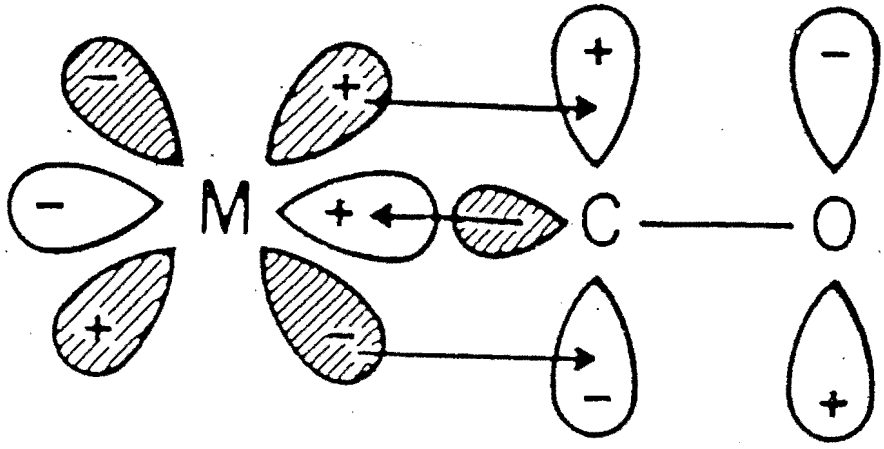

Figure 1.8 : π back-bonding between carbon monoxide and a transition metal atom

1.6.3. Dicobalt octacarbonyl

Cobalt metal alone is a bluish-white, ferromagnetic metal with a melting point of 1493°C (*49*). It is unreactive unless in a very finely divided state, dissolves slowly in mineral acids and can form a variety of oxides (CoO, Co_3O_4 and Co_2O_3). Its outer orbital electron configuration is $3d^7 4s^2$ and has well-documented oxidation states ranging from -1 to +4 (*49*). Cobalt metal or cobalt salts can react with carbon monoxide to form carbonyls; of particular importance in this project is the dimeric dicobalt octacarbonyl, $Co_2(CO)_8$, in which the cobalt is zerovalent and there is a bond directly between the two cobalt atoms (see **Figure 1.9**).

$Co_2(CO)_8$ is a convenient starting material for preparing many cobalt compounds because it is commercially available, easily purified and undergoes a wide variety of reactions (*49*). At S.T.P. it is an orange, crystalline solid with a melting point of 51-52°C with decomposition. It is thermally unstable in the absence of CO and at room temperature in an inert atmosphere slowly loses CO to form $Co_4(CO)_{12}$ and ultimately cobalt metal. As a solid, each molecule has two bridging carbonyl groups but in solution or the gas phase, there are two non-bridged isomers also present in equilibrium with the bridged form and with each other (*49*). The three forms are shown in **Figure 1.9**.

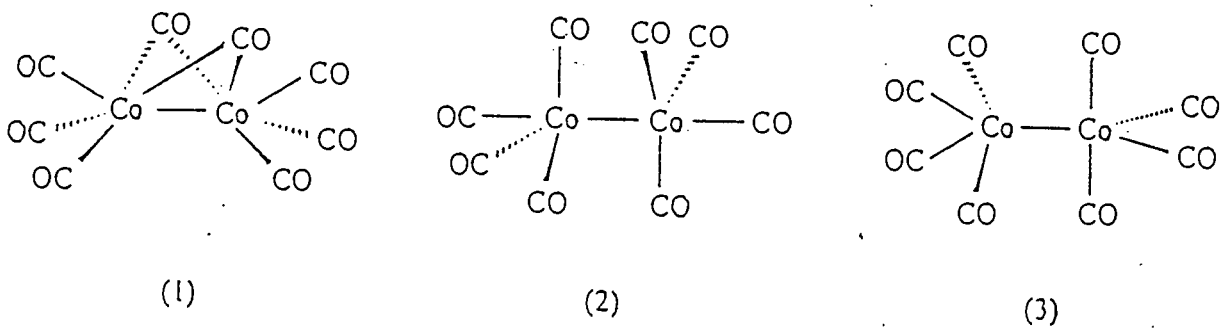

Figure 1.9 : Three Dicobalt Octacarbonyl isomers

1.6.4. Some important reactions of dicobalt octacarbonyl

1.6.4.1 Oxidation reactions

$Co_2(CO)_8$ is easily oxidised by air, halogens and oxidising agents. In air, olive-green CoO (*48*) is formed while at 400-500°C, Co_2O_3 (*50*) or Co_3O_4 (*48*) is formed.

1.6.4.2. Reduction reactions

$Co_2(CO)_8$ is readily reduced from Co(0) to Co(-I) by metals and by hydrogen. Under hydroformylation conditions, the reduction is due to hydrogen to form the hydride, $HCo(CO)_4$, the hydroformylation catalyst precursor. The reaction of $Co_2(CO)_8$ with hydrogen is shown in equation (4).

$$Co_2(CO)_8 + H_2 \rightarrow 2\ HCo(CO)_4 \qquad \text{.....(4)}$$

1.6.4.3. Disproportionation reactions

$Co_2(CO)_8$ reacts with bases under mild conditions (atmospheric pressure and room temperature) to form ionic complexes. Arsines, stilbines and phosphines are all bases which have been used extensively in such disproportionation reactions (*49,51-56,57,58*). For the hydroformylation reaction, phosphines have been found to modify $Co_2(CO)_8$ in such a way to give the most commercially desirable combination of distribution of products and catalyst activity and have consequently received the most attention in this field.

Monodentate phosphines (general formula PR_3 with R = alkyl or phenyl groups) form complexes of the type $[Co(CO)_3(PR_3)_2]^+[Co(CO)_4]^-$ while bidentate phosphines (frequently $R_{(1)}R_{(2)}P(CH_2)_nPR_{(3)}R_{(4)}$ where R = alkyl or phenyl groups) form complexes of the type $[Co_2(CO)_4(L\text{-}L)_3]^{2+}\{[Co(CO)_4]^-\}_2$ or $[Co(CO)_3(L\text{-}L)]^+[Co(CO)_4]^-$ where L-L is the bidentate phosphine (*53*). The monodentate phosphines can also react with $Co_2(CO)_8$ to form

complexes of the type $[Co(CO)_{5-n}(PR_3)_n]Y$ (Y=anion), but the complexes for n>2 are more difficult to form, requiring particular conditions (ie. **not** simply the addition of phosphine to a solution of $Co_2(CO)_8$) (*49,57,58*).

The reaction between $Co_2(CO)_8$ and triphenylphosphine, PPh_3 (monodentate phosphine), is shown as equation (5) (*54*).

$$Co_2(CO)_8 + 2PPh_3 \rightarrow [Co(CO)_3(PPh_3)_2]^+[Co(CO)_4]^- + CO \quad \text{..... (5)}$$

The reaction between $Co_2(CO)_8$ and bis(diphenylphosphino)ethane, DPPE (bidentate phosphine), is shown as equation (6) (*53*).

$$2Co_2(CO)_8 + 3DPPE \rightarrow [Co_2(CO)_4(DPPE)_3]^{2+}\{[Co(CO)_4]^-\}_2 + 4CO \quad \text{..... (6)}$$

1.6.4.4. Substitution reactions

Phosphines (both bidentate and monodentate) react with $Co_2(CO)_8$ at higher temperatures (>30°C) to produce covalent complexes. The monodentate phosphines can substitute for up to six of the carbonyl groups to from a cobalt complex of the type $[Co_2(CO)_{8-n}L_n]$, where n=1-6 (*49*), although n>2 is difficult to achieve (and consequently much fewer papers have been published about these complexes (*59-61*)). The monodentate phosphines form disubstituted complexes of the type $[Co(CO)_3(PR_3)]_2$ (*49,51,54,56,62,63*) and monosubstituted complexes of the type $Co_2(CO)_7(PR_3)$ (*49,51,64*) while the bidentate phosphines form complexes of the type $[Co(CO)_2(L\text{-}L)]_2$ or $[Co_2(CO)_6(L\text{-}L)]$ (*52,53,55,65*).

The reaction between $Co_2(CO)_8$ and triphenylphosphine, PPh_3 (monodentate phosphine), to form a disubstituted dimer is shown as equation (7) (*54*). **Figure 1.10** is a pictorial representation of the triphenylphosphine-substituted cobalt carbonyl molecule.

$$Co_2(CO)_8 + 2PPh_3 \rightarrow [Co(CO)_3(PPh_3)]_2 + 2CO \quad \text{..... (7)}$$

The reaction between $Co_2(CO)_8$ and triphenylphosphine to form a monosubstituted dimer is shown as equation (8) (*51,64*).

$$Co_2(CO)_8 + PPh_3 \rightarrow Co_2(CO)_7(PPh_3) + CO \quad \text{..... (8)}$$

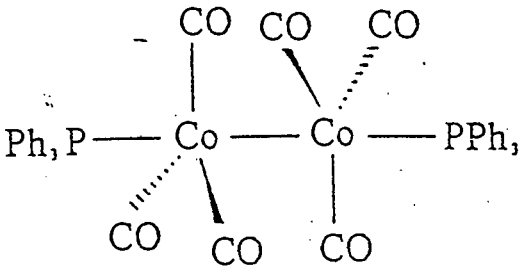

Figure 1.10 : The $[Co(CO)_3(PPh_3)]_2$ molecule

The reaction between $Co_2(CO)_8$ and bis(diphenylphosphino)ethane, DPPE (bidentate phosphine), is shown as equation (9) (*53*). **Figure 1.11** is a pictorial representation of the DPPE-substituted cobalt carbonyl molecule.

$$Co_2(CO)_8 + 2DPPE \rightarrow [Co(CO)_2(DPPE)]_2 + 4CO \quad \text{..... (9)}$$

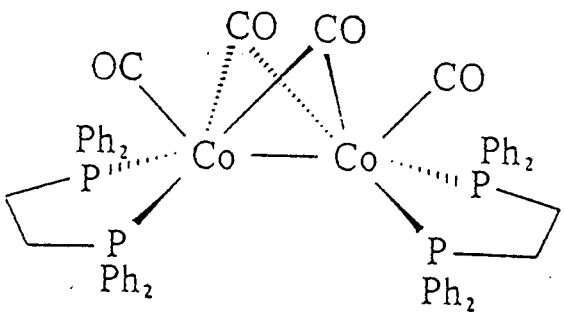

Figure 1.11 : The $[Co(CO)_2(DPPE)]_2$ molecule

1.7. HETEROGENIZING HYDROFORMYLATION CATALYSTS

Much research has gone into immobilising hydroformylation catalysts to simplify catalyst recovery. This research has been done almost exclusively on the rhodium catalysts for two reasons:

- the major oxo product required for many years has been n-butanal and rhodium is the best catalyst for this in terms of activity, selectivity and operating costs (*1*).
- rhodium is about 300 times more expensive than cobalt, so even a small loss results in high running costs.

The development of this field has gone through four distinct phases from the early 1970's to the present day.

1.7.1. Polymeric supports

In the early seventies, efforts were made to chemically bind rhodium to an insoluble polymeric support, either via one of the ligands of the complex or replacement of one of the ligands by a functional group on the support. $Rh(CO)Cl(Ph_3P)_2$ was incorporated into a crosslinked polystyrene containing functional groups of nitrogen, phosphorus or sulphur and 1-hexene was hydroformylated quite successfully; there was "very little" rhodium leaching and the catalyst had activity, selectivity and yield similar to homogeneous catalysts (*40*).

Cobalt carbonyl was also "immobilised", this time on poly-2-vinylpyridine; the mechanism here, though, was not strictly immobilisation but the enabling of an apparent controlled, reversible release of cobalt catalyst to the liquid phase reaction medium (*40*). This appeared to provide a mechanism whereby catalyst poisons were overridden or destroyed.

Such research has continued into the nineties (*1*) but the essential problems with organic substrates (discussed in Section 1.3.1.) and the fact that leaching of the rhodium from the support has not been sufficiently minimised has resulted in these catalysts never being put into operation on an industrial scale.

1.7.2. Zeolite supports

The next phase, from the mid seventies to the mid eighties, involved researching the use of zeolites as supports for rhodium hydroformylation catalysts; cobalt catalysts were apparently not considered at all.

The zeolites used were mainly the faujasite zeolites X and Y and zeolite A. The zeolites were almost exclusively ion-exchanged with $RhCl_3.xH_2O$ and then placed under hydroformylation conditions (syngas at 1-3 atm, temperature 50-150°C) (*66-68,69,70,71*); one method used the tris-allyl rhodium, $Rh(C_3H_5)_3$, as the ion-exchange precursor and phosphines were also added to the catalyst to mimic the homogeneous system (*72*). All these systems showed promising trends in terms of activity and selectivity and the rhodium was retained on the zeolite to a certain extent. Furthermore, the zeolite was seen to be a far superior support to the polymeric organic substrates (cf. Section 1.3.1., Section 1.3.2. and ref. *70*). However, as was the case for the polymeric supports, leaching of the rhodium was never minimised enough to warrant commercialising a process.

1.7.3. Supported liquid (aqueous) phase catalysts

The next innovation involved dissolving a rhodium complex in a thin layer of high boiling, low volatility solvent, adsorbed on a solid support; the catalyst was usually $HRh(CO)(PPh_3)_3$ dissolved in a layer of PPh_3 (*1*). However, this catalyst was only suitable for the hydroformylation of gas phase systems because liquid reagents and products solubilised the liquid layer leading, again, to leaching of the catalyst from the support. This problem was alleviated by replacing the liquid film by water, using a water soluble rhodium complex and anchoring the rhodium-containing water film to a highly hydrophilic support, eg. silica; the rhodium complex was water-solubilised by introducing a highly polar substituent, such as sulphonate or carboxylic acid groups, into the phosphine ligands on the rhodium (*1,73,74*). However, this catalyst type has also not been commercialised as of yet (*1*); it appears that deactivation of the catalyst and loss of the solvent phase are still problematic.

1.7.4. Homogeneous aqueous-phase catalysts

The logical extension to supported aqueous phase catalysts was the preparation of a homogeneous rhodium catalyst dissolved in water and contacted with the hydrocarbon reagents under hydroformylation conditions, using water as the mobile "support". In fact, research was done at Rhône-Poulenc in the late 1970's to the early 1980's and a suitable catalyst, $HRh(CO)[P(m\text{-}sulphophenyl\text{-}Na)_3]_3$, was developed which was adapted for commercial use by Ruhr-chemie in 1984 (*1,42,75,76*). The industrial process is very simple and economic compared to any other setup in operation: high activity, n:iso ratio of up to 97/3, small losses of rhodium and ease of catalyst separation (simple decantation of an aqueous phase).

The newest development in this field is an apparent improvement on the abovementioned bi-phasic system: a single-phase rhodium-ionic phosphine catalyst (*46*). In this system, the rhodium complex is soluble in hydrocarbon reactants but, after reaction, can be induced to separate out as a polar phase by as simple a mechanism as cooling the reaction medium down (although more often a water-solubilizing agent is added). The significance of this is that, unlike the bi-phasic system mentioned above which is restricted to low molecular weight alkenes with low water solubility, the single-phase catalyst can be used in the hydroformylation of less volatile olefins such as octene, dodecene and styrene. Union Carbide have carried out runs on an experimental unit using this catalyst (*46*) but an industrial-scale process does not appear to have been developed yet.

(Water-soluble cobalt catalysts do not appear to have been studied as extensively as rhodium.)

1.8. AIM OF THIS PROJECT

The aim of this project is to form a cobalt complex encapsulated within the supercages of zeolite Y for use as a hydroformylation catalyst. The intention is that the cobalt catalyst will still function in a similar way to its homogeneous equivalent in terms of activity and selectivity but will be much easier to separate from the reaction medium after the reaction is complete. Both rhodium and cobalt are known to be very active catalysts for hydroformylation, as previously mentioned, and were the two catalysts considered for this

project.

Much research has been done on encapsulating rhodium within zeolite Y without much success. Since rhodium is so expensive, even losses on the level of parts per billion can make a process not economically viable. In other words, any rhodium-zeolite hybrid must result in a catalyst with no leaching whatsoever and this is a very stringent, maybe even impossible, requirement to fulfill.

Cobalt complexes encapsulated in zeolites have been reported in the literature (*7,31*) and appear to be very successful. However, these complexes are oxygen-binders; cobalt hydroformylation catalysts have not been reported. Because of this as well as the fact that cobalt is much cheaper than rhodium (*77*), it was decided to carry out research on encapsulating cobalt as a hydroformylation catalyst.

An active and stable catalyst which is used for hydroformylation is dicobalt octacarbonyl ($Co_2(CO)_8$) reacted with a monodentate tertiary phosphine, PR_3 (R = alkyl or phenyl) or a multidentate phosphine. The method envisaged for encapsulation involved reacting $Co_2(CO)_8$ with phosphines inside the zeolite cages and it was decided to use solvent impregnation to achieve encapsulation, ie. solutions of the phosphine and $Co_2(CO)_8$ were added consecutively to a sample of zeolite Y at room temperature to produce the impregnated zeolite catalysts.

It was decided to use both a monodentate tertiary phosphine (ethyldiphenylphosphine, PPh_2Et) and a bidentate phosphine (1,2-bisdiphenylphosphino(ethane), DPPE). The reason for trying a bidentate phosphine is as follows. Hydroformylation conditions involve a high partial pressure of CO at high temperature which can shift the equilibrium shown in equation (1) (see Section 1.5.3.) so as to produce unsubstituted cobalt carbonyl and free phosphine ligand. The method of encapsulation of the cobalt complex within the zeolite requires the substituted cobalt carbonyl complex, so if the phosphine is removed, both phosphine and cobalt carbonyl can leach out of the zeolite. It was envisaged that the "double bite" of the DPPE on cobalt could possibly ensure that at least one of the phosphorus atoms in the DPPE remains attached to cobalt at all times, thereby retaining the "mast" of the "ship-in-a-bottle".

CHAPTER 2

Experimental procedures

2. EXPERIMENTAL PROCEDURES

In this project, five batches of impregnated zeolite catalyst were produced. Two batches of zeolite were impregnated with about 4.5% cobalt by mass and are subsequently referred to as "high-cobalt catalysts" or 4ph/co and 4pp/co in this thesis; the other three batches of zeolite were impregnated with about 0.1%-0.2% cobalt and are subsequently referred to as "low-cobalt catalysts" or 0.2ph/co, 0.2co/ph and 0.2pp/co (see p47 and p52 for code definitions).

2.1. ANALYTICAL EQUIPMENT

2.1.1. Gas Chromatograph (GC)

The GC used for analysis of solutions was a Varian 3400 with a heated, on-line, ultrabore injector and a flame ionization detector. The integrator was a Hewlett Packard 3396 Series II. The column installed was a 50m PONA column with an internal diameter of 0.2 mm and a crosslinked, methylsilicone gum as stationary phase.

Only liquid samples were analysed and were prepared by mixing about 2ml of sample solution with 1ml of acetone in a small sample vial. 1.0μl of sample was injected into the column using a 25μl Hamilton #802 microliter syringe. The injection procedure used was described in the Varian 3000 Series Gas Chromatograph operator's manual and involved the following:

- Flush the syringe with acetone
- Expel acetone, then carefully retract plunger in air to the 1.0μl mark; a small amount of acetone is present in the syringe due to needle holdup
- Submerge needle tip into the sample solution and slowly draw a few microliters of sample into the syringe
- Remove the syringe needle from the sample solution and expel sample until the plunger reaches the 2μl mark
- Retract the syringe plunger in air to pull the sample load fully into the body of the syringe
- Insert needle of syringe fully into the injector, inject the sample and quickly remove needle

The injector and detector were held at 300°C and the GC temperature program used for all samples was as follows:

- 60°C for 20 minutes
- ramp up to 250°C at 10°C per minute
- hold at 250°C for 4 minutes

2.1.2. Infrared spectrophotometer (IR)

The infrared spectrophotometer used for analysis of both liquid and solid samples was a Perkin-Elmer Paragon 1000 FT-IR machine. Liquid samples were analysed in a cell consisting of two sodium chloride plates. Zeolite samples and certain solid complexes were analysed as solid discs. The solid sample was ground up with KBr using a pestle and mortar, pressed into a 10mm disc using a press with a pressure of 10-12 tons per square foot, then mounted in a plastic frame for analysis. All samples were analysed over the range 4000-400 cm^{-1}; the region 2200-1700 cm^{-1} of all IR spectra was reported to show the carbonyl stretching frequency range in greater detail. The resolution used was 2.0 cm^{-1} and the minimum peak intensity recognised by the machine was 2.00 absorbance units.

2.1.3. Atomic Absorption spectrometer (AA)

The spectrometer used for atomic absorption (AA) analyses was a Varian SpectraAA-30 with a DS-15 Data Station. Solutions of dissolved zeolite samples were prepared as described in Section 2.4.4. and were analysed to determine the cobalt loading on the zeolite samples.

2.1.4. BET equipment

The BET machine used to dehydrate certain zeolite samples was an ASAP 2000 Chemi System and is shown in **Figure 2.1**. The dehydration ports are shown on the left of the figure; in the picture are two flasks already fitted into the ports and the heating mantles have been placed around the bulbs of the flasks. Vacuum is drawn by a 2-stage mechanical pump and the heating mantles are glass-wool lined bags which are placed over the bulb of the flasks

containing the sample to be dehydrated.

2.1.5. Nuclear Magnetic Resonance spectrometer (NMR)

^{31}P NMR spectra were recorded on a Varian VXR-200 with a switchable probe and recording frequency of 80 MHz. Phosphoric acid (H_3PO_4) was used as internal reference standard and chemical shifts were reported in ppm, downfield of phosphoric acid (δ = 0.00 ppm)

2.1.6. Microscope for melting point analysis

Melting points of complexes were determined on a Kofler hotstage microscope (Reichert Thermovar) and are uncorrected.

2.2. EXPERIMENTAL APPARATUS

2.2.1. Reaction vessel

The reaction vessel was a stainless steel autoclave with internal dimensions 9cm depth by 7cm diameter ($\approx$350cm^3) (see **Figure 2.2**). The pressure relief valve was set to crack at about 110 bar. During the experimental runs, the autoclave was lagged with ceramic wool to prevent excess heat loss because the temperature programmer controlled the temperature of the heating mantle and not of the autoclave contents. Heat transfer away from the autoclave lead to considerable differences in temperature between the setpoint of the programmer and the actual temperature inside the reactor (up to 40° C at a setpoint of 200° C with no lagging compared to $\pm$1° C at 180° C with lagging). The cross section of the autoclave (in **Figure 2.2**) only shows the pressure gauge and the pressure relief valve; the autoclave lid also had a needle valve fitted which served as both inlet and outlet port for gas reagent (syngas) and for releasing the pressure if needed. The liquid and/or solid reagents were loaded into the autoclave before the lid was clamped into place. The contents were stirred using a magnetic stirrer and a Teflon-coated magnetic bar, the bar being placed in the autoclave together with the reagents. A heating rate of about 4.5° C/minute was used to obtain the final reaction temperature of 180° C, ie. reaction temperature was reached in about 30-40 minutes.

2.2.2. Glassware used in the washing of zeolites with solvents

Impregnated zeolites were washed under nitrogen with various solvents and the glassware used to carry out this operation is shown in **Figure 2.3**. This setup was used to allow the impregnated zeolite samples to be suction filtered and washed with solvent under an inert atmosphere. The nitrogen was passed into the system via the upper tap and a vacuum was drawn from the lower tap.

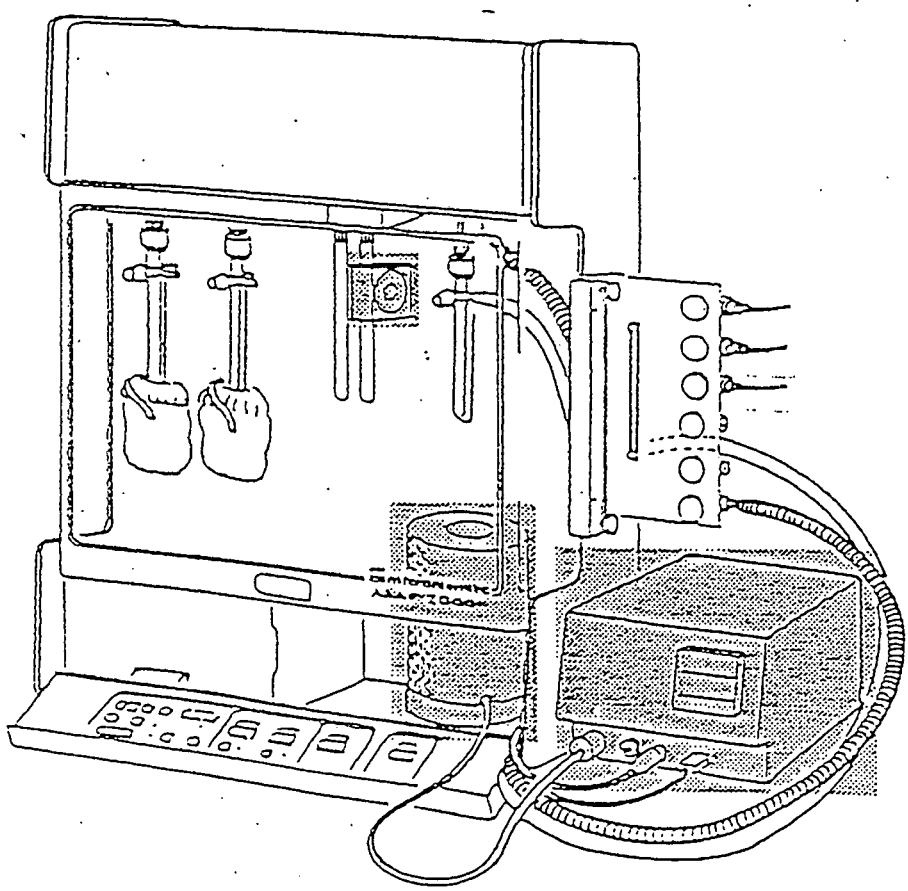

Figure 2.1 : The ASAP 2000 Chemi System

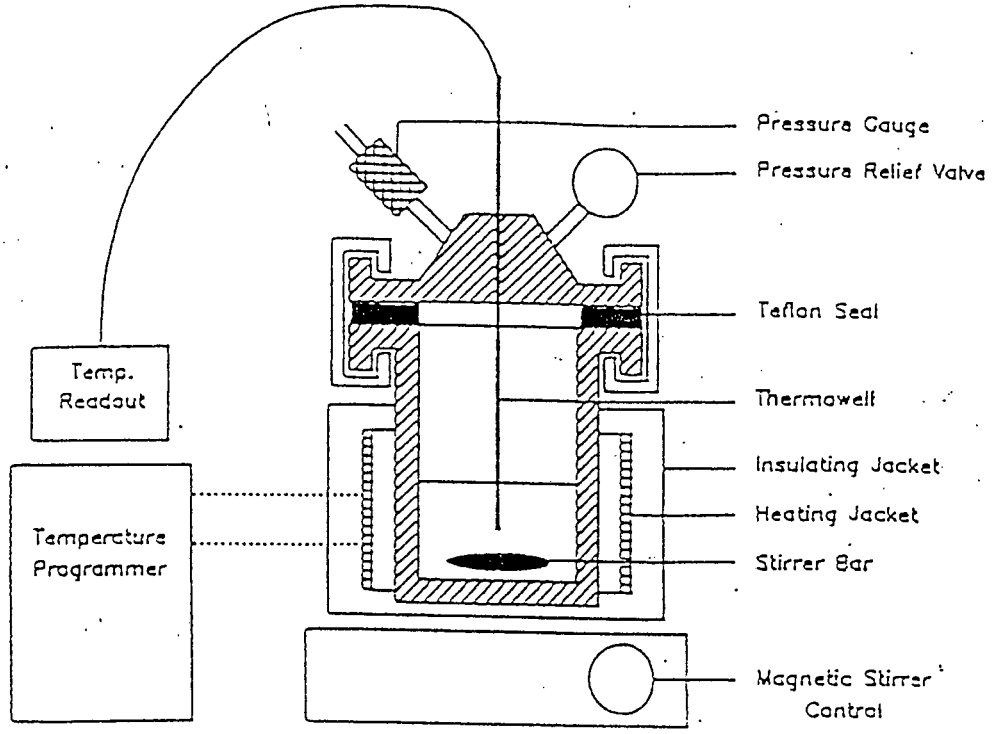

Figure 2.2 : Autoclave used to carry out reactions

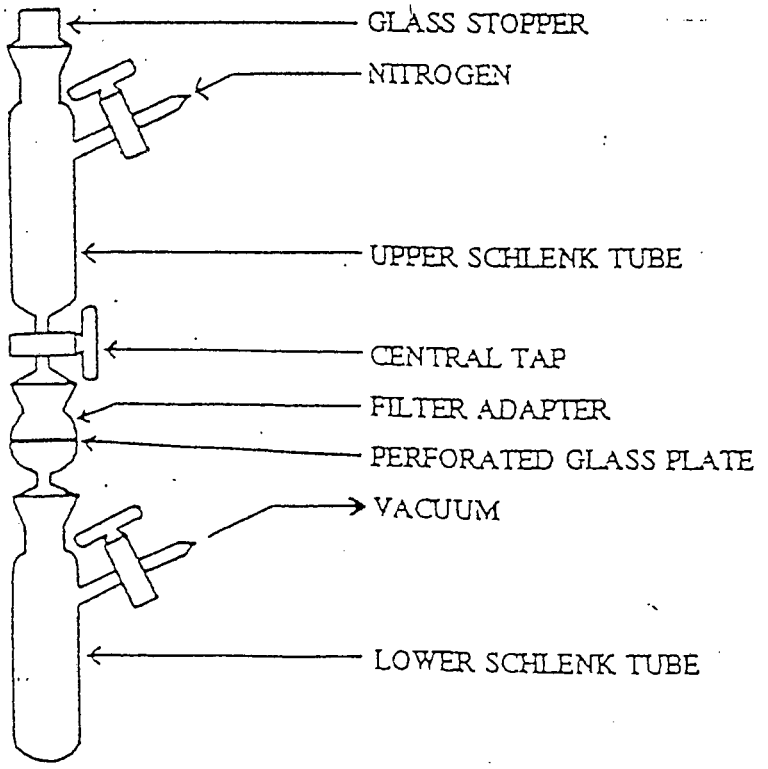

Figure 2.3 : Glassware used to carry out suction-filtered washing of samples under an inert atmosphere

2.2.3. Glassware used in zeolite dehydration

The amounts of impregnated zeolite produced for the high-cobalt batches was smaller than for the low-cobalt batches. The glassware used in the dehydration of the zeolites before impregnation differed for the high-cobalt and low-cobalt batches because it was not practical to produce the larger batches using the BET equipment.

For the high-cobalt batches, the glassware used for dehydrating the zeolite samples consisted of a set of round bottom flasks with a bulb volume of about 10 cm^3 and a neck length of 240mm; these flasks were designed to be used on the BET machine. The flasks were sealed with a stopper that contained a spring-loaded ball valve. The ball was usually in the "closed" position but was depressed by insertion into the BET machine port, exposing the contents of the flask to the contents of the BET machine header. This was helium gas or a vacuum and thus kept the sample in the flask isolated from the atmosphere between the time of the dehydration procedure and eventual use of the sample in an experiment.

For the low-cobalt batches, no specialised glassware was used. The equipment used is mentioned in Section 2.6.1.

2.3 CHEMICALS USED IN EXPERIMENTS

2.3.1. Solvents

The solvents used were the following: n-hexane, dichloromethane, benzene, 1-decanol, and 1-decene. The hexane, dichloromethane and benzene were LAB grade, the 1-decanol and 1-decene were analytical grade. The hexane, benzene and dichloromethane were dried by distillation from sodium wire under nitrogen using benzophenone as an indicator.

2.3.2. Dicobalt octacarbonyl

Dicobalt octacarbonyl, $Co_2(CO)_8$, was purchased from Fluka in Switzerland and stored in a freezer under argon gas. The cobalt carbonyl was not purified in any way before use.

However, the cobalt carbonyl used was always only minimally oxidised, being mainly a dark orange in colour with a minimal purple surface colouring, the purple being the colour of the cobalt oxide.

2.3.3. Tertiary and bidentate phosphines

The phosphines used were the following:

- ethyldiphenylphosphine, PPh_2Et
- 1,2 bis(diphenylphosphino)ethane, DPPE

Both phosphines were obtained from Sigma-Aldrich in the United States.

2.3.4. Reagents used in the hydroformylation reactions

1-Decene of 94%+ purity was purchased from Merck and Sigma-Aldrich. The internal standard used in hydroformylation reactions was hexadecane of 99%+ purity and was also purchased from Merck and Sigma-Aldrich. The syngas used was 2:1 ratio H_2:CO and was purchased from FEDGAS MG, South Africa; the hydrogen and CO used to make up the syngas were grade 5.0 and grade 2.0 respectively.

2.3.5. Zeolite Y

Na-Y zeolite was obtained from AKZO Nobel in The Netherlands with a Si:Al ratio of 5:1.

2.4. GENERAL EXPERIMENTAL PROCEDURES

This section describes all procedures which either do not relate directly to the impregnation of zeolites with cobalt or which are common to both the high-cobalt and low-cobalt zeolites.

2.4.1. Calculation of molecule sizes

As mentioned in Section 1.8., the envisaged encapsulation procedure involved reaction of $Co_2(CO)_8$ with a tertiary phosphine. Both the $Co_2(CO)_8$ and the phosphine must obviously be able to enter the pores of the zeolite structure to allow a possible ship-in-a-bottle synthesis procedure. $Co_2(CO)_8$ has been used frequently for ship-in-a-bottle applications and was found to easily enter the zeolite Y structure via the 7.5Å pores; however, selection of an appropriate phosphine required the calculation of the smallest diameters of a number of phosphines since these were not forthcoming in the literature.

The molecular modelling program BIOSYM was used on a Silicon Graphics machine to build and optimise the structure of various phosphine molecules. For each phosphine molecule, the three-dimensional Cartesian coordinates (x, y and z) of each atom in the molecule was recorded and used in a True Basic computer program to calculate the smallest diameter of the molecule.

2.4.2. Reaction of $Co_2(CO)_8$ with phosphines in solution

$Co_2(CO)_8$ was reacted with DPPE and also with PPh_2Et in solution to compare the compounds formed in solution to those formed in the Na-Y zeolite during the impregnation procedure at room temperature.

2.4.2.1. Reaction of $Co_2(CO)_8$ with PPh_2Et

(i) Preparation of the ionic species, $[Co(CO)_3(PPh_2Et)_2]^+[Co(CO)_4]^-$

The procedure used was adapted from the procedures used by Thornhill and Manning to produce ionic cobalt carbonyl-phosphine complexes (*53*). PPh_2Et (0.30g, 1.40 mmol) was added to dry hexane (15 cm^3) in a round-bottomed flask under a nitrogen atmosphere. Hexane (15 cm^3) was also placed in a beaker and both the round-bottomed flask and the beaker were placed in an ice-bath. When the temperature of the solvent in both containers reached 0-2°C, $Co_2(CO)_8$ (0.50g, 1.46 mmol) was added to the beaker and the solution in the

beaker was then poured into the round-bottomed flask. The flask was left in an ice bath until no more gas was evolved (~15-20 min.). The final solid formed was insoluble in hexane and formed large orange clumps. The supernatant hexane solution was colourless and was decanted out of the flask, leaving the solid behind; the resultant crystals were bright orange platelets which were washed again with hexane. A nitrogen stream was passed over the solid to partially dry it, then the sample was rigorously dried under a vacuum of 0.01mm Hg. The yield was 38.6 mol% based on phosphine (0.20g, 0.27 mmol).

(ii) Preparation of the covalent species, $[Co(CO)_3(PPh_2Et)]_2$

The procedure used was adapted from the procedures used by Manning to produce disubstituted covalent cobalt carbonyl-phosphine complexes (*54*). $Co_2(CO)_8$ (0.43g, 1.26 mmol) was added to dry benzene (40 cm^3) in a two-necked round-bottomed flask together with a Teflon-coated stirrer bar. A nitrogen line was joined to a tap fitted into one neck of the flask and the contents were kept under nitrogen. PPh_2Et (0.54g, 2.52 mmol) was added and the contents refluxed under nitrogen for 3 hours with stirring. The benzene was removed using a rotary evaporator and the resulting dark-brown crystals were washed with hexane. The crystals were then redissolved in benzene and recrystallised by mixing the benzene solution with hexane and placing the flask in a freezer overnight. The solution was suction filtered and the dark brown, needle-like crystals were retrieved from the filter paper. A nitrogen stream was passed over the crystals to partially dry them, then the sample was rigorously dried under a vacuum of 0.01mm Hg. The yield was 28.5 mol% based on phosphine (0.26g, 0.36 mmol).

(iii) Preparation of the covalent species, $[Co_2(CO)_7(PPh_2Et)]$

The procedure used was adapted from the procedures used by Szabó *et al* to produce monosubstituted covalent cobalt carbonyl-phosphine complexes (*51*). $Co_2(CO)_8$ (0.43g, 1.26 mmol) was added to dry benzene (40 cm^3) in a two-necked round-bottomed flask together with a Teflon-coated stirrer bar. A nitrogen line was joined to a tap fitted into one neck of the flask and the contents were kept under nitrogen. PPh_2Et (0.54g, 2.52 mmol) was added and the contents refluxed under nitrogen for 3 hours while being stirred. A large

excess of $Co_2(CO)_8$ (4.00g, 11.72 mmol) was added to the solution and the solution was stirred under carbon monoxide atmosphere (atmospheric pressure) at room temperature for 48 hours. The solution was then passed through an alumina column to chromatographically separate out the different fractions. A mixture of hexane:dichloromethane of 3:1 ratio by volume was used and three fractions were obtained. The first fraction contained unreacted $Co_2(CO)_8$, the second fraction was the desired fraction and the third fraction contained $[Co(CO)_3(PPh_2Et)]_2$. A very viscous black-brown oil was recovered from this second fraction by removal of solvent on a rotary evaporator and partial drying with a stream of nitrogen. The oil was then dried rigorously under a vacuum of 0.01mm Hg. Dark-drown platelets were retrieved in a yield of 19.0 mol% based on phosphine (0.03g, 0.06 mmol); only 5 cm^3 of the final solution was chromatographically columned to isolate the desired product for further analysis and the yield was calculated accordingly.

2.4.2.2. Reaction of $Co_2(CO)_8$ with DPPE

(i) Preparation of the ionic species, $[Co_2(CO)_4(DPPE)_3]^{2+}\{[Co(CO)_4]^-\}_2$

The procedure used was adapted from the procedures used by Thornhill and Manning to produce ionic cobalt carbonyl-phosphine complexes (*53*). DPPE (0.12g, 0.30 mmol) was added to acetone (25 cm^3) in a round-bottomed flask. Acetone (15 cm^3) was also placed in a beaker and both the round-bottomed flask and the beaker were placed in an ice-bath. When the temperature of the solvent in both containers reached 0-2°C, $Co_2(CO)_8$ (0.10g, 0.29 mmol) was added to the beaker and the solution in the beaker was then poured into the round-bottomed flask. The flask was left in the ice bath until no more gas was evolved in the solution. The yellow crystals were then recrystallised from a methanol acetone mixture and isolated by filtration. A nitrogen stream was passed over the crystals to partially dry them, then the sample was rigorously dried under a vacuum of 0.01mm Hg. The yield was 10.0% based on phosphine (0.011g, 0.01 mmol).

(ii) Preparation of the covalent species, $[Co(CO)_2(DPPE)]_2$

This procedure was the same as the procedure used by Pedersen and Robinson to produce

covalent cobalt carbonyl-phosphine complexes (*65*). $Co_2(CO)_8$ (0.23g, 0.68 mmol) was added to dry benzene (50 cm^3) in a two-necked round-bottomed flask together with a Teflon-coated stirrer bar. A nitrogen line was joined to a tap fitted into one neck of the flask and the contents were kept under nitrogen. DPPE (1.10g, 2.76 mmol) was added and the contents refluxed under nitrogen for 3 hours while being stirred. The benzene was removed using a rotary evaporator and the resulting red-brown crystals were redissolved in dichloromethane (30 cm^3) and recrystallised by addition of acetonitrile (20 cm^3). The solution was suction filtered and the red-brown crystals retrieved, washed with hexane and dried using a nitrogen stream. The yield was 92.6% based on $Co_2(CO)_8$ (0.68g, 0.63 mmol).

2.4.3. Ion-exchange modification of zeolite Y

The form of the zeolite used was Na-Y. To get Co-Y, an ion-exchange procedure was carried out to exchange some of the sodium ions with cobalt ions. The procedure followed was that of Yoshida *et al* (*23*) and was used to produce zeolites containing ~3% cobalt by mass.

Na-Y zeolite (10.91g) was placed in a glass autoclave with 200 cm^3 of distilled water and a Teflon-coated stirrer bar and $Co(NO_3)_2 \cdot 6H_2O$ (2.00g, 6.9 mmol) was added to the solution. The solution was stirred using a magnetic stirrer and was refluxed for 11.5 hours. The solution was allowed to stand for 15 hours and then suction filtered. The solid remaining on the filter paper was washed with 1 litre of distilled water and then scraped off into a beaker containing 1 litre of distilled water. This solution was then suction filtered to retrieve the zeolite. The zeolite was placed in a porcelain crucible and dried for 1 hour at 123°C.

2.4.4. AA measurements to determine cobalt loading of zeolite samples

Zeolite samples were analysed using atomic absorption spectroscopy to determine the cobalt loading of the zeolite. This involved dissolving the zeolite with 48% hydrofluoric acid (HF) and then diluting with distilled water. However, the cobalt complexes present on the zeolite (especially the phosphine complexes) were insoluble in both water and HF. The zeolite samples were therefore heated in a furnace in air to oxidise the cobalt complexes which formed cobalt species soluble in water after treatment with HF. The following procedure was

used for both the high-cobalt and low-cobalt zeolites. The amounts of sample given are for the high-cobalt zeolites; for the low-cobalt zeolites, 0.185g of sample was dissolved in HF and diluted up to 50 cm^3.

Zeolites impregnated with $Co_2(CO)_8$ and a phosphine were placed in a number of small (10 cm^3) ceramic crucibles and placed in a furnace at room temperature. The samples were then heated in the furnace according to the following temperature program:

- heat to 200°C over 30 minutes
- maintain at 200°C for 2 hours
- heat to 500°C over 1 hour
- maintain at 500°C for 12 hours

The samples changed colour from yellow or orange to light blue after this heating procedure. The samples (0.015g) were dissolved in HF (5 cm^3) in a number of plastic beakers (50 cm^3) and then diluted up to 100 cm^3 in a number of plastic volumetric flasks. The contents of the flasks were then analysed using AA to determine the concentration of cobalt in solution, enabling the calculation of the mass of cobalt present on the zeolite sample of weight 0.015g ie. the mass % cobalt loading could then be calculated. The exact formulae and procedure used in the mass percent calculation is described in **APPENDIX A.** The mass percent loadings for all pertinent zeolite samples are listed in a **Table 3.4** and **Table 3.11** in Chapter 3.

2.4.5. Washing of impregnated zeolites with solvents

The impregnated Na-Y zeolites were washed a number of times with different solvents. A new batch of zeolite was used for each set of washings with a particular solvent. 1g of catalyst was used in each set of washings and the following solvents were used: hexane, dichloromethane, 1-decanol and 1-decene.

The procedure for washing each sample was the following:

- place a new piece of filter paper on the perforated glass plate in the filter adapter and assemble the apparatus, as shown in **Figure 2.3**
- flush the apparatus with nitrogen
- moisten the filter paper with solvent and place 1g of catalyst sample on the filter paper
- place 20 cm^3 of solvent in the top Schlenk tube while keeping the centre tap closed (see **Figure 2.3**)
- seal the top Schlenk tube with a glass stopper, pass nitrogen into the top Schlenk tube and draw a vacuum on the bottom Schlenk tube
- open the centre tap to deposit the solvent onto the filter paper and allow the aliquot of solvent to filter through the zeolite sample into the bottom Schlenk tube
- remove the solution from the lower Schlenk tube and carry out an IR analysis of this solution
- repeat the washing of the sample with 20 cm^3 aliquots of solvent until no carbonyl stretching frequencies are visible in the IR spectrum of the aliquot which has passed through the zeolite sample

2.5. EXPERIMENTAL PROCEDURES PERTAINING TO HIGH-COBALT CATALYSTS

2.5.1. Dehydration of zeolite prior to impregnation

About 4g of white Na-Y zeolite was heated in an oven at 200°C for 2 hours in air at atmospheric pressure to remove physisorbed water and then placed hot into a 10 cm^3 flask and sealed with a self-sealing stopper. The flask was then inserted into the BET machine port and a heating mantle placed around the bulb. The sample was slowly evacuated until 0.6-0.8 mm Hg pressure was reached and then evacuated quickly while heating the sample to 250°C over the period of an hour. The sample was evacuated for at least six hours at 250°C, the criteria for ceasing the evacuation being that the pressure in the flask dropped below 0.01 mm Hg.

2.5.2. Impregnation of zeolites with $Co_2(CO)_8$ and ligands

Two sets of impregnations were carried out at room temperature:

- Na-Y impregnated with PPh_2Et followed by $Co_2(CO)_8$: 4ph/co
- Na-Y impregnated with DPPE followed by $Co_2(CO)_8$: 4pp/co

2.5.2.1. Impregnation of Na-Y with PPh_2Et followed by $Co_2(CO)_8$ (4ph/co)

White, dehydrated Na-Y zeolite (11.69g) was placed in a 100 cm^3 two-necked round bottom flask containing dry hexane (30 cm^3) together with a Teflon-coated stirrer bar. A nitrogen line was joined to a tap fitted into one neck of the flask and the contents were kept under a flow of nitrogen. PPh_2Et (4.02g, 18.8 mmol) was added in 4 equal portions over a period of 10 minutes. The second neck of the flask was then closed by a glass stopper and the contents stirred with a magnetic stirrer for 7 hours under nitrogen at room temperature. $Co_2(CO)_8$ (1.59g, 4.7 mmol) was dissolved in dry hexane (30 cm^3) and added over a period of 10 minutes to the contents of the flask. The maximum cobalt loading possible was thus 4.7% by mass. The P:Co ratio used was 2:1 (18.8 mmoles P vs 9.4 mmoles Co; there are 2 mmoles Co per mmole $Co_2(CO)_8$). The flask was then resealed and the contents stirred under nitrogen for 2 days at room temperature to allow diffusion of the cobalt carbonyl throughout the zeolite crystals. After this period, the zeolite had turned an orange-brown colour, while the solution was colourless. The impregnated zeolite was then separated from the solution by centrifuging the flask contents and was placed in a round-bottom flask. The zeolite was partially dried by blowing a stream of nitrogen into the flask. The flask was then evacuated to remove as much of the solvent as possible and weighed periodically throughout the evacuation procedure. Evacuation was stopped when the flask attained a constant weight. The final impregnated zeolite was a light mustard yellow in colour and about 14g was ultimately obtained.

2.5.2.2. Impregnation of Na-Y with DPPE followed by $Co_2(CO)_8$ (4pp/co)

White, dehydrated Na-Y (11.73g) was placed in a 100 cm^3 two-necked round bottom flask containing dry benzene (30 cm^3) together with a Teflon-coated stirrer bar. A nitrogen line was joined to a tap fitted into one neck of the flask and the contents were kept under a flow of nitrogen. DPPE (6.08g, 15.3 mmol) was added, the second neck closed by a glass stopper and the contents stirred with a magnetic stirrer for 6 hours under nitrogen at room temperature. $Co_2(CO)_8$ (2.57g, 7.5 mmol) was dissolved in dry benzene (30 cm^3) and added over a period of 10 minutes to the contents of the flask. The maximum cobalt loading possible was thus 7.6% by mass of cobalt on zeolite; the P:Co ratio used was 2:1. The flask was then resealed and the contents stirred under nitrogen at room temperature for 4 days to allow diffusion of the cobalt carbonyl throughout the zeolite crystals. After this period, the zeolite had turned an orange-brown colour. The impregnated zeolite was then separated from the solution by centrifuging the flask contents and placed in a round-bottom flask. The zeolite was partially dried by blowing a stream of nitrogen into the flask. The flask was then evacuated to remove as much of the solvent as possible and weighed periodically throughout the evacuation procedure. Evacuation was stopped when the flask attained a constant weight. The final impregnated zeolite was orange in colour and about 19g was ultimately obtained.

2.5.3. Hydroformylation reactions using homogeneous catalysts

Two reactions were carried out with a homogeneous $Co_2(CO)_8$/ligand catalyst (one with ligand = DPPE, one with ligand = PPh_2Et) for comparison of product distribution and activity with the impregnated zeolite catalysts. The conditions of the reactions are shown in **Table 2.1**.

A typical run was carried out as follows. The 1-decene and hexadecane were placed in the autoclave which was then flushed with nitrogen for about 5 minutes. The $Co_2(CO)_8$ and the appropriate phosphine were added while keeping the contents under nitrogen and the autoclave was then sealed. The autoclave was placed in the heating mantle and heated to operating temperature before the syngas was added. After reaching operating temperature, the autoclave was pressurised with syngas to the operating pressure and then sealed, ie. the autoclave was charged with a specific amount of syngas and the pressure was not maintained throughout

reaction. The pressure inside the autoclave was monitored over the five hour reaction period to monitor the extent of reaction. After five hours, the autoclave was removed from the heating mantle to cool down to room temperature and then depressurised. The liquid reaction mixture was analysed using infrared spectroscopy and gas chromatography.

Table 2.1 : Operating conditions for homogeneously-catalysed reactions (high cobalt system)

OPERATING CONDITION	AMOUNT
Reaction time	5 hours
Reaction temperature	180° C
Initial reaction pressure (not maintained)	80 bar
Syngas	2:1 ratio of H_2:CO
Olefin reagent	20g 1-Decene
Internal standard	5.2g Hexadecane
Amount of cobalt	0.04g
P:Co ratio	2:1

2.5.4. Single hydroformylation reactions using zeolite catalysts

Four reactions were carried out using the following catalysts:

- 4ph/co
- 4pp/co
- Na-Y zeolite ion-exchanged to form Co-Y
- pure, non-impregnated Na-Y zeolite sample as a blank run

The conditions of the reactions are given in **Table 2.1**, except that about 1g of impregnated zeolite was used as catalyst in each run (contained about 0.04g cobalt). Also, the typical

procedure followed for a run is analogous to that given in Section 2.5.3. The liquid product solution was analysed using infrared spectroscopy and gas chromatography. The zeolite remaining in the autoclave was washed with hexane to remove all product solution and any cobalt catalyst that had possibly leached out of the zeolite (ie. on the surface of the zeolite crystals) and analysed using infrared spectroscopy.

2.5.5. Reactions using impregnated zeolites under hydroformylation conditions with decane (no alkene reagent)

Reactions were carried out using 4ph/co and 4pp/co. The conditions of the reactions are given in **Table 2.1**. These reactions were carried out to see what the effect of the reaction temperature and pressure was on the catalyst in the absence of alkene reagent. Essentially, the operating procedure is identical to that described in Section 2.5.4. except that 1-decene was replaced with an equivalent amount of n-decane.

2.5.6. Recycling of impregnated zeolite catalysts

Each "set" of reactions carried out with a zeolite catalyst involved three consecutive hydroformylation batch reactions in which the catalyst sample used in one run was "recycled", ie. the exact same sample was used for each of the three consecutive reactions. Two "sets" of reactions were carried out with each of 4ph/co and 4pp/co.

The two sets were not duplicate runs. The second of the two sets of runs differed from the first in one important respect: an amount of phosphine (PPh_2Et for 4ph/co and DPPE for 4pp/co) was added to the **first run** of the set such that the moles of phosphorus added to the solution via the phosphine was equal to twice the moles of cobalt **initially present** on the impregnated zeolite catalyst (ie. before the first run in a set was carried out). The reason for adding extra phosphine was similar to the reason for adding excess phosphine to a homogenously-catalysed system. Hydroformylation at relatively low CO partial pressures (lower than 100 bar at 200°C) decomposes $Co_2(CO)_8$, so excess phosphine is added to ensure the formation of the more stable phosphine-substituted cobalt complex (see Section 1.5.3.). Adding the extra phosphine to the system was carried out to check if the activity of the

cobalt-zeolite catalyst was actually compromised by decomposition of the "ship-in-a-bottle" complex in the zeolite if no extra phosphine was added.

After completion of each reaction in a set, the liquid reagent/product mixture was removed for analysis leaving the zeolite behind in the autoclave. The zeolite was washed with octane to remove any residual liquid from the previous batch and a new batch of reagent (1-decene and hexadecane) was added to the autoclave. The next reaction was then carried out. The conditions and procedure for each reaction were exactly the same as mentioned in Section 2.5.4.

2.6. EXPERIMENTAL PROCEDURES PERTAINING TO LOW-COBALT CATALYSTS

2.6.1. Dehydration of zeolite prior to impregnation

About 80g of white Na-Y zeolite was placed in three ceramic crucibles and placed in a furnace at room temperature. The furnace was then heated up according to the following temperature program:

- heat to 100°C over 30 minutes, maintain at 100°C for 1 hour
- heat to 200°C over 30 minutes, maintain at 200°C for 1 hour
- heat to 300°C over 30 minutes, maintain at 300°C for 1 hour
- heat to 400°C over 30 minutes, maintain at 400°C for at least 12 hours

After this, the zeolite was allowed to cool for 15 minutes in a desiccator before being transferred to a 1 litre Buchner flask; the flask was flushed continuously with nitrogen during the transfer. The flask had been sealed and weighed before the transfer and was sealed and weighed after transfer to obtain the mass of dry zeolite present in the flask.

2.6.2. Impregnation of zeolites with $Co_2(CO)_8$ and ligands

Three sets of impregnations were carried out at room temperature:

- Na-Y impregnated with PPh_2Et followed by $Co_2(CO)_8$: 0.2ph/co
- Na-Y impregnated with $Co_2(CO)_8$ followed by PPh_2Et : 0.2co/ph
- Na-Y impregnated with DPPE followed by $Co_2(CO)_8$: 0.2pp/co

2.6.2.1. Impregnation of Na-Y with PPh_2Et followed by $Co_2(CO)_8$ (0.2ph/co)

White, dehydrated Na-Y zeolite (74.11g) was placed in a 1 litre Buchner flask. Dry hexane (750 cm^3) was added to the flask together with a Teflon-coated stirrer bar. A nitrogen line was joined to the side arm of the Buchner flask and the contents were kept under a flow of nitrogen. PPh_2Et (1.11g, 5.2 mmol) was added over a period of 1 minute, the neck of the flask sealed with a plastic stopper and the contents stirred with a magnetic stirrer for about 20 hours under nitrogen. $Co_2(CO)_8$ (0.45g, 1.3 mmol) was dissolved in dry hexane (100 cm^3) and added over a period of 2-3 minutes to the contents of the flask. The maximum cobalt loading possible was thus 0.2% by mass of cobalt on zeolite; the P:Co ratio used was 2:1. The flask was then resealed and the contents stirred under nitrogen for about 20 hours. After this period, the zeolite had turned a light yellow-green colour, while the solution was colourless. Most of the supernatant solution was then removed by pipette from the flask and the remaining wet zeolite was dried using a stream of nitrogen until the zeolite could flow as a powder. The zeolite was then placed in a round-bottom flask and the flask evacuated at room temperature to remove as much of the solvent as possible. The flask was weighed periodically throughout the evacuation procedure and evacuation was stopped when the flask attained a constant weight. The final impregnated zeolite was a white-grey colour with a green tint and about 86g was ultimately obtained. It should be noted that the total weight obtained at the end of impregnation is larger than expected if the masses of the components are added up (74.11g+1.11g+0.45g=75.67g). This was probably due to some of the solvent (hexane) being retained on the zeolite. This solvent could only be removed under vacuum together with heating of the sample. This was undesirable in case the cobalt species present on the zeolite decomposed under vacuum and raised temperatures. In all the other cases of

impregnation with 0.2% cobalt loading, the final batch of zeolite weighed more than the individual components and it was assumed that adsorbed solvent was the cause.

2.6.2.2. Impregnation of Na-Y with $Co_2(CO)_8$ followed by PPh_2Et (0.2co/ph)

White, dehydrated Na-Y zeolite (75.71g) was placed in a 1 litre Buchner flask. Dry hexane (600 cm^3) was added to the flask together with a Teflon-coated stirrer bar. A nitrogen line was joined to the side arm of the Buchner flask and the contents were kept under a flow of nitrogen. $Co_2(CO)_8$ (0.448g, 1.3 mmol) was dissolved in dry hexane (200 cm^3) and added over a period of 2-3 minutes to the contents of the flask. The neck of the flask was sealed with a plastic stopper and the contents stirred with a magnetic stirrer for 15 minutes under nitrogen. The period of stirring was shorter than the previous case because $Co_2(CO)_8$ alone is known to decompose fairly quickly on zeolite Y (*11*,*33*). The maximum cobalt loading possible was thus 0.2% by mass of cobalt on zeolite. PPh_2Et (1.12g, 5.2 mmol) was then added over a period of 1 minute (ie. P:Co ratio used was 2:1). The flask was then resealed and the contents stirred under nitrogen for about 20 hours. After this period, the zeolite had turned a light yellow-green colour, while the solution was colourless. Most of the supernatant solution was then removed by pipette from the flask and the remaining wet zeolite was dried using a stream of nitrogen until the zeolite could flow as a powder. The zeolite was then placed in a round-bottom flask and the flask evacuated at room temperature to remove as much of the solvent as possible. The flask was weighed periodically throughout the evacuation procedure and evacuation was stopped when the flask attained a constant weight. The final impregnated zeolite was a white-grey colour with a green tint and about 86g was ultimately obtained.

2.6.2.3. Impregnation of Na-Y with DPPE followed by $Co_2(CO)_8$ (0.2pp/co)

White, dehydrated Na-Y zeolite (76.38g) was placed in a 1 litre Buchner flask. Dry benzene (500 cm^3) was added to the flask together with a Teflon-coated stirrer bar. A nitrogen line was joined to the side arm of the Buchner flask and the contents were kept under a flow of nitrogen. DPPE (1.04g, 2.6 mmol) was dissolved in benzene (100 cm^3) and added over a period of 1 minute, the neck of the flask sealed with a plastic stopper and the contents stirred

with a magnetic stirrer for about 20 hours under nitrogen. $Co_2(CO)_8$ (0.443g, 1.3 mmol) was dissolved in dry benzene (100 cm^3) and added over a period of 2-3 minutes to the contents of the flask. The maximum cobalt loading possible was thus 0.2% by mass of cobalt on zeolite; the P:Co ratio used was 2:1. The flask was then resealed and the contents stirred under nitrogen for about 20 hours. After this period, the zeolite had turned a light yellow, while the solution was colourless. Most of the supernatant solution was then removed by pipette from the flask and the remaining wet zeolite was dried using a stream of nitrogen until the zeolite could flow as a powder. The zeolite was then placed in a round-bottom flask and the flask evacuated to remove as much of the solvent as possible. The flask was weighed periodically throughout the evacuation procedure and evacuation was stopped when the flask attained a constant weight. The final impregnated zeolite was a light yellow in colour and about 87g was ultimately obtained.

2.6.3. Hydroformylation reactions using homogeneous catalysts

A series of hydroformylation reactions were carried out with homogeneous $Co_2(CO)_8$/ligand catalysts; some of the runs were with DPPE as ligand while others were with PPh_2Et as ligand. The conditions of the reactions are shown in **Table 2.2**.

These runs were carried out for three reasons:

1. Repetition of runs using the same catalyst to show the reproducibility of the experimental setup.
2. For comparison of product distribution and activity with the impregnated zeolite catalysts.
3. Varying of the phosphorus to cobalt ratio (P:Co ratio) in the system to see the effect on catalyst activity and product distribution.

A typical run was carried out as follows. The 1-decene and hexadecane were placed in the autoclave which was then flushed with nitrogen for 5 minutes. The $Co_2(CO)_8$ and the appropriate phosphine were added while keeping the contents under nitrogen and the autoclave was then sealed. The autoclave was pressurised to 52 bar with syngas at room temperature (equivalent to about 79 bar at 180°C) and the inlet valve closed. The autoclave was placed

in the heating mantle and heated to operating temperature (about 30 minutes) before the inlet valve was again opened, this time to a pressure of 80 bar syngas and this pressure was maintained over the reaction period of a further two hours. After two hours, the autoclave was removed from the heating mantle to cool down to room temperature and depressurised. The liquid reaction mixture was then analysed using infrared spectroscopy and gas chromatography.

Table 2.2 : Operating conditions for homogeneously-catalysed reactions (low cobalt systems)

OPERATING CONDITION	AMOUNT
Reaction time	2 hours
Reaction temperature	180°C
Reaction pressure	80 bar (maintained)
Syngas	2:1 ratio of H_2:CO
Olefin reagent	30g 1-Decene
Internal standard	15g Hexadecane
Amount of cobalt	0.01g
P:Co ratio	2:1, 5:1 and 10:1

2.6.4. Recycling of impregnated zeolite catalysts

Two "sets" of reactions were carried out with each of the three low-cobalt catalysts (0.2ph/co, 0.2co/ph and 0.2pp/co). Each "set" involved a series of three consecutive hydroformylation reactions in which the zeolite sample used in one run was "recycled", ie. the exact same sample was used for three reactions in succession. The conditions of the reactions are given in **Table 2.2**. Essentially, the operating procedure is identical to that described in Section 2.6.3. except that 5g of impregnated zeolite was used instead of $Co_2(CO)_8$ and phosphine. This 5g of impregnated zeolite contained the same mass of cobalt as was added to the system

in the homogeneously-catalysed cases (ie. 0.01g cobalt)

For each of the three catalysts, the second of the two sets of reactions differed from the first in one important respect : an amount of phosphine (PPh_2Et for 0.2ph/co and 0.2co/ph and DPPE for 0.2pp/co) was added at the start of **each reaction of the set** such that the moles of phosphorous added to the solution via the phosphine was equal to twice the moles of cobalt present on the impregnated zeolite catalyst before the first reaction was carried out. Note that the absolute amount of phosphine added was the same for each reaction in a set. Also note that this procedure is different to the procedure followed with the high-cobalt catalysts, 4ph/co and 4pp/co. In the case of the high-cobalt catalysts, the phosphine was only added to the first reaction (see Section 2.5.6.).

After each reaction was complete, the liquid reagent/product mixture together with the zeolite was removed, placed into two 40 cm^3 centrifuge tubes and centrifuged to separate the zeolite and the liquid. The supernatant solution was removed for analysis by IR and GC while the zeolite, still wet with a small amount of liquid, was retained in the centrifuge tubes. The appropriate amount of 1-decene for another reaction was added to the centrifuge tubes and the contents mixed together so that the zeolite was suspended in the 1-decene. The appropriate amount of hexadecane was added to the autoclave together with the contents of the two centrifuge tubes and the autoclave flushed with nitrogen. If the set involved adding extra phosphine to the system, the phosphine was weighed out into the autoclave at this stage. The autoclave was then sealed and the next reaction was carried out with the conditions and procedure exactly the same as mentioned above.

At the end of a set of reactions, the zeolite was analysed by IR to detect cobalt carbonyl species and analysed by AA to determine cobalt loading.

CHAPTER 3

Results

3. RESULTS

3.1. CALCULATION OF MOLECULE SIZES

As mentioned in Section 2.4.1., the smallest cross-sectional diameters of various molecules were calculated using the computer modelling package BIOSYM and a True Basic computer program. The calculated diameters of the molecules are listed in **Table 3.1.**

Table 3.1 : Smallest molecular diameters calculated for various tertiary and bidentate phosphines and cobalt carbonyl complexes

	PHOSPHINE/COMPLEX	SMALLEST CROSS-SECTIONAL DIAMETER (Å)
1	Na-Y pore	7-8
	Na-Y supercage diameter	13
2	$Co_2(CO)_8$	3.7
3	$PPhMe_2$	5.4
	$HCo(CO)_3(PPhMe_2)$	7.2
4	PPh_2Me	6.8
	$HCo(CO)_3(PPh_2Me)$	8.1
5	$PPhEt_2$	6.3
	$HCo(CO)_3(PPhEt_2)$	7.8
6	PPh_2Et	7.5
	$HCo(CO)_3(PPh_2Et)$	8.4
7	DPPE	10.1
8	P-n-Bu_3	7.8
9	PPh_3	9.8

The reason for considering this particular subset of the numerous tertiary alkyl and phenyl phosphines was that these phosphines were immediately available in the laboratory.

For each of the first four phosphines (listed 3-6), the size of one other complex is also listed. This complex is formed when $Co_2(CO)_8$ and the phosphine react with each other under hydroformylation conditions and is the proposed active catalytic species which takes part in the catalytic cycle forming alcohols and aldehydes from alkenes (see **Figure 1.6** and **Figure 1.7** in Chapter 1).

The criterion for selecting a phosphine to use in impregnating zeolite Y was that the phosphine was small enough to fit through the pores of zeolite Y while the cobalt carbonyl hydride complexes were too large to do so. PPh_2Me and PPh_2Et, as shown in **Table 3.1**, fit this criterion. PPh_2Et, was selected over PPh_2Me because its hydride complex was calculated to be larger. This fact is important in trying to ensure encapsulation: the pores of zeolite Y are usually 7.5Å, but atomic vibrations can result in oscillation of the pore sizes between 7-8Å.

A very important point to note is that DPPE is too large to enter the pores of the zeolite so the question might arise as to why this phosphine was used. The DPPE molecule is different to the monodentate phosphines because it should have a certain flexibility in the ethyl chain linking the two phosphorus atoms, unlike the monodentate phosphines which are closer to molecular "balls". Thus, although the smallest diameter of a rigid DPPE molecule is too large to enter the pores, flexibility in the ethyl chain might allow it to diffuse into the cages. The reason for using DPPE rather than some other bidentate phosphine was because DPPE is also a phosphine in which the phosphorus atoms each have a similar environment to those in PPh_2Et, making it a bidentate analogy to PPh_2Et. Finally, the fact that it is a bidentate, chelating phosphine was hoped to have a beneficial effect on stabilising the substituted cobalt carbonyl species present under hydroformylation and would possibly improve the effectiveness of encapsulation if it did manage to diffuse into the zeolite cages.

3.2. REACTIONS OF $Co_2(CO)_8$ WITH TERTIARY OR BIDENTATE PHOSPHINES IN SOLUTION

The reaction of $Co_2(CO)_8$ with PPh_2Et and with DPPE in solution were investigated to compare the compounds formed in solution to those formed in the Na-Y zeolite during the impregnation procedure. **Table 3.2** shows the colour, melting point, ^{31}P NMR peaks and elemental analyses for all the compounds synthesized. **Table 3.3** lists the ν(CO) bands in the infrared spectra of the compounds synthesized and also lists, for comparison, the ν(CO) bands of pertinent compounds reported in the literature.

3.2.1. Reaction of $Co_2(CO)_8$ with PPh_2Et

Complexes formed from the reaction of $Co_2(CO)_8$ and tertiary alkyl and phenyl phosphines have been reported extensively in the literature, as mentioned in Section 1.6.4.. However, PPh_2Et as a ligand does not seem to have been so reported. Thus, all the synthesized complexes have been characterised by IR, melting point, elemental analysis, colour and ^{31}P NMR.

The ^{31}P NMR spectrum of PPh_2Et is shown in **Figure 3.1**. The large peak at -11.1 ppm is of PPh_2Et while the peak at a shift of 34.3 ppm is of the phosphine oxide. This characteristic NMR spectrum of PPh_2Et was used to identify any unreacted PPh_2Et present in any other of the samples analysed by ^{31}P NMR. An expansion of the region -10.4 ppm to -12.2 ppm is also included on the right hand side of the spectrum. This was a standard procedure used to report NMR spectra when the main spectrum did not show all peaks clearly and separately.

3.2.1.1. Reaction of $Co_2(CO)_8$ with PPh_2Et at 0° C under a nitrogen atmosphere

The reaction of $Co_2(CO)_8$ with PPh_2Et was carried out in hexane at ca. 0° C under nitrogen. This gave the complex $[Co(CO)_3(PPh_2Et)_2]^+[Co(CO)_4]^-$ **[1]** in 39% yield as orange crystals. The infrared spectrum of **[1]** is shown in **Figure 3.2** and the ^{31}P NMR spectrum is shown in **Figure 3.3**. The theoretical molar mass of **[1]** was calculated to be 742.5 $g.mol^{-1}$ and from this, the calculated mass percent distribution was calculated to be C: 56.6%%, H: 4.1%.

Elemental analysis gave C: 56.5%, H: 4.2%.

3.2.1.2. Reaction of $Co_2(CO)_8$ with PPh_2Et in benzene refluxed under a nitrogen atmosphere

The reaction of $Co_2(CO)_8$ with PPh_2Et was carried out in refluxing benzene under nitrogen. This gave the complex $[Co(CO)_3(PPh_2Et)]_2$ **[3]** in 29% yield as dark brown crystals. The infrared spectrum of **[3]** is shown in **Figure 3.4** and the ^{31}P NMR spectrum is shown in **Figure 3.5**. The molar mass of **[3]** was calculated to be 714.4 $g.mol^{-1}$ and from this, the calculated mass percent distribution was calculated to be C: 57.1%, H: 4.2%. Elemental analysis gave C: 57.5%, H: 4.5%.

3.2.1.3. Reaction of $Co_2(CO)_8$ with PPh_2Et in benzene at 20° C under a CO atmosphere

The reaction of $Co_2(CO)_8$ with PPh_2Et was carried out at 20° C in benzene under 1 atmosphere of CO. This gave two isomers of the complex $Co_2(CO)_7(PPh_2Et)$, a non-bridged complex **[7]** and a carbonyl-bridged complex **[8]**, inseparable from one another. The yield of **[7]** and **[8]** was 19% in the form of dark brown crystals. The infrared spectrum of **[7]** and **[8]** is shown in **Figure 3.6** and the ^{31}P NMR spectrum is shown in **Figure 3.7**. The theoretical molar mass of **[7]/[8]** was calculated to be 528.0 $g.mol^{-1}$ and from this, the calculated mass percent distribution was calculated to be C: 47.7%, H: 2.9%. Elemental analysis gave C: 45.0%, H: 2.9%.

3.2.2. Reaction of $Co_2(CO)_8$ with DPPE

Since these complexes are reported in the literature (*53,65*), only the infrared spectra, colour and melting points are reported in this thesis.

3.2.2.1. Reaction of $Co_2(CO)_8$ with DPPE at 0° C under a nitrogen atmosphere

The reaction of $Co_2(CO)_8$ with DPPE was carried out in hexane at ca. 0° C under nitrogen. This gave the complex $[Co_2(CO)_4(DPPE)_3]^{2+}\{[Co(CO)_4]^-\}_2$ **[12]** in 10% yield as yellow

crystals. The infrared spectrum of [12] is shown in **Figure 3.8.**

3.2.2.2. Reaction of $Co_2(CO)_8$ with DPPE in benzene refluxed under a nitrogen atmosphere

The reaction of $Co_2(CO)_8$ and DPPE was carried out refluxed in benzene under nitrogen. This gave the complex $[Co(CO)_2(DPPE)]_2$ [13] in 93% yield as red-brown crystals. The infrared spectrum of [13] is shown in **Figure 3.9.**

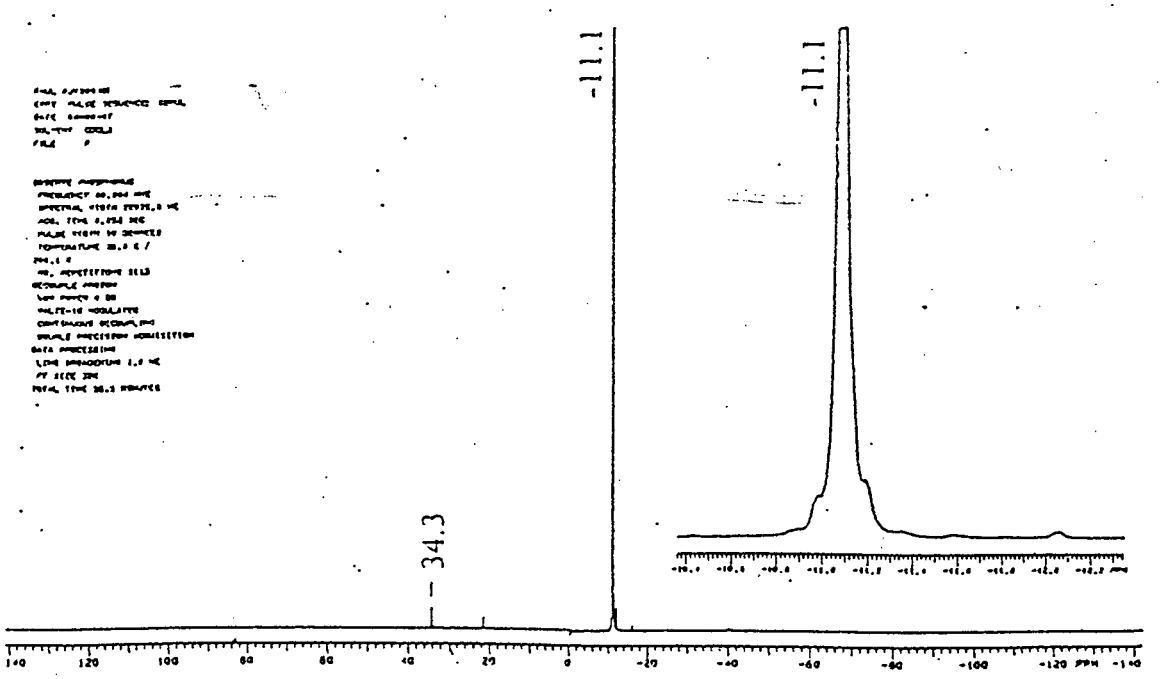

Figure 3.1 : ^{31}P NMR spectrum of a $CDCl_3$ solution of PPh_2Et at 25°C

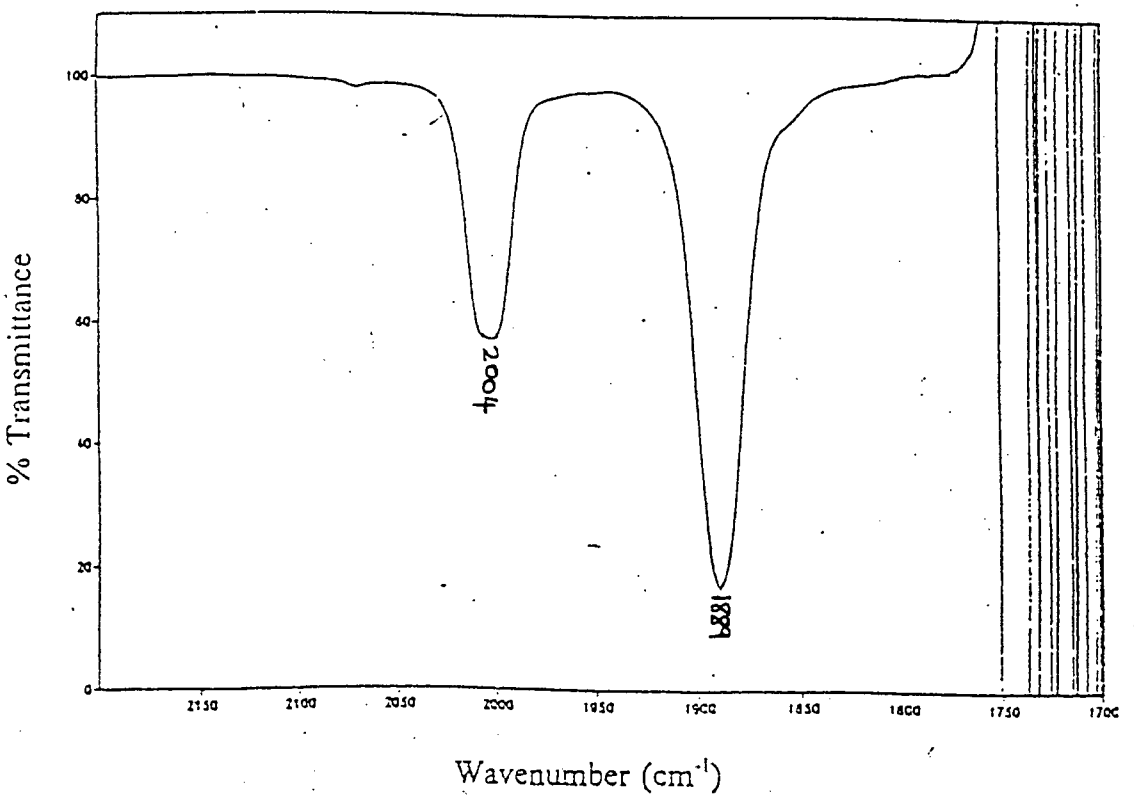

Figure 3.2 : Infrared spectrum at 25°C in the ν(CO) region of an acetone solution of $[Co(CO)_3(PPh_2Et)_2]^+[Co(CO)_4]^-$

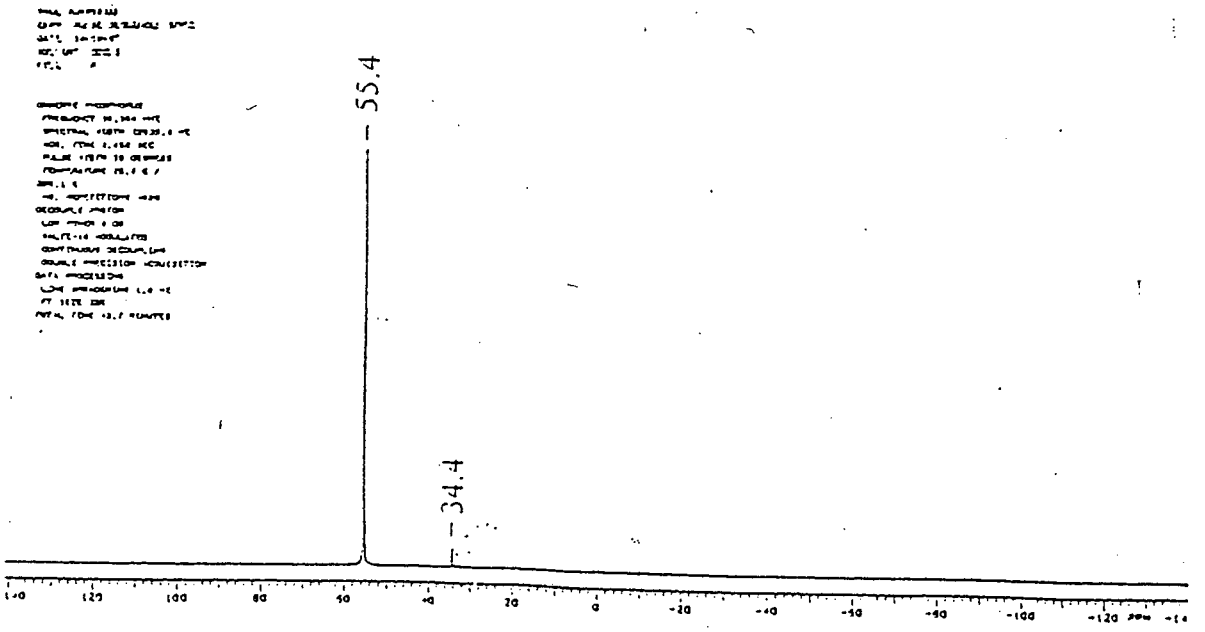

Figure 3.3 : ^{31}P NMR spectrum of a $CDCl_3$ solution of $[Co(CO)_3(PPh_2Et)_2]^+[Co(CO)_4]^-$ at 25°C

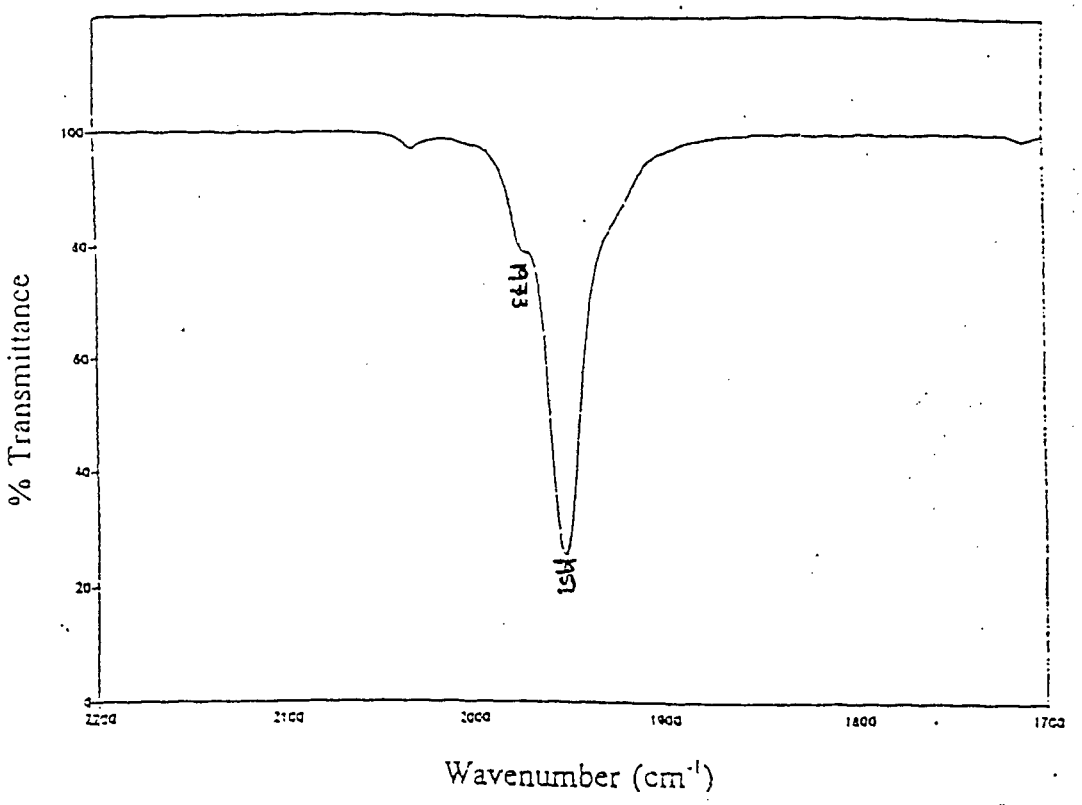

Figure 3.4 : Infrared spectrum at 25°C in the ν(CO) region of a $CHCl_3$ solution of $[Co(CO)_3(PPh_2Et)]_2$

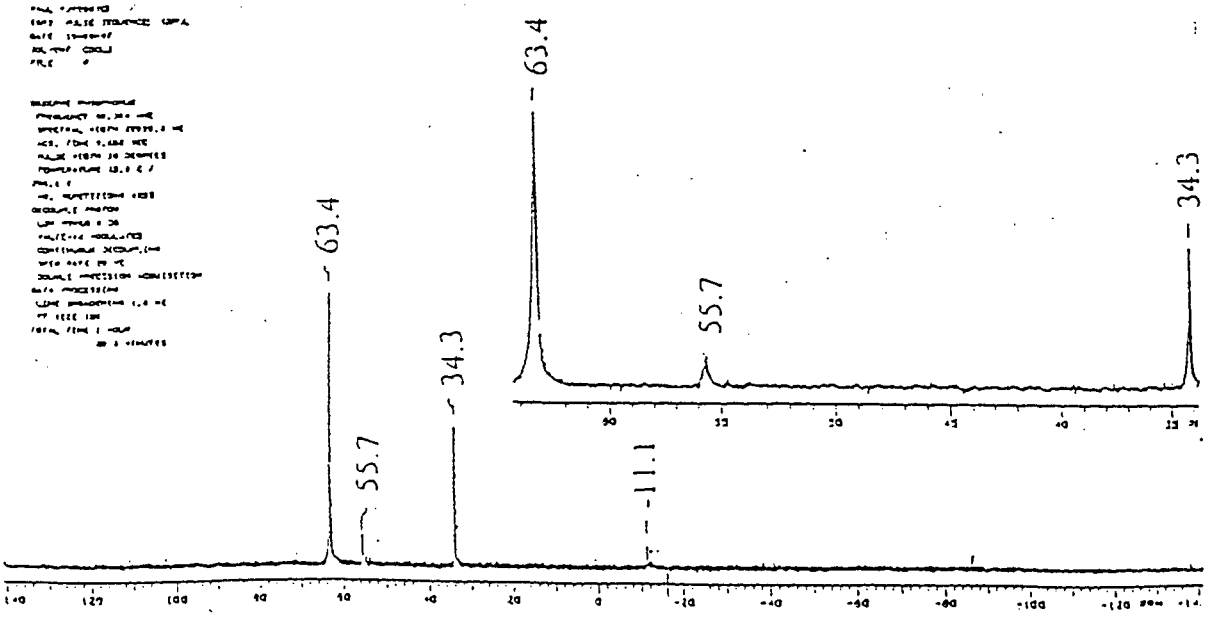

Figure 3.5 : ^{31}P NMR spectrum of a $CDCl_3$ solution of $[Co(CO)_3(PPh_2Et)]_2$ at 25°C

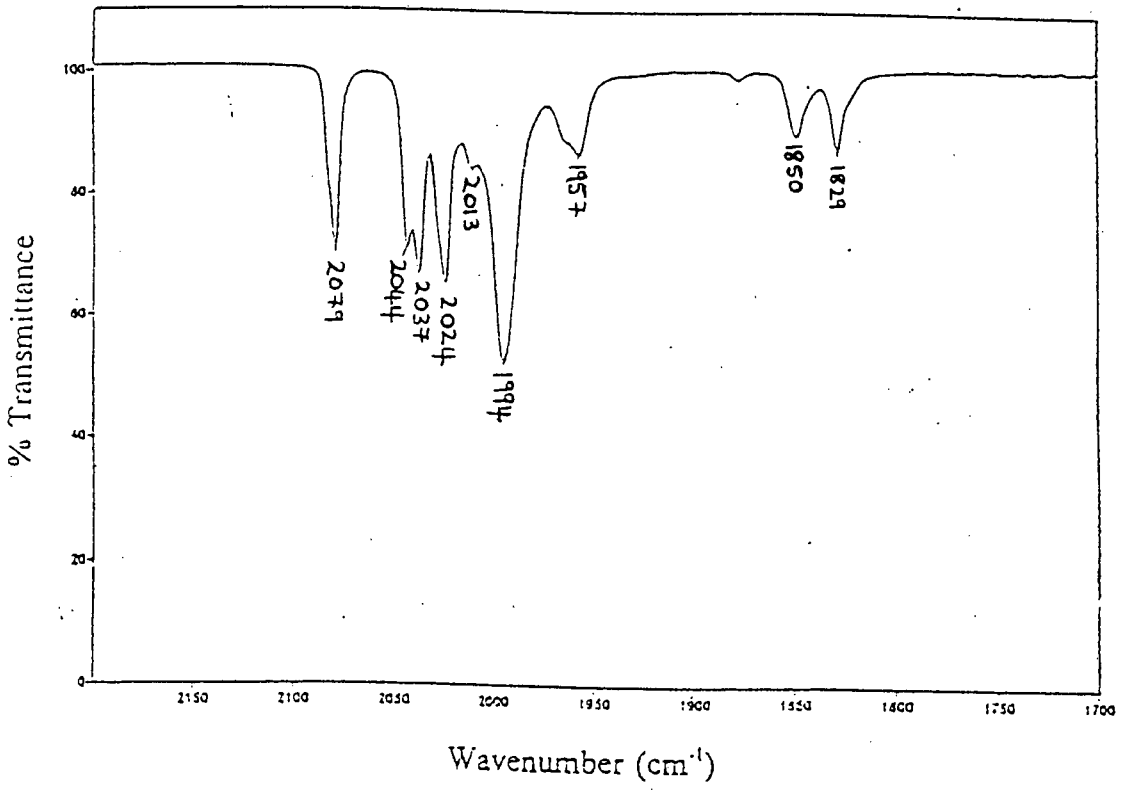

Figure 3.6 : Infrared spectrum at 25°C in the ν(CO) region of a hexane solution of $Co_2(CO)_7(PPh_2Et)$

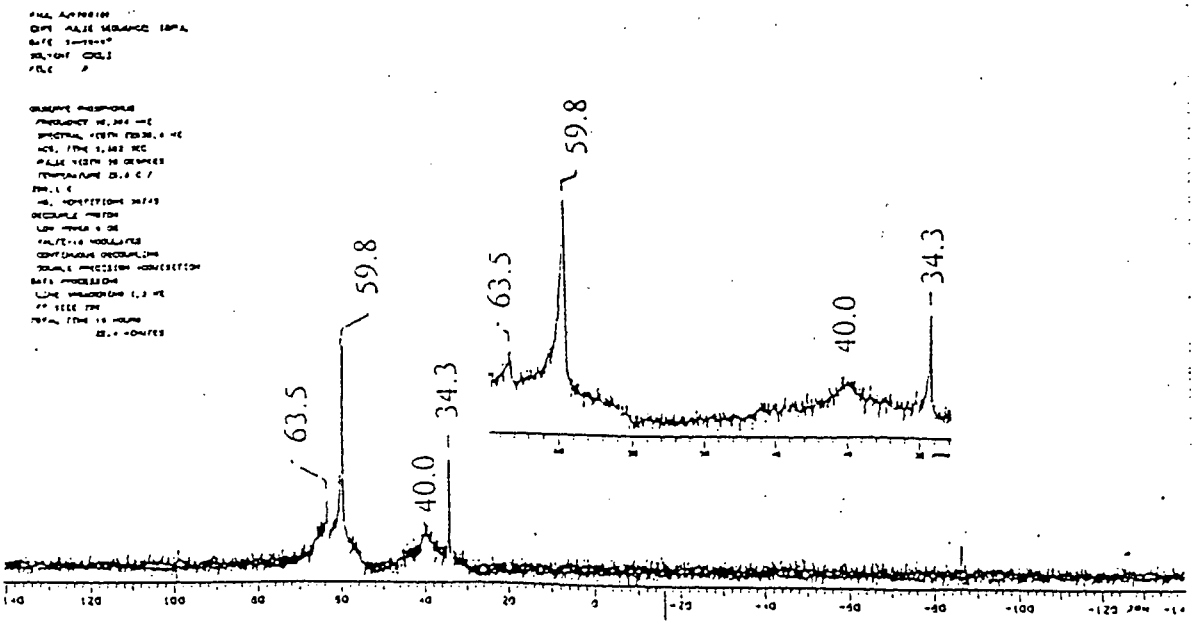

Figure 3.7 : ^{31}P NMR spectrum of a $CDCl_3$ solution of $Co_2(CO)_7(PPh_2Et)$ at 25°C

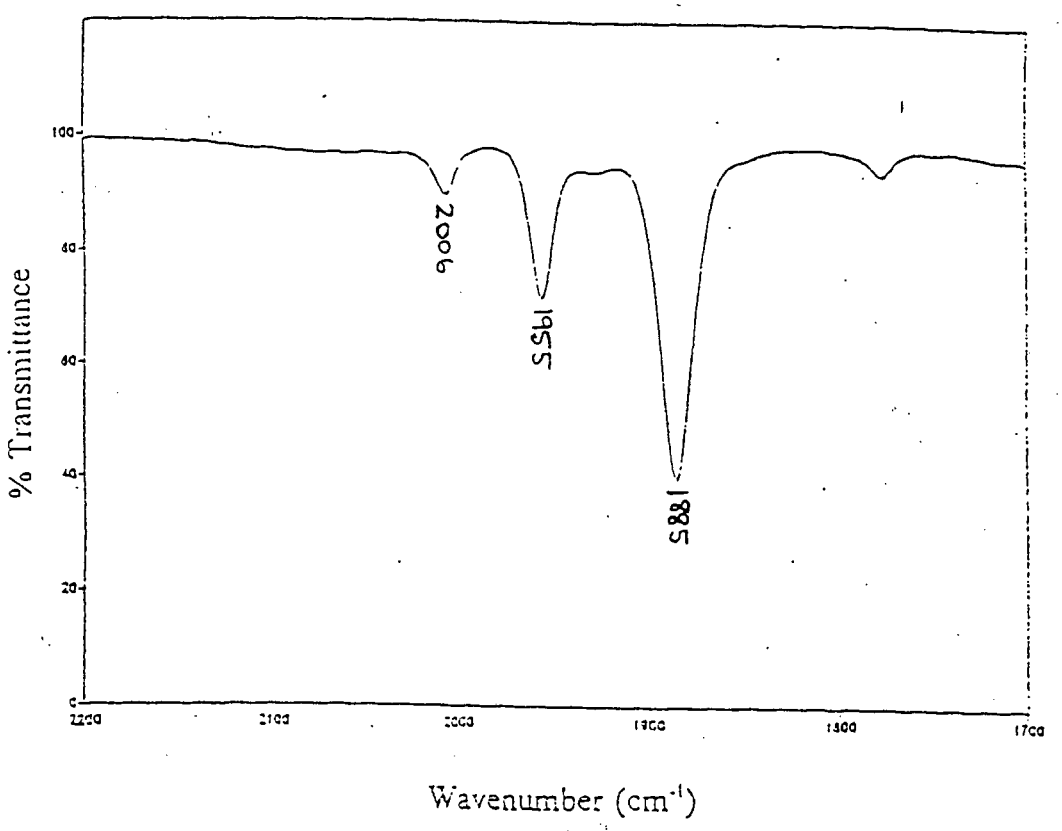

Figure 3.8 : Infrared spectrum at 25°C in the ν(CO) region of a THF solution of $[Co_2(CO)_4(DPPE)_3]^{2+}\{[Co(CO)_4]^-\}_2$

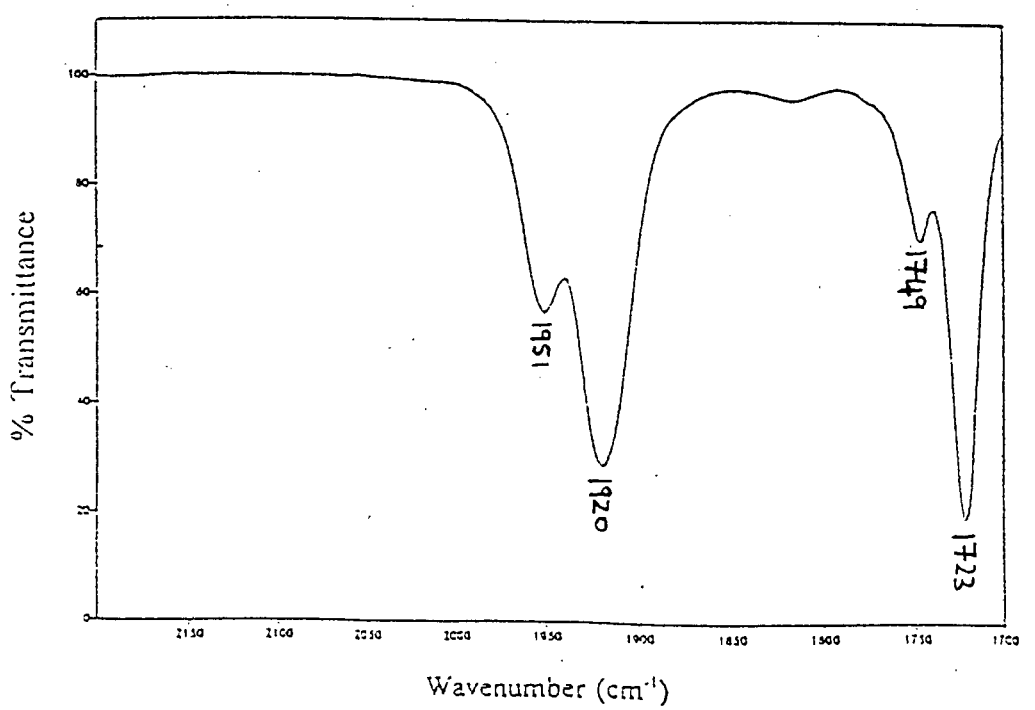

Figure 3.9 : Infrared spectrum at 25°C in the ν(CO) region of a CH_2Cl_2 solution of $[Co(CO)_2(DPPE)]_2$

Table 3.2 : Colour, yields, ^{31}P NMR, elemental analysis and melting points of cobalt carbonyl-phosphine complexes

Compound	Compound number	Colour of crystals	Yield (%)	^{31}P NMR peaks relative to H_3PO_4 (δ = 0.00 ppm)	Elemental analysis Found (Calc.)		Melting points
					C	H	
$[Co(CO)_3(PPh_2Et)_2]^+[Co(CO)_4]^-$	**[1]**	orange	39%	55.4, 34.4	56.5% (56.6%)	4.2% (4.1%)	85-90°C dec
$[Co(CO)_3(PPh_2Et)]_2$	**[3]**	dark brown	29%	63.4, 55.7, 34.3, -11.1	57.5% (57.1%)	4.5% (4.2%)	121-123°C
$[Co(CO)_7(PPh_2Et)]$	**[7]/[8]**	dark brown	19%	63.5, 59.8, 40.0, 34.3	45.0% (47.7%)	2.9% (2.9%)	dec
$[Co_2(CO)_4(DPPE)_3]^{2+}\{[Co(CO)_4]^-\}_2$	**[12]**	yellow	10%	---	---	---	281-285°C dec
$[Co(CO)_2(DPPE)]_2$	**[13]**	red-brown	93%	---	---	---	223-228°C

---- : no analysis was performed

dec : decomposed

Table 3.3 : IR data of cobalt carbonyl-phosphine complexes

Synthesized compound	Compound number	ν(CO) bands, cm^{-1} (solvent)	IR data of cobalt compounds reported in literature			
			Compound	Compound number	ν(CO) bands, cm^{-1} (solvent)	Ref.
$[Co(CO)_3(PPh_2Et)_2]^+[Co(CO)_4]^-$	[1]	2004 s, 1889 vs (acetone)	$[Co(CO)_3(PPh_3)_2]^+[Co(CO)_4]^-$	[2]	2008 s, 1887 vs (acetone)	(*78*)
$[Co(CO)_3(PPh_2Et)]_2$	[3]	1973 sh. 1951 vs ($CHCl_3$)	$[Co(CO)_3(PPh_3)]_2$	[4]	1977 sh, 1957 vs ($CHCl_3$)	(*54*)
$Co_2(CO)_7(PPh_2Et)$	[7][a]	2079 s, 2024 s 2013 sh. 1994 vs, 1957 w (hexane)	$Co_2(CO)_7(PPh_3)$ [a]	[11]	2079 s, 2026 s, 2010 sh, 1996 vs, 1964 m (hexane)	(*51,79*)
	[8][b]	2079 s, 2044 s, 2037 s, 1850 w, 1829 w (hexane)	$Co_2(CO)_7(PEt_3)$ [a]	[9]	2077 m, 2025 s, 1988 vs, 1972 vw (alkanes)	(*64*)
			$Co_2(CO)_7(PEt_3)$ [b]	[10]	2081 w, 2039 m, 2037 s, 1850 m, 1827 m (alkanes)	(*64*)
$[Co_2(CO)_4(DPPE)_3]^{2+}\{[Co(CO)_4]^-\}_2$	[12]	2006 w, 1955 m, 1885 vs (THF)	$[Co_2(CO)_4(DPPE)_3]^{2+}\{[Co(CO)_4]^-\}_2$	[12]	2007 w, 1955 m, 1885 vs (THF)	(*53*)
$[Co(CO)_2(DPPE)]_2$	[13]	1951 m, 1920 vs, 1749 w sh, 1723 vs (CH_2Cl_2)	$[Co(CO)_2(DPPE)]_2$	[13]	1957, 1922, 1752, 1728 [c] (CS_2)	(*53*)
					1970 s, 1920 vs, 1753 m, 1728 vs (CH_2Cl_2)	(*65*)

a : cobalt-cobalt bond is not bridged by carbonyl ligands in this isomer

b : cobalt-cobalt bond is bridged by carbonyl ligands in this isomer

c : relative peak intensities were not provided in the literature

3.3. ION-EXCHANGE MODIFICATION OF ZEOLITE Y

The Na^+ counter-ions in Na-Y were exchanged for Co^{2+} ions from aqueous solution (see Section 2.4.3.). In the case of 100% exchange, the zeolite would be referred to as Co-Y; for partial exchange, the zeolite would be referred to as CoNa-Y. Total exchange would give a loading of 20% cobalt by mass, so an exchange to produce 3-4% cobalt was CoNa-Y zeolite. The IR spectrum was not obtained for this catalyst since there were no characteristic bands in the carbonyl range (2200-1700 cm^{-1}); rather, just the AA analyses were done to get the mass% loading of cobalt. The exact cobalt loading of the ion-exchanged zeolite was 3.12% from AA analysis.

3.4. IMPREGNATION OF ZEOLITE Y WITH $Co_2(CO)_8$ AND TERTIARY OR BIDENTATE PHOSPHINE LIGANDS

All impregnations of zeolites were carried out at room temperature (20-25° C) throughout the entire impregnation procedure. The identification codes for each catalyst are given in parentheses indicating the approximate cobalt mass% loading, then the order of impregnation of compounds, ie. "Ax/y" means "zeolite loaded with ~A% cobalt and impregnated with x followed by y" (ph = PPh_2Et, pp = DPPE, co = $Co_2(CO)_8$). For example, 4ph/co means "zeolite loaded with ~4% cobalt and impregnated with PPh_2Et followed by $Co_2(CO)_8$".

3.4.1. High-cobalt catalysts (~4.5% cobalt)

3.4.1.1. Na-Y zeolite impregnated with PPh_2Et followed by $Co_2(CO)_8$ (4ph/co)

The IR spectrum in the ν(CO) region of the impregnated zeolite is shown in **Figure 3.10.** Three bands are evident at 2007 cm^{-1}, 1999 cm^{-1} and 1884 cm^{-1}, indicating that a cobalt carbonyl species was present. It is suspected that the two peaks at 2007 and 1999 cm^{-1} are in actual fact one peak split into two by the effect of solid-state splitting (the sample was mixed with KBr and pressed into a disc to obtain the IR spectrum).

3.4.1.2. Na-Y zeolite impregnated with DPPE followed by $Co_2(CO)_8$ (4pp/co)

The IR spectrum in the ν(CO) region of the resultant impregnated zeolite is shown in **Figure 3.11**. Three bands are evident at 2007 cm^{-1}, 1951 cm^{-1} and 1878 cm^{-1}, indicating the presence of a cobalt carbonyl complex on the zeolite.

3.4.2. Low-cobalt catalysts (~0.2% cobalt)

3.4.2.1. Na-Y zeolite impregnated with PPh_2Et followed by $Co_2(CO)_8$ (0.2ph/co)

The IR spectrum in the ν(CO) region of the impregnated zeolite is shown in **Figure 3.12**. Three bands are evident at 2084 cm^{-1}, 2022 cm^{-1} and 1983 cm^{-1} indicating the presence of a cobalt carbonyl complex on the zeolite. It should be noted that the bands observed in **Figure 3.12** differ considerably from the bands observed in **Figure 3.10** for impregnation with the same compounds at a higher cobalt loading. This indicates that the species present in 0.2ph/co was different to the species present in 4ph/co.

3.4.2.2. Na-Y zeolite impregnated with $Co_2(CO)_8$ followed by PPh_2Et (0.2co/ph)

The IR spectrum in the ν(CO) region of the impregnated zeolite is identical to that of the zeolite 0.2ph/co, shown in **Figure 3.12**.

3.4.2.3. Na-Y zeolite impregnated with DPPE followed by $Co_2(CO)_8$ (0.2pp/co)

The IR spectrum in the ν(CO) region of the impregnated zeolite is shown in **Figure 3.13**. Two peaks are evident at 2006 cm^{-1} and 1951 cm^{-1}. These two peaks are almost identical to two of the peaks shown in **Figure 3.11**. However, the absence of the third peak indicates that the species present in 0.2pp/co was different to the species in 4pp/co.

The exact cobalt loadings of all five batches of catalysts were determined using AA analysis and are included in **Table 3.4** together with pertinent IR data.

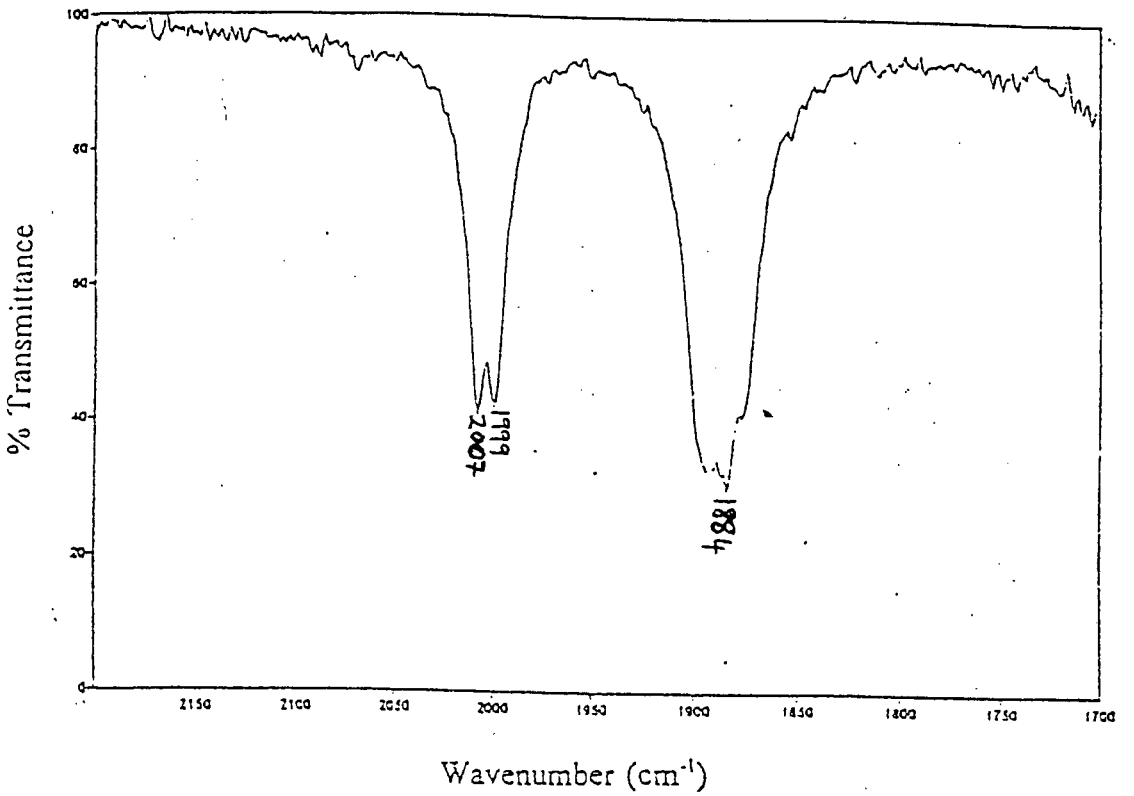

Figure 3.10 : Infrared spectrum at 25°C in the ν(CO) region of 4ph/co in KBr

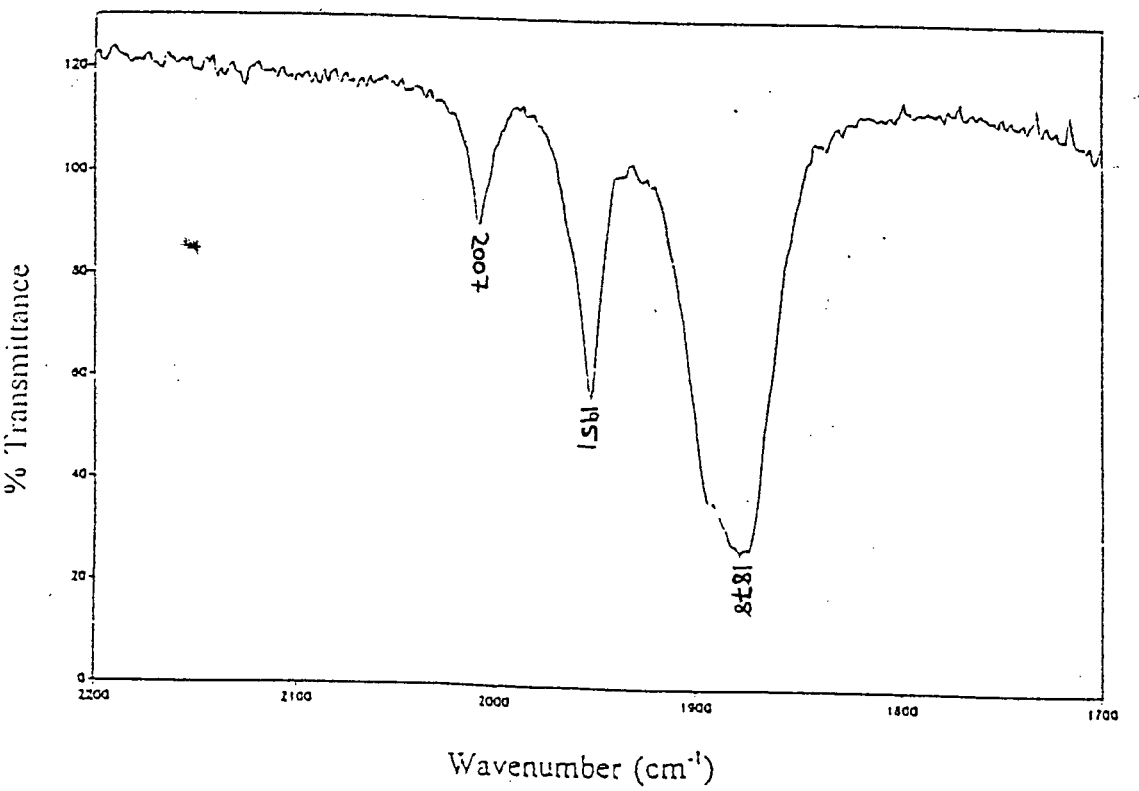

Figure 3.11 : Infrared spectrum at 25°C in the ν(CO) region of 4pp/co in KBr

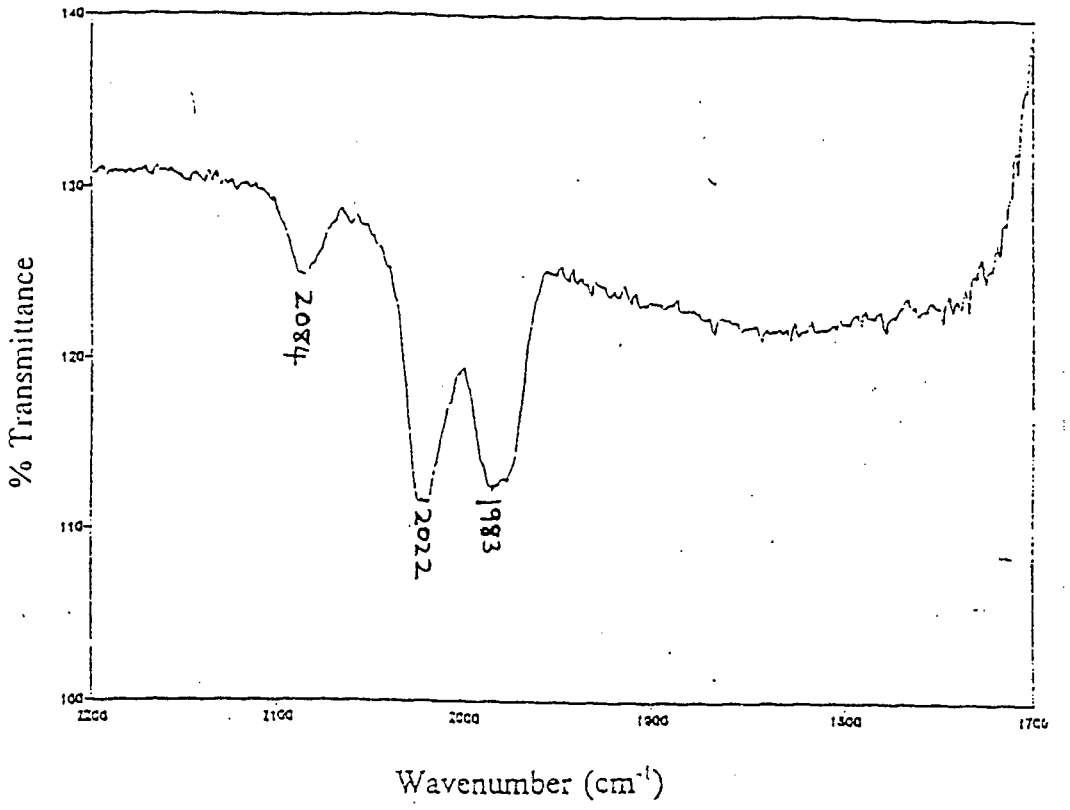

Figure 3.12 : Infrared spectrum at 25°C in the ν(CO) region of 0.2ph/co and 0.2co/ph in KBr

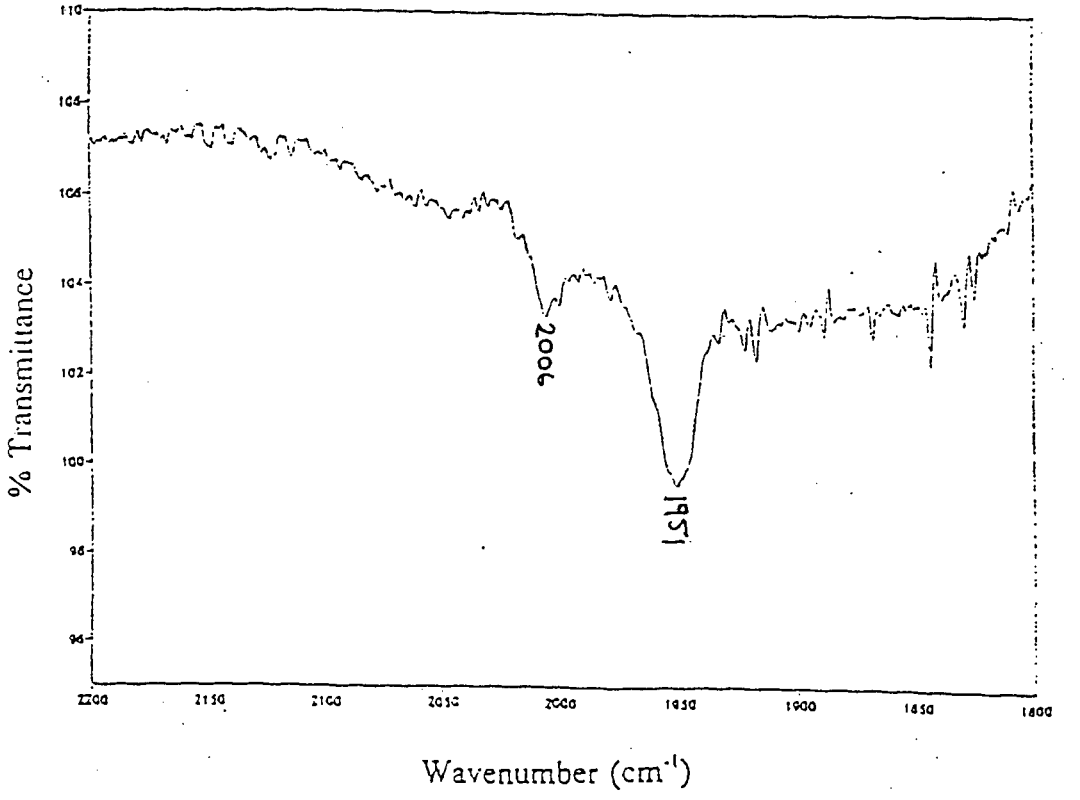

Figure 3.13 : Infrared spectrum at 25°C in the ν(CO) region of 0.2pp/co in KBr

Table 3.4 : Summary of IR spectra (in the ν(CO) region) and cobalt loadings of impregnated zeolite catalysts

CATALYST	ORDER OF IMPREGNATION		ν(CO) bands, cm^{-1} (all samples on KBr)	MASS % COBALT [a]	COBALT ATOMS PER NaY SUPERCAGE
	FIRST COMPONENT	SECOND COMPONENT			
4ph/co	PPh_2Et	$Co_2(CO)_8$	2007 vs, 1999 vs, 1884 vs	4.38%	10
4pp/co	DPPE	$Co_2(CO)_8$	2007 m, 1951 s, 1878 vs	4.71%	11
0.2ph/co	PPh_2Et	$Co_2(CO)_8$	2084 w, 2022 vs, 1983 vs	0.20%	0.5
0.2co/ph	$Co_2(CO)_8$	PPh_2Et	same as 0.2ph/co	0.20%	0.5
0.2pp/co	DPPE	$Co_2(CO)_8$	2006 w, 1951 m	0.13%	0.3

a : [(Mass of cobalt)/(Mass of zeolite support)] x 100% ; see APPENDIX A

3.5. WASHING OF IMPREGNATED ZEOLITES WITH SOLVENTS

The impregnated zeolites described in Sections 3.4.1. and 3.4.2. were washed with a number of solvents to see what effect they would have on the complex remaining on the zeolite after the impregnation procedure (see washing procedure in Section 2.4.5.). These washings were a preliminary test to see if the complex remained on/in the zeolite in its initial form or if it was washed off (ie. was not encapsulated or anchored).

3.5.1. High-cobalt catalysts

This section describes the effects of washing 4ph/co and 4pp/co with hexane, dichloromethane, 1-decanol and 1-decene. The results of the AA analyses of the zeolites before and after washing are summarised in **Table 3.5.**

(i) Hexane

Hexane was used to check the effect of a non-polar solvent on the species present in the zeolite. The IR spectra of the hexane filtered through both 4ph/co and 4pp/co show no ν(CO) bands. Furthermore, the IR spectra of the zeolites after washing were identical to the original spectra (cf. **Figure 3.10** and **Figure 3.11**). 100% of the cobalt was retained on 4ph/co while 98% of the cobalt remained on 4pp/co after washing.

(ii) Dichloromethane

Dichloromethane was used to check the effect of a more polar solvent on the species present in the zeolite. The IR spectra in the ν(CO) region for a series of washes is shown in **Figure 3.14** and **Figure 3.15** for 4ph/co and 4pp/co respectively. In both cases, very strong ν(CO) bands are evident for the IR spectrum of the first aliquot of dichloromethane with the intensity of the bands decreasing for subsequent aliquots. IR analysis of 4ph/co and 4pp/co after washing showed no ν(CO) bands. 14% of the cobalt remained on 4ph/co while only 4% of the cobalt was retained on 4pp/co after washing.

(iii) 1-Decanol

1-Decanol was used to check the effect of possible reaction products (undecanols) on the species present on the zeolites. The IR spectra of the 1-decanol filtered through both 4ph/co and 4pp/co showed no ν(CO) bands. Furthermore, the IR spectrum of the zeolites after washing were identical to the original spectra (**Figure 3.10** and **Figure 3.11**). However, **Table 3.5** does indicate that some cobalt has been washed off the 4ph/co. Possibly the complex was sparingly soluble in 1-decanol and very small amounts (not detected by IR) were removed from the exterior of the zeolite crystals in each wash. 86% of the cobalt remained on 4ph/co while 98% of the cobalt was retained on 4pp/co after washing.

(iv) 1-Decene

1-Decene was used to check the effect of the reagent used in the hydroformylation reactions on the species present on the zeolites. The IR spectra of the 1-decene filtered through both 4ph/co and 4pp/co show no ν(CO) bands. Furthermore, the IR spectra of the zeolites after washing were identical to the original spectra (cf. **Figure 3.10** and **Figure 3.11**). 95% of the cobalt remained on 4ph/co and 100% of the cobalt remained on 4pp/co after washing.

3.5.2. Low-cobalt catalysts

0.2ph/co, 0.2co/ph and 0.2pp/co were washed with hexane, dichloromethane and 1-decene. IR spectra of all aliquots of solvents filtered through any of the catalysts did not show any ν(CO) bands and AA analyses showed that 100% of the cobalt was retained in the zeolite supports of all three catalysts.

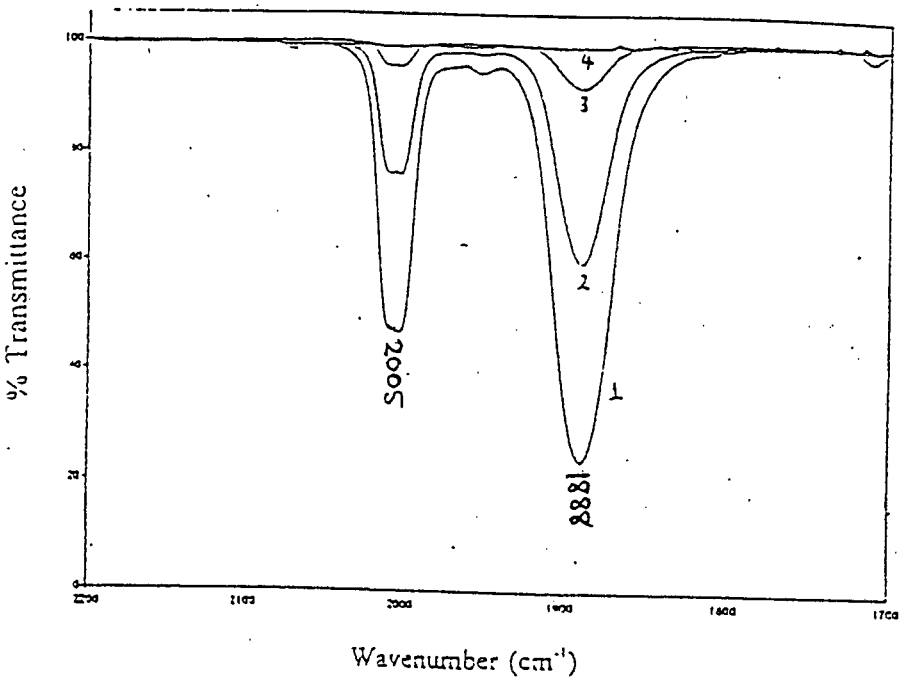

Figure 3.14 : Infrared spectra at 25°C in the ν(CO) region of dichloromethane aliquots filtered through 4ph/co (1-4 : aliquots 1-4)

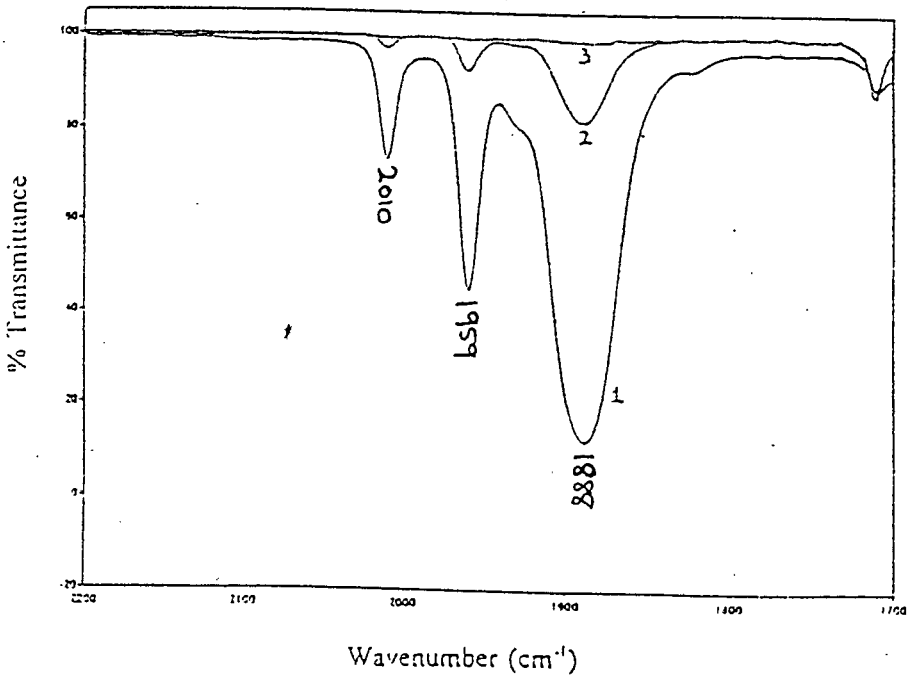

Figure 3.15 : Infrared spectra at 25°C in the ν(CO) region of dichloromethane aliquots filtered through 4pp/co (1-3 : aliquots 1-3)

Table 3.5 : Results of AA analyses carried out on 4ph/co and 4pp/co after washing with various solvents

	Mass % of cobalt after washing	**Cobalt fraction remaining on zeolite support**
4ph/co initial mass % cobalt: **4.38%**		
Hexane	4.38%	1.00
Dichloromethane	0.61%	0.14
1-Decanol	3.74%	0.86
1-Decene	4.15%	0.95
4pp/co initial mass % cobalt : **4.71%**		
Hexane	4.60%	0.98
Dichloromethane	0.17%	0.04
1-Decanol	4.63%	0.98
1-Decene	4.70%	1.00

3.6. USE OF HIGH-COBALT CATALYSTS UNDER REACTION CONDITIONS

Carbon balances, conversions and selectivities for all reactions were calculated using the procedure outlined in **APPENDIX B**. This procedure is also applicable to the reactions with the low-cobalt catalysts discussed in Section 3.7.

3.6.1. Hydroformylation reactions using homogeneous catalysts (as base case)

Reactions were carried out with $Co_2(CO)_8$ and either PPh_2Et or DPPE for comparison of product distribution and activity with the impregnated zeolite catalysts. The results are summarised in **Table 3.6**. Experiment PJV123 is the reaction using $Co_2(CO)_8$ and PPh_2Et while PJV122 is the reaction using $Co_2(CO)_8$ and DPPE. These reactions are compared to the

appropriate reactions with impregnated zeolites in Section 3.6.3.3. and Section 3.6.3.4..

3.6.2. Reactions under hydroformylation conditions in decane (no alkene reagent)

Experiments were carried out using 4ph/co and 4pp/co. These reactions were carried out to see the effect of the reaction temperature and pressure on the hybrid zeolite catalyst in the absence of alkene reagent.

3.6.2.1. 4ph/co

The IR spectrum of the solution after completion of the experiment with 4ph/co is shown in **Figure 3.16**. One main ν(CO) band is visible at 1960 cm^{-1}, indicating the presence of a cobalt carbonyl species in solution. The infrared spectrum of 4ph/co after reaction is also shown in **Figure 3.16**. Two ν(CO) bands are in evidence at 1956 cm^{-1} and 1933 cm^{-1} indicating that there was still a cobalt carbonyl species present on the zeolite support, either due to encapsulation within the zeolite crystals or due to attachment (physical or chemical) to the walls of the zeolite crystals (inside or outside surfaces).

3.6.2.2. 4pp/co

The IR spectrum of the solution after the experiment with 4pp/co was completed is shown in **Figure 3.17**. A large number of ν(CO) bands are visible at 2051 cm^{-1}, 2023 cm^{-1}, 2014 cm^{-1}, 1992 cm^{-1}, 1977 cm^{-1} and 1965 cm^{-1}, indicating the presence of at least one, but very likely more than one, cobalt carbonyl species in solution. The infrared spectrum of 4pp/co after reaction is also shown in **Figure 3.17**. One very weak band at 1936 cm^{-1} suggests that there was still a cobalt carbonyl species present on the zeolite support, but the weakness and bad resolution of the band indicates a very low concentration of a carbonyl complex.

3.6.3. Hydroformylation reactions using zeolite catalysts

Single reactions (ie. no recycle of zeolite samples from one reaction to another) were carried out with non-impregnated NaY zeolite, CoNa-Y zeolite, 4ph/co and 4pp/co under

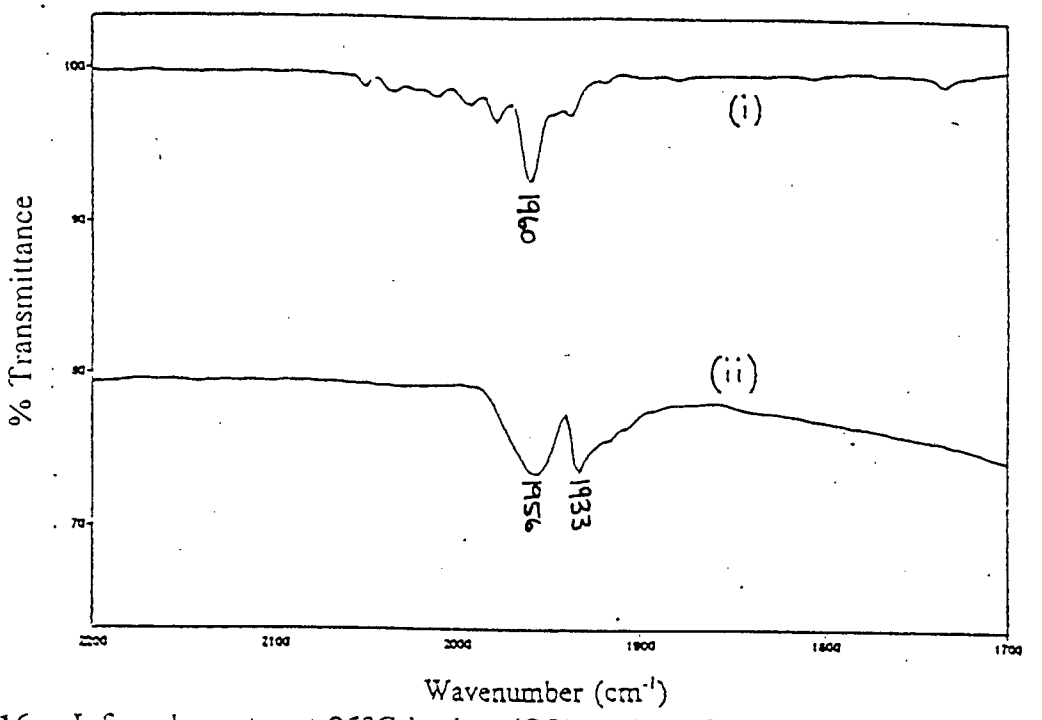

Figure 3.16 : Infrared spectra at 25°C in the ν(CO) region of (i) reaction solution and (ii) 4ph/co zeolite (mixed with KBr), after the experiment using 4ph/co in decane under hydroformylation conditions

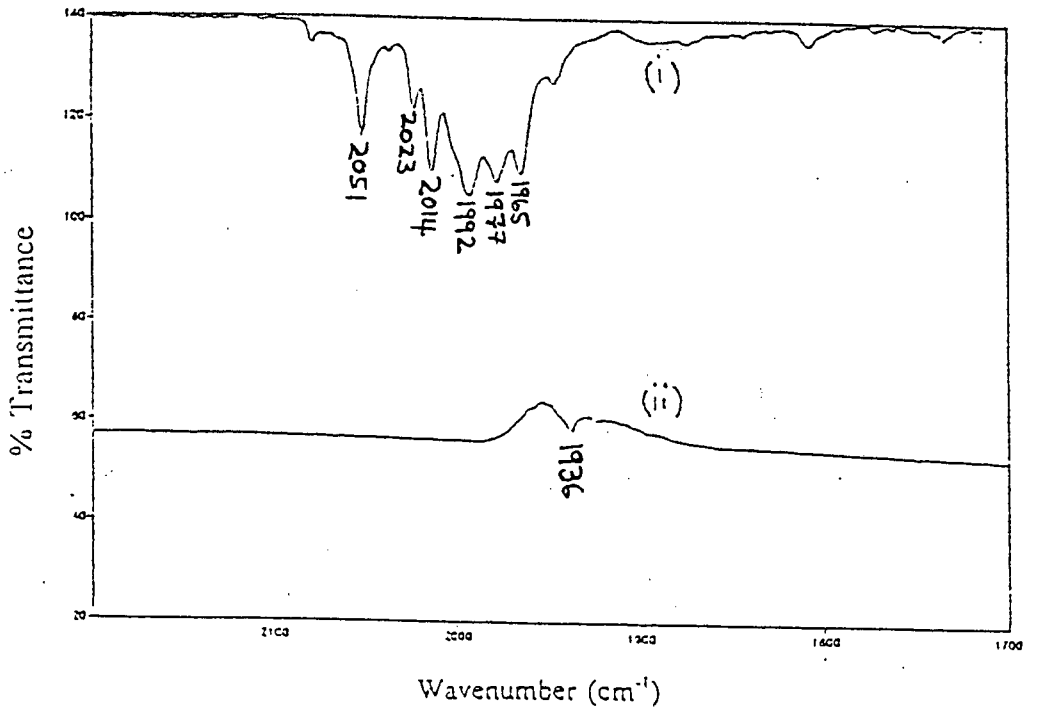

Figure 3.17 : Infrared spectra at 25°C in the ν(CO) region of (i) reaction solution and (ii) 4pp/co zeolite (mixed with KBr), after the experiment using 4pp/co in decane under hydroformylation conditions

hydroformylation conditions. The blank run with just 1-decene, hexadecane and no catalyst or zeolite was carried out but is not recorded in the tables; GC analysis showed that there was no difference between the starting solution and the final solution. **Table 3.6** summarises the results discussed in this section.

3.6.3.1. Non-impregnated Na-Y zeolite as a blank run

Experiment PJV95 involved using plain Na-Y zeolite to see if the zeolite support results in any conversion of 1-decene to hydroformylation products or by-products. The result in **Table 3.6** indicates that there is no effect of the zeolite support on the reaction medium.

3.6.3.2. Na-Y zeolite ion-exchanged to form Co-Y

Experiment PJV96 involved using CoNa-Y to see if the Co^{2+} ions present as counter-ions could catalyse hydroformylation. The result in **Table 3.6** indicates that no hydroformylation products were formed. Nothing else could be inferred from the result because the mass balance was really poor. This was due to the fact that the products constituting the 25% conversion appeared on the GC trace at a longer residence time than hexadecane as a closely-bunched, poorly-resolved lump of peaks. These peaks were not identified but it was assumed that they were heavy by-products, possibly oligomers of decene.

3.6.3.3. 4ph/co

Catalysis with 4ph/co gave a higher conversion (63%) compared to the analogous homogenous catalysis (48%) but gave a lower proportion of linear products (1.6 compared to 2.6).

IR spectra of the solutions (after reaction) for both PJV116 and PJV123 showed a ν(CO) band at 1957 cm^{-1}, indicating that the same cobalt carbonyl complex was present in solution in both the homogeneously-catalysed and heterogeneously-catalysed reactions. In the case of PJV116, this means that cobalt had leached out of the zeolite and into solution.

Table 3.6 : Summary of single hydroformylation reactions carried out with homogeneous catalysts as well as the zeolite catalysts NaY, CoNa-Y, 4ph/co and 4pp/co [a]

CATALYSTS USED FOR HYDROFORMYLATION		Mass of zeolite used (g)	Concentration of cobalt ($g.l^{-1}$)	P:Co ratio [b]	Conver. [b]	n:iso ratio [c]	alc:ald ratio [c]	Selectivities			Carbon Balance
								Decane	Aldehydes	Alcohols	
NaY	(PJV95)	2.3	0	0	0%	N/A	N/A	0%	0%	0%	94.20%
CoNa-Y	(PJV96)	3.4	1.06	0	25.6%	N/A	N/A	0%	0%	0%	70.14%
$Co_2(CO)_8$ + PPh_2Et	(PJV123)	0	1.37	2	48.28%	2.55	2.74	15.7%	21.0%	57.5%	103.1%
4ph/co	(PJV116)	1	1.04	1 *	63.25%	1.59	2.44	13.2%	21.0%	51.2%	102.98%
$Co_2(CO)_8$ + **DPPE**	(PJV122)	0	1.29	2	87.19%	1.00	18.26	8.9%	4.7%	84.9%	91.75%
4pp/co	(PJV109)	1	1.14	1.5 *	82.78%	0.80	16.90	9.9%	4.9%	82.8%	88.31%

a : Initial pressure = 80 bar, temperature (maintained) = 180°C, reaction time = 5 hours

b : P:Co = phosphorus:cobalt, Conver. = conversion

c : n:iso = (linear products):(branched products), alc:ald = alcohols:aldehydes

* : Not determined by analysis; assumed due to species initially present on the zeolites (see Section 4.2.)

N/A : Not applicable; ratio involves division by zero

3.6.3.4. 4pp/co

Catalysis using 4pp/co gave the same results as for homogeneous catalysis. IR spectra of the solutions (after reaction) for PJV109 and PJV122 showed the same set of ν(CO) bands but the complexes present could not be identified. This indicates that the same cobalt complex or complexes are present in the solution after reaction for both reactions and also indicates that cobalt leached from the zeolite into solution.

3.6.4. Recycling of impregnated zeolite catalysts

Two sets of hydroformylation reactions were carried out with each of 4ph/co and 4pp/co in which the catalyst used in one reaction was "recycled", as described in Section 2.5.6. **Table 3.7** summarises the results discussed in this section. Unfortunately, no AA analyses of the zeolites were carried out after reaction, so the final mass% cobalt remaining on the zeolite supports was not quantified.

Some of the sets involved adding "extra" phosphine to the system before reaction was carried out (see Section 2.5.6.). The extra phosphine was only added to the first reaction of a set. Enough phosphine was added to ensure that the moles of phosphorus added to the system via the phosphine was twice the moles of cobalt present on the zeolite before the start of the first reaction.

3.6.4.1. 4ph/co

Recycling of 4ph/co led to decreasing conversions (63% to 3%), decrease in the linearity of the products (1.6 to 0.9) and a decrease in the selectivity to alcohol compared to aldehyde (2.44 down to 0.03).

As mentioned in Section 3.6.3.3., the IR spectrum of the solution after the first reaction, PJV116, showed that cobalt had leached from the zeolite and was present in solution as a cobalt carbonyl complex. In the IR spectra of the solutions from PJV117 and PJV118 after reaction, no ν(CO) bands were observed, ie. there were no cobalt carbonyl complexes present

in solution. The IR spectrum of the zeolite after the third reaction showed no ν(CO) bands indicating that no cobalt carbonyl complex remained on the zeolite.

3.6.4.2. 4ph/co with extra PPh_2Et added

This set of reactions was identical to those mentioned in Section 3.6.4.1. except that extra PPh_2Et was added to the solution before the first reaction, PJV119. Recycling of 4ph/co, similar to the previous case, led to decreasing conversions (59% to 4%). In reactions PJV120 and PJV121, no aldehydes or alcohols were detected, so no trends could be observed for product distribution.

The IR spectrum of the solution after reaction PJV119 showed a ν(CO) band at 1956 cm^{-1}, similar to that observed for PJV116, indicating that cobalt had leached from the zeolite and was present in solution as a cobalt carbonyl complex. In the IR spectra of the solutions from PJV120 and PJV121 after reaction, no ν(CO) bands were observed, ie. there were apparently no cobalt carbonyl complexes present in solution. The IR spectrum of the zeolite after the third reaction showed no ν(CO) bands indicating that no cobalt carbonyl complex remained on the zeolite.

3.6.4.3. 4pp/co

Recycling of 4pp/co led to decreasing conversions (83% to 10%). The linearity of the products remained constant for two of the three reactions and there was a sharp decrease in the selectivity to alcohol compared to aldehyde (16.9 down to 0.04). As mentioned in Section 3.6.3.4., the IR spectrum of the solution after reaction PJV109 showed that cobalt had leached from the zeolite and was present in solution as a cobalt carbonyl complex, although the species could not be identified. In the IR spectra of the solutions from PJV110 and PJV111 after reaction, no carbonyl bands were observed, ie. there were apparently no cobalt carbonyl complexes present in solution. The IR spectrum of the zeolite after the third reaction showed no ν(CO) bands indicating that no cobalt carbonyl complex remained on the zeolite.

3.6.4.4. 4pp/co with extra DPPE added

This set of reactions was identical to those mentioned in Section 3.6.4.3. except that extra DPPE was added to the solution before the first reaction, PJV112. Recycling of 4pp/co, unlike the previous case, led to an initial increase in conversion from 12% in reaction PJV112 to 31% in reaction PJV113. This conversion was maintained in reaction PJV114 and this performance instigated the carrying out of a fourth reaction. The conversion in this fourth reaction dropped dramatically to 7%. The linearity of the products for all four reactions remained roughly the same (n:iso of 0.74-0.91) but the selectivity to aldehydes compared to alcohols increased sharply after the first reaction and in the final reaction, PJV115, no alcohol was detected by GC analysis. The IR spectrum of the solution after reaction PJV112 showed ν(CO) bands indicating that cobalt had leached from the zeolite and was present in solution as a cobalt carbonyl complex. In the IR spectra of the solutions from PJV113-115 after reaction, no ν(CO) bands were observed, ie. there were apparently no cobalt carbonyl complexes present in solution. No ν(CO) bands were observed in the IR spectrum of the zeolite after the fourth reaction indicating that no cobalt carbonyl complex remained on the zeolite.

3.7. USE OF LOW-COBALT CATALYSTS UNDER REACTION CONDITIONS

3.7.1. Hydroformylation reactions using homogeneous catalysts (as base case)

The homogeneously catalysed reactions described in this section were essentially carried out for comparison of catalyst activity and product distribution with reactions using the 0.2ph/co, 0.2co/ph and 0.2pp/co catalysts. However, it was also decided to test the reproducibility of the experiments as well as testing the effect of varying the P:Co ratio on catalyst activity and product distribution. All the results are summarised in **Table 3.8**.

3.7.1.1. Reproducibility tests

Five reactions were carried out with $Co_2(CO)_8$ and phosphine ligands; three reactions with PPh_2Et as ligand and two reactions with DPPE as ligand.

Table 3.7 : Summary of recycle reactions carried out with 4ph/co and 4pp/co [a]

EXPERIMENT CODES	Reaction number	P:Co ratio	Initial conc. of cobalt ($g.l^{-1}$) [b]	Conversion	n:iso ratio	alc:ald ratio	Selectivities			Carbon Balance
							Decane	Aldehydes	Alcohols	
4ph/co										
PJV116	1	1 *	1.04	63.25%	1.59	2.44	13.2%	21.0%	51.2%	102.98%
PJV117	2	---	---	15.15%	0.92	0.05	5.7%	86.0%	4.6%	93.27%
PJV118	3	---	---	2.57%	0.94	0.03	12.4%	65.8%	2.2%	92.68%
4ph/co + extra PPh,Et										
PJV119	1	3 *	1.04	58.54%	2.83	5.13	15.1%	11.8%	60.5%	99.12%
PJV120	2	---	---	5.50%	N/A	N/A	0%	0%	0%	101.28%
PJV121	3	---	---	3.81%	N/A	N/A	0%	0%	0%	101.76%
4pp/co										
PJV109	1	1.5 *	1.14	82.78%	0.80	16.90	9.9%	4.9%	82.8%	88.31%
PJV110	2	---	---	16.51%	0.83	0.04	8.0%	84.4%	3.3%	101.47%
PJV111	3	---	---	10.36%	N/A	N/A	0%	0%	0%	97.30%
4pp/co+ extra DPPE										
PJV112	1	3.5 *	1.14	12.02%	0.91	0.36	49.5%	29.3%	10.7%	107.80%
PJV113	2	---	---	31.07%	0.75	0.02	10.0%	85.7%	2.1%	97.84%
PJV114	3	---	---	33.32%	0.74	0.04	9.6%	86.1%	3.1%	97.19%
PJV115	4	---	---	6.74%	0.81	0	0%	68.0%	0%	99.77%

a : Initial pressure = 80 bar, temperature (maintained) = 180°C, reaction time = 5 hours

b : Total initial liquid volume = 40 cm^3 (decene:hexadecane 2:1)

--- : Indicates that the value is unknown.

* : Not determined by analysis; assumed due to species initially present on the supports (see Section 4.2)

N/A : Not applicable; ratio involves division by zero

(i) $Co_2(CO)_8$ and PPh_2Et

The three reactions carried out are referred to as PJV159, PJV160 and PJV162. The average conversion and average selectivities to decane, aldehyde and alcohol are, respectively: 53.1%, 7.3%, 70.3% and 19.6%. From the small scatter observed in the results (see **Table 3.8**), the reproducibility of the experimental setup is considered to be good.

(ii) $Co_2(CO)_8$ and DPPE

The two reactions carried out are referred to as PJV165 and PJV166. The average conversion and average selectivities to decane, aldehydes and alcohols are, respectively: 87.2%, 8.4%, 68.1% and 21.9%. These reactions were carried out to confirm reproducibility and the results appear to affirm reproducibility (see **Table 3.8**).

3.7.1.2. Effect of varying P:Co ratio

(i) $Co_2(CO)_8$ and PPh_2Et

As the P:Co ratio was increased, the conversion decreased and the linearity of products increased. The alcohol to aldehyde ratio does not show a definite trend.

(ii) $Co_2(CO)_8$ and DPPE

As the P:Co ratio was increased, the conversion decreased dramatically (about 14-fold) while the linearity of the products increased. The alcohol to aldehyde ratio decreased sharply together with a large increase in the relative amounts of decane (i.e. hydrogenation product of the 1-decene).

Figure 3.18 and **Figure 3.19** are graphical representations of the trends observed in these homogeneously catalysed reactions. In **Figure 3.18**, the system considered is of $Co_2(CO)_8$ and PPh_2Et; the first three bars in each category represent the results in the reproducibility experiments while the following two bars show the effect of increasing the P:Co ratio. In

Figure 3.19, the system considered is of $Co_2(CO)_8$ and DPPE; the first two bars in each category represent the results in the reproducibility experiments while the following two bars show the effect of increasing the P:Co ratio.

3.7.2. Recycling of impregnated zeolite catalysts

Each "set" of reactions carried out with catalysts 0.2ph/co, 0.2co/ph and 0.2pp/co consisted of three consecutive hydroformylation reactions in which the impregnated zeolite sample used in one reaction was "recycled", as described in Section 2.6.4. Two "sets" were carried out for each of the catalysts, one set involving no addition of extra phosphine to the system while the other set involved addition of extra phosphine to the system **before each and every reaction in a set**. The amount of phosphine added to the system contained moles of phosphorus equal to twice the moles of cobalt present on the zeolite before the first reaction in a set was started, ie. the same absolute amount of phosphine was added to each run. Note that this is different to the procedure followed with the high-cobalt catalysts and is also mentioned in Section 2.6.4.

Carbon balances, conversions, n:iso ratios and alcohol:aldehyde ratios for all the reactions are summarised in **Table 3.9**. The three experiment codes for each set of reactions corresponds (in numerical order) to the recycle number shown beneath the heading of each column, eg. for "**0.2ph/co**", PJV171 corresponds to reaction 1, PJV172 corresponds to reaction 2 and PJV173 corresponds to reaction 3. Duplicate sets were carried out with certain catalysts and are entered under the same heading in **Table 3.9**, eg. under "**0.2ph/co + extra PPh_2Et**", set PJV191-PJV193 and set PJV197-PJV199 are duplicate sets.

Table 3.10 summarizes the product distribution for each of the sets of reactions while **Table 3.11** shows the change in cobalt loading of the catalysts before and after each set of three reactions. For example: for "**0.2ph/co**", the initial cobalt loading is for 0.2ph/co before the first reaction (PJV171) was carried out and the final cobalt loading is for 0.2ph/co after the third consecutive reaction (PJV173) had been carried out.

Table 3.8 : Summary of reactions carried out with homogeneous catalysts (low-cobalt system) [a]

EXPERIMENT CODES	Concentration of cobalt ($g.l^{-1}$) [b]	P:Co ratio	Conversion	n:iso ratio	alc:ald ratio	Selectivities			Carbon Balance
						Decane	Aldehydes	Alcohols	
$Co_2(CO)_8$ + PPh_2Et									
PJV159 *	0.15	2	52.7%	1.15	0.30	7.2%	68.8%	20.8%	96.7%
PJV160 *	0.15	2	53.7%	1.13	0.26	7.2%	71.8%	18.6%	99.6%
PJV162 *	0.15	2	52.8%	1.12	0.28	7.4%	70.3%	19.3%	97.9%
PJV163	0.14	5	37.7%	2.03	0.32	10.2%	64.2%	20.4%	99.5%
PJV164	0.14	10	30.6%	3.54	0.33	13.7%	57.9%	19.3%	100.9%
$Co_2(CO)_8$ + DPPE									
PJV165 **	0.15	2	86.6%	0.80	0.35	8.3%	66.3%	22.9%	100.1%
PJV166 **	0.15	2	87.8%	0.75	0.30	8.4%	69.9%	20.9%	100.5%
PJV168	0.15	5	5.9%	2.80	0.19	26.5%	42.8%	8.3%	96.6%
PJV167	0.15	10	5.6%	2.58	0.19	28.6%	37.4%	7.1%	99.1%

a : Pressure (maintained) = 80 bar, temperature (maintained) = 180°C, reaction time = 2 hours

b : Total initial liquid volume = 60 cm^3 (decene:hexadecane 2:1)

* , ** : Duplicate reactions

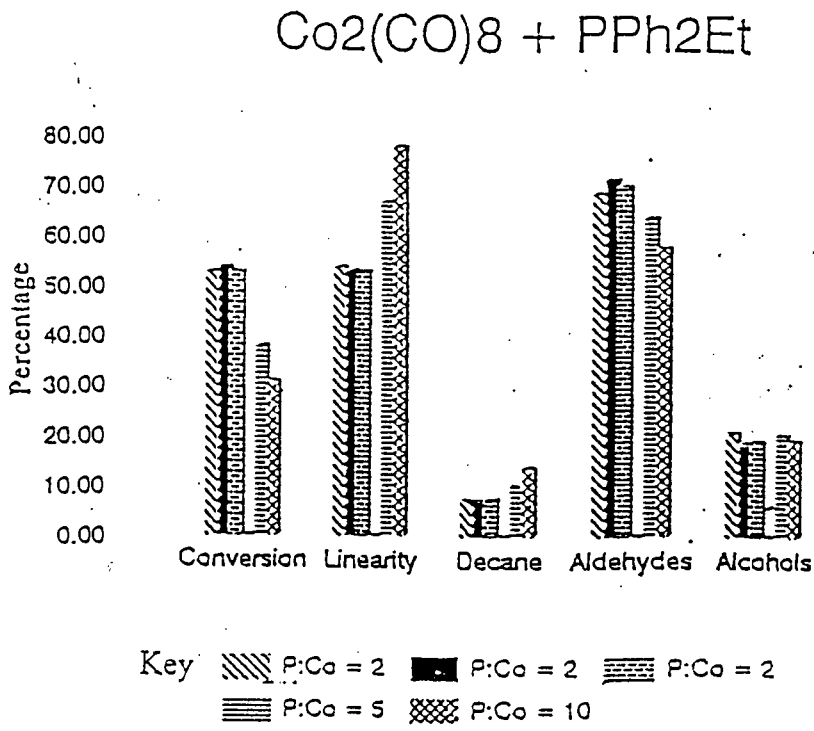

Figure 3.18 : Bar chart showing trends observed when $Co_2(CO)_8$ and PPh_2Et are used for homogeneously-catalysed hydroformylation of 1-decene

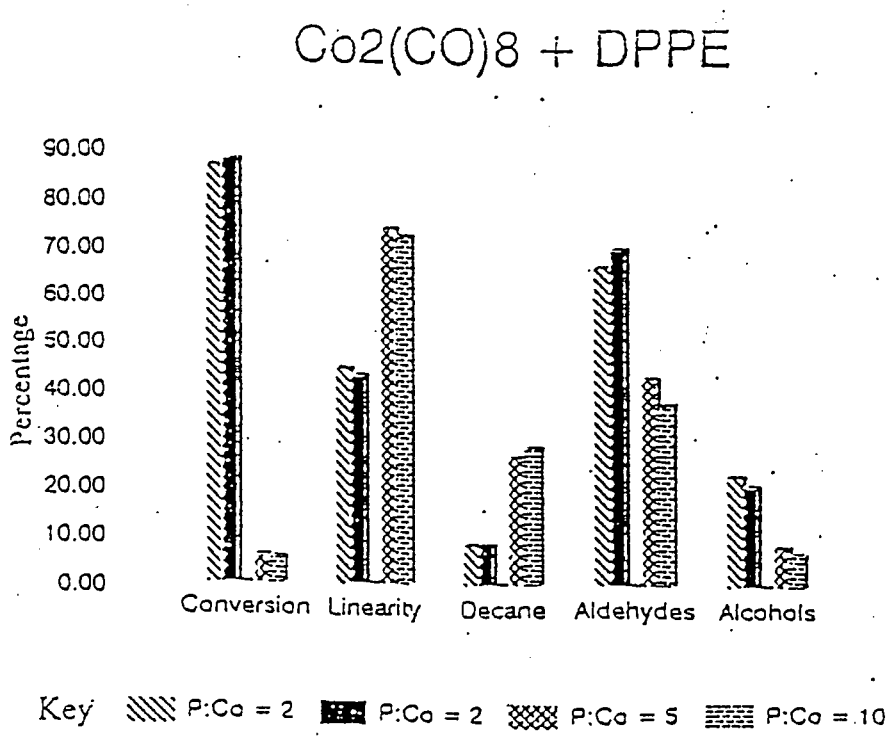

Figure 3.19 : Bar chart showing trends observed when $Co_2(CO)_8$ and DPPE are used for homogeneously-catalysed hydroformylation of 1-decene

Table 3.9 : Summary of recycle reactions carried out with 0.2ph/co, 0.2co/ph and 0.2pp/co [a]

EXPERIMENT CODES	P:Co ratio	Initial conc. of cobalt ($g.l^{-1}$) [b]	C balance			Conversion			n:iso ratio			Alcohol:aldehyde ratio		
Reaction number →			1	2	3	1	2	3	1	2	3	1	2	3
Homogenous : $Co_2(CO)_8$ + PPh_2Et (Average from **Table 3.8**)	2	0.15	98%	N/A	N/A	53.10%	N/A	N/A	1.13	N/A	N/A	0.28	N/A	N/A
0.2ph/co														
PJV171-PJV173	0.5 *	0.14	100%	100%	103%	24.19%	7.56%	4.45%	0.81	0.81	0.80	0.02	0	0
0.2ph/co + extra PPh_2Et														
PJV191-PJV193	2.5 *	0.14	97%	100%	100%	16.46%	16.48%	15.94%	0.95	1.54	1.74	0.03	0.09	0.11
PJV197-PJV199	2.5 *	0.14	102%	100%	99%	16.94%	16.10%	13.56%	0.92	1.60	1.96	0.02	0.09	0.10
0.2co/ph														
PJV177-PJV179	0.5 *	0.14	104%	101%	102%	16.17%	2.01%	1.59%	0.83	1.25	N/A	0	0	N/A
0.2co/ph + extra PPh_2Et														
PJV180-PJV182	2.5 *	0.14	96%	100%	103%	2.07%	14.84%	14.90%	1.98	1.74	1.71	0	0.11	0.08
PJV194-PJV196	2.5 *	0.14	96%	99%	103%	1.29%	12.72%	13.29%	no iso.	1.85	1.84	0	0.07	0.07
Homogeneous : $Co_2(CO)_8$ + DPPE (Average from **Table 3.8**)	2	0.15	100%	N/A	N/A	87.20%	N/A	N/A	0.78	N/A	N/A	0.33	N/A	N/A
0.2pp/co														
PJV183-PJV185	3 *	0.14	96%	102%	99%	23.81%	3.30%	1.05%	0.74	0.86	N/A	0.02	0.08	N/A
0.2pp/co + extra DPPE														
PJV186-PJV188	5 *	0.14	96%	98%	99%	0.94%	0.94%	0.91%	N/A	N/A	N/A	N/A	N/A	N/A

a : Pressure (maintained) = 80 bar, temperature (maintained) = 180°C, reaction time = 2 hours

b : Total initial liquid volume = 60 cm^3 (decene:hexadecane = 2:1)

* : Not determined by analysis; assumed, for the first reaction, due to the species initially present on the zeolite (see Section 4.2.)

N/A : Not Applicable

Table 3.10 : Product distributions of recycle reactions carried out with 0.2ph/co, 0.2co/ph and 0.2pp/co

EXPERIMENT CODES	Selectivities								
	Decane			Aldehydes			Alcohols		
Reaction number →	1	2	3	1	2	3	1	2	3
Homogenous : $Co_2(CO)_8$ + PPh_2Et (Average from **Table 3.8**)	7.3%	N/A	N/A	70.3%	N/A	N/A	19.6%	N/A	N/A
0.2ph/co									
PJV171-PJV173	8.0%	8.9%	9.6%	89.2%	83.7%	78.9%	1.7%	0%	0%
0.2ph/co + extra PPh_2Et									
PJV191-PJV193	8.8%	12.0%	12.4%	85.4%	77.0%	75.2%	2.7%	7.1%	8.3%
PJV197-PJV199	8.7%	12.3%	12.8%	86.7%	78.2%	75.7%	1.9%	7.3%	7.6%
0.2co/ph									
PJV177-PJV179	7.5%	13.1%	44.4%	91.0%	53.0%	0%	0%	0%	0%
0.2co/ph + extra PPh_2Et									
PJV180-PJV182	24.1%	13.4%	13.3%	60.0%	70.1%	77.9%	0%	7.7%	6.3%
PJV194-PJV196	25.0%	12.6%	12.8%	71.2%	76.6%	75.5%	0%	5.7%	5.4%
Homogeneous : $Co_2(CO)_8$ + DPPE (Average from **Table 3.8**)	8.4%	N/A	N/A	68.1%	N/A	N/A	21.9%	N/A	N/A
0.2pp/co									
PJV183-PJV185	8.6%	11.4%	18.4%	87.5%	58.4%	0%	1.6%	4.5%	0%
0.2pp/co + extra DPPE									
PJV186-PJV188	19.0%	17.7%	12.2%	0%	0%	0%	0%	0%	0%

Table 3.11 : Cobalt loading of 0.2ph/co, 0.2co/ph and 0.2pp/co before and after each set of recycle reactions

EXPERIMENT CODES	Cobalt loading (obtained from AA analyses)		
	Initial loading (mass % cobalt)	Final loading (mass % cobalt)	% cobalt remaining (final/initial)
0.2ph/co			
PJV171-PJV173	0.2	0.18	90%
0.2ph/co + extra PPh_2Et			
PJV191-PJV193	0.2	0.12	60%
PJV197-PJV199	0.2	0.08	40%
0.2co/ph			
PJV177-PJV179	0.2	0.19	95%
0.2co/ph + extra PPh_2Et			
PJV180-PJV182	0.2	0.08	40%
PJV194-PJV196	0.2	0.12	60%
0.2pp/co			
PJV183-PJV185	0.13	0.13	100%
0.2pp/co + extra DPPE			
PJV186-PJV188	0.13	0.13	100%

3.7.2.1. 0.2ph/co

Recycling of 0.2ph/co resulted in a decrease in conversion (24% to 4.5%) while the linearity of the products remained constant (0.8). Selectivity to decane increased slowly while selectivity to aldehydes and alcohols decreased. The amount of cobalt retained on the zeolite after the third reaction, PJV173, was 90%; however, this cobalt was not in the form of a carbonyl complex because no peaks were observed in the ν(CO) region of the IR spectrum

of the zeolite. No ν(CO) bands were observed in the IR spectra of the reaction solutions after any of the three reactions indicating that no cobalt carbonyl species were present in solution.

3.7.2.2. 0.2ph/co with extra PPh_2Et added

These two duplicate sets of reactions (PJV191-PJV193 and PJV197-PJV199) were similar to the set of reactions PJV171-PJV173 (see Section 3.7.2.1.) except that extra PPh_2Et was added to the reaction medium before each reaction. The conversion was constant for all three reactions (~16%) while the n:iso ratio of the products steadily increased (0.9 to 1.8). Selectivities to both decane and alcohols increased while selectivity to aldehydes decreased. The amount of cobalt retained on the zeolite after all three reactions was about 50%. The cobalt was in the form of some carbonyl complex because two peaks at 2002 cm^{-1} and 1902 cm^{-1} were present in the IR spectrum of the zeolite. ν(CO) bands were observed in the IR spectra of the solutions after each of the three reactions, indicating the presence of cobalt carbonyl species in solution. However, these species could not be identified.

3.7.2.3. 0.2co/ph

Recycling of 0.2co/ph resulted in a decrease in conversion (16% to 1.6%) while the linearity of the products appeared to increase slightly (0.8 to 1.25). Selectivity to decane increased sharply while selectivity to aldehydes decreased sharply; alcohols did not appear to have been formed in any of the reactions. The amount of cobalt retained on the zeolite after the third reaction (PJV179) was 95%; however, this cobalt was not in the form of a carbonyl complex because no ν(CO) bands were observed in the IR spectrum of the zeolite. No ν(CO) bands were observed in the IR spectra of the solutions after any of the reactions, indicating that no cobalt carbonyl species were present in solution.

3.7.2.4. 0.2co/ph with extra PPh_2Et added

These two duplicate sets of reactions (PJV180-PJV182 and PJV194-PJV196) were similar to the set of reactions PJV177-PJV179 (see Section 3.7.2.3.) except that extra PPh_2Et was added to the reaction medium before each reaction. The conversion was very low (1-2%) for the

first reaction but increased and steadied at about 14% conversion for the next two reactions. The n:iso ratio of the products remained fairly constant (1.7-2.0) for the second and third reaction as did selectivities to decane, aldehydes and alcohols. The anomalous results for the first reaction were very likely a function of the very low (almost negligible conversions) of 1-2%. The amount of cobalt retained on the zeolite after all three reactions was about 50%. The cobalt on the zeolite was in the form of some unidentified carbonyl complex, indicated by the presence of ν(CO) bands in the IR spectrum of the zeolite. The IR spectra of the reaction solutions showed ν(CO) bands after each of the three reactions, indicating the presence of cobalt carbonyl species in solution after reaction. However, these species could not be identified because the bands were broad and weak.

3.2.7.5. 0.2pp/co

Recycling of 0.2pp/co resulted in a decrease in conversion (24% to 1%) while the linearity of the products appeared to increase slightly (0.7 to 0.9). Selectivities to decane and alcohols increased while selectivity to aldehydes decreased sharply. The amount of cobalt retained on the zeolite after the third reaction (PJV185) was 100%; however, this cobalt was not in the form of a carbonyl complex because no ν(CO) bands were observed in the IR of the zeolite. No ν(CO) bands were observed in the IR spectra of any of the solutions.

3.2.7.6. 0.2pp/co with extra DPPE added

These reactions (PJV186-PJV188) were similar to PJV183-PJV185 (see Section 3.2.7.5.) except that extra DPPE was added to the reaction medium before each reaction. The conversion for all three reactions was negligible (<1%) and only some decane (no alcohols or aldehydes) was detected by GC analysis. The amount of cobalt retained on the zeolite after all three reactions was 100%. The cobalt was in the form of some carbonyl complex because three peaks at 2087 cm^{-1}, 2041 cm^{-1} and 2016 cm^{-1} were present in the IR spectrum of the zeolite. No ν(CO) bands were observed in the IR spectra of any of the solutions.

CHAPTER 4

Discussion

4. DISCUSSION

4.1. SYNTHESIS OF COBALT COMPOUNDS

The reactions of $Co_2(CO)_8$ with PPh_2Et or with DPPE in solution were investigated to compare the compounds formed to those formed on the Na-Y zeolite during the impregnation procedure. All complexes that were synthesized were characterised by IR analysis and melting point measurements. The various complexes synthesized by reaction of $Co_2(CO)_8$ with PPh_2Et were further characterised by ^{31}P NMR and elemental analysis.
^{31}P NMR and IR spectra of the complexes are shown in **Figures 3.2-3.9** and all data are summarised in **Table 3.2** and **Table 3.3** (see Section 3.2.).

4.1.1. Reaction of $Co_2(CO)_8$ with PPh_2Et

4.1.1.1. Reaction of $Co_2(CO)_8$ with PPh_2Et at 0°C under a nitrogen atmosphere

The reaction of $Co_2(CO)_8$ with PPh_2Et was carried out in hexane at ca. 0°C under nitrogen. This gave the complex $[Co(CO)_3(PPh_2Et)_2]^+[Co(CO)_4]^-$ **[1]** in 39% yield in the form of orange crystals.

The ^{31}P NMR spectrum of a solution of **[1]** shows two singlet peaks (see **Figure 3.3**), one at 55.4ppm due to **[1]** and one at 34.4 ppm due to ethyldiphenylphosphine oxide, $OPPh_2Et$ (see **Figure 3.1** and Section 3.2.1.1.). The single peak at 55.4 ppm indicates that in **[1]**, both phosphorus atoms are in the same environment. This is as expected for the proposed structure of $[Co(CO)_3(PR_3)_2]^+[Co(CO)_4]^-$ (R = alkyl or phenyl) formed by the reaction of monodentate tertiary phosphines and $Co_2(CO)_8$ at low temperatures (*49,78*). The cation, $[Co(CO)_3(PR_3)_2]^+$, is proposed to be a trigonal bipyramid with both phosphines occupying the axial positions, as shown in **Figure 4.1** (resulting in a single peak in a ^{31}P NMR spectrum of a solution of $[Co(CO)_3(PR_3)_2]^+[Co(CO)_4]^-$).

The infrared spectrum of **[1]** in the ν(CO) region is interpreted by comparison with that of a similar complex, $[Co(CO)_3(PPh_3)_2]^+[Co(CO)_4]^-$ **[2]** in acetone (see **Table 3.3**, *78*). The IR

spectrum of [2] shows two ν(CO) bands at 2008 cm^{-1} and 1887 cm^{-1}. The 2008 cm^{-1} band is assigned to the cation while the 1887 cm^{-1} band is assigned to the anion (*78*). This is very similar to the IR spectrum of [1] in the same solvent (see **Figure 3.2**) which shows bands at 2004 cm^{-1} and 1889 cm^{-1}.

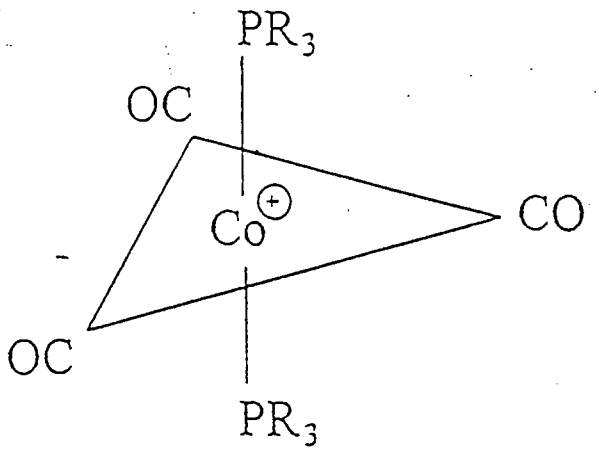

Figure 4.1 : Structure of the cation $[Co(CO)_3(PR_3)_2]^+$ (R = alkyl or phenyl)

4.1.1.2. Reaction of $Co_2(CO)_8$ with PPh_2Et in benzene refluxed under a nitrogen atmosphere

The reaction of $Co_2(CO)_8$ with PPh_2Et was carried out in benzene refluxed under nitrogen. This gave the complex $[Co(CO)_3(PPh_2Et)]_2$ [3] in 29% yield in the form of dark brown crystals.

The ^{31}P NMR spectrum of a solution of the dark brown crystals shows four singlet peaks (see **Figure 3.5**) at 63.4 ppm, 55.7 ppm, 34.4 ppm and -11.1 ppm. The peaks at -11.1 ppm and 34.4 ppm correspond to PPh_2Et and $OPPh_2Et$ respectively (see **Figure 3.1**). The peak at 55.7 ppm corresponds to [1], identified in Section 4.1.1.1. (see **Figure 3.3**). We assign the remaining singlet at 63.4 ppm to compound [3]. The singlet indicates that both phosphorus atoms in [3] are in the same environment. This is as expected for the proposed structure of $[Co(CO)_3(PR_3)]_2$ (R = alkyl or phenyl) formed by the reaction of monodentate tertiary

phosphines and $Co_2(CO)_8$ at elevated temperatures (*49,54*). Each cobalt is bonded to one phosphine in the axial position and three carbonyl groups in a trigonal planar arrangement, as shown in **Figure 1.10** (*49,54,62,63*).

The infrared spectrum of **[3]** in the ν(CO) region (shown in **Figure 3.4**) is interpreted by comparison with that of a similar complex, $[Co(CO)_3(PPh_3)]_2$ **[4]** in chloroform (see **Table 3.3**, *54*). The IR spectrum of **[4]** shows two ν(CO) bands at 1977 cm^{-1} and 1957 cm^{-1} (*54*). This is very similar to the IR spectrum of **[3]** in the same solvent showing bands at 1973 cm^{-1} and 1951 cm^{-1}.

The melting point obtained for **[3]** was 121-123°C. This fits a trend observed for some $[Co(CO)_3(PR_3)]_2$ complexes (**[5]**: R = PEt_3, **[6]**: R = $PPhEt_2$) reported by Manning (*54*): **[5]** has a melting point of 182-184°C and **[6]** has a melting point of 129-131°C, indicating a decrease in the melting point as ethyl groups of the tertiary phosphine are replaced by phenyl groups.

4.1.1.3. Reaction of $Co_2(CO)_8$ with PPh_2Et in benzene at 20°C under a CO atmosphere

The reaction of **[3]** with $Co_2(CO)_8$ and PPh_2Et was carried out at 20°C in benzene under 1 atmosphere pressure of CO. Two isomers of $Co_2(CO)_7(PPh_2Et)$ (non-bridged isomer : **[7]**; carbonyl-bridged isomer : **[8]**) were formed in 19% yield in the form of dark brown crystals. **[7]** and **[8]** could not be separated from each other.

The ^{31}P NMR spectrum of a solution of **[7]** and **[8]** (see **Figure 3.7**) shows two well-resolved singlets at 59.8 ppm and 34.3 ppm and two poorly resolved peaks at 63.5 ppm and 40 ppm. The poor quality of this spectrum is most likely due to the fact that the monosubstituted cobalt-tertiary phosphine complexes are unstable in solution (*51*). The peak at 34.3 ppm is due to the phosphine oxide, $OPPh_2Et$ while the peak at 63.5 ppm can be assigned to **[3]** (see **Figure 3.5**). The remaining two peaks at 59.8 ppm and 40 ppm are assigned to the two isomers, **[7]** and **[8]**.

Only four monosubstituted dimers of the type $Co_2(CO)_7(PR_3)$ have been reported in the

literature, namely $Co_2(CO)_7(PEt_3)$ (non-bridged isomer : **[9]**; carbonyl-bridged isomer : **[10]**) (*64*) as well as $Co_2(CO)_7(PPh_3)$ **[11]**, $Co_2(CO)_7(PBu_3)$ and $Co_2(CO)_7\{P(C_6H_{11})_3\}$ (*51,79*). Only Capron-Cotigny and Poilblanc (*64*) observed and reported carbonyl-bridged isomers. Furthermore, only the IR spectra of these complexes are reported. In the IR spectrum of **[7]** and **[8]**, there are nine distinguishable ν(CO) bands (see **Figure 3.6** and **Table 3.3**). The five bands for **[7]** at 2079 cm^{-1}, 2024 cm^{-1}, 2013 cm^{-1}, 1994 cm^{-1} and 1957 cm^{-1} correspond very closely to the five bands reported for **[9]** and **[11]** at 2079 cm^{-1}, 2026 cm^{-1}, 2010 cm^{-1}, 1996 cm^{-1}, and 1964 cm^{-1} (*51,79*). The five bands for **[8]** at 2079 cm^{-1}, 2044 cm^{-1}, 2037 cm^{-1}, 1850 cm^{-1} and 1829 cm^{-1} are similar to the five bands reported for **[10]** at 2081 cm^{-1}, 2039 cm^{-1}, 2037 cm^{-1}, 1850 cm^{-1} and 1827 cm^{-1} (*64*). The bands at 1850 cm^{-1} and 1827 cm^{-1}, indicating bridging carbonyls, confirm that **[8]** is present. The single band at 2079 cm^{-1} is assumed to consist of two overlapping bands at almost the same frequency, one band for **[7]** and one band for **[8]**.

4.1.2. Reaction of $Co_2(CO)_8$ with DPPE

4.1.2.1. Reaction of $Co_2(CO)_8$ with DPPE at 0°C under a nitrogen atmosphere

The reaction of $Co_2(CO)_8$ with DPPE was carried out in hexane at ca. 0°C under nitrogen. This gave the complex $[Co_2(CO)_4(DPPE)_3]^{2+}\{[Co(CO)_4]^-\}_2$ **[12]** in 10% yield as yellow crystals.

The infrared spectrum of **[12]** in the ν(CO) region (see **Figure 3.8** and **Table 3.3**) shows three bands at 2006 cm^{-1}, 1955 cm^{-1} and 1885 cm^{-1}. These bands are very similar to those reported by Thornhill and Manning (*53*) for **[12]** at 2007 cm^{-1}, 1955 cm^{-1} and 1885 cm^{-1}.

4.1.2.2. Reaction of $Co_2(CO)_8$ with DPPE in benzene refluxed under a nitrogen atmosphere

The reaction of $Co_2(CO)_8$ with DPPE was carried out in benzene refluxed under nitrogen. This gave the complex $[Co(CO)_2(DPPE)]_2$ **[13]** in 93% yield as red-brown crystals.

The infrared spectrum of **[13]** in the ν(CO) region (see **Figure 3.9** and **Table 3.3**) shows four bands at 1951 cm^{-1}, 1920 cm^{-1}, 1749 cm^{-1} and 1723 cm^{-1}. The last three of these bands correlate very closely with those reported for **[13]** in the literature. Pedersen and Robinson report ν(CO) bands at 1920 cm^{-1}, 1753 cm^{-1} and 1728 cm^{-1} in CH_2Cl_2 (*65*); Thornhill and Manning report ν(CO) bands at 1922 cm^{-1}, 1752 cm^{-1} and 1728 cm^{-1} in CS_2 (*53*). However, the first peak reported by Pedersen and Robinson was at 1970 cm^{-1} while Thornhill and Manning report it at 1957 cm^{-1}; this discrepancy cannot be explained on the basis of different solvents (CH_2Cl_2 vs CS_2) because the shift is too large (> 20 cm^{-1}). It was noted that Pedersen and Robinson reported the IR spectrum of the analogous $[Co(CO)_2(DPPM)]_2$ as showing a strong peak at 1957 cm^{-1} with a weak one at 1970 cm^{-1}. This, combined with the correlation between the results obtained in this thesis and the results of Thornhill and Manning, suggests that a peak at about 1955 cm^{-1} is correct for **[13]**.

4.2. IMPREGNATION OF ZEOLITES WITH $Co_2(CO)_8$ AND TERTIARY OR BIDENTATE PHOSPHINE LIGANDS

4.2.1. Na-Y zeolite impregnated with PPh_2Et followed by $Co_2(CO)_8$ (4ph/co)

The IR spectrum in the ν(CO) region of the impregnated zeolite is shown in **Figure 3.10**. The three peaks observed at 2007 cm^{-1}, 1999 cm^{-1} and 1884 cm^{-1} indicate the presence of a cobalt carbonyl complex on the zeolite. It is suspected that the two peaks at 2007 cm^{-1} and 1999 cm^{-1} are actually one peak split into two by the effect of solid-state splitting (the sample was mixed with KBr and pressed into a disc to obtain the IR spectrum).

The spectrum in **Figure 3.10** is very similar to the IR spectrum obtained for **[1]** shown in **Figure 3.2**. **[1]** was mixed with KBr and Na-Y zeolite and pressed into a disc. The IR spectrum of this disc showed two bands in the carbonyl region, one at about 2002 cm^{-1} (showing slight splitting) and one at 1883 cm^{-1}. From this, it was concluded that the cobalt species present in catalyst 4ph/co was $[Co(CO)_3(PPh_2Et)_2]^+[Co(CO)_4]^-$.

4.2.2. Na-Y zeolite impregnated with DPPE followed by $Co_2(CO)_8$ (4pp/co)

The IR spectrum in the ν(CO) region of the impregnated zeolite is shown in **Figure 3.11**. The three peaks observed at 2007 cm^{-1}, 1951 cm^{-1} and 1878 cm^{-1} indicate that a cobalt carbonyl species was present on the zeolite.

The IR spectrum in **Figure 3.11** is very similar to the IR spectrum obtained for **[12]** shown in **Figure 3.8**. **[12]** was mixed with KBr and Na-Y and pressed into a disc. The IR spectrum of this disc showed three bands at 2005 cm^{-1}, 1953 cm^{-1} and 1887 cm^{-1}. From this, it was concluded that the cobalt species present in catalyst 4pp/co was $[Co_2(CO)_4(DPPE)_3]^{2+}\{[Co(CO)_4]^-\}_2$.

4.2.3. Na-Y zeolite impregnated with PPh_2Et followed by $Co_2(CO)_8$ (0.2ph/co)

The IR spectrum in the ν(CO) region of the impregnated zeolite is shown in **Figure 3.12**. Three bands were observed at 2084 cm^{-1}, 2022 cm^{-1} and 1983 cm^{-1} indicating the presence of a cobalt carbonyl complex on the zeolite. It should be noted that the bands observed in **Figure 3.12** differ considerably from the bands observed in **Figure 3.10** in 4ph/co (higher cobalt loading). This indicates that the species present in 0.2ph/co was different to the species present in 4ph/co.

This IR spectrum does not resemble the spectrum of **[1]**, which only shows two ν(CO) bands (see **Figure 3.2**). Rather, it more closely resembles the IR spectrum of either **[3]** mixed with Na-Y and KBr (shown in **Figure 4.2**) or **[7]**, the unbridged isomer of $Co_2(CO)_7(PPh_2Et)$. It should be noted that the IR spectrum in the ν(CO) region of **[3]** mixed with Na-Y and KBr is different to the IR spectrum of **[3]** in solution (compare **Figure 4.2** with **Figure 3.4**). **[3]** was the only synthesized cobalt complex for which this was the case; **[1]**, **[7]**/**[8]**, **[12]** and **[13]** all produced similar IR spectra in the ν(CO) region, whether in solution or mixed with Na-Y and KBr. The IR spectrum of [3] showed three ν(CO) bands at 1972 cm^{-1}, 1950 cm^{-1} and 1933 cm^{-1}. The shifts of these three bands from the bands in the IR spectrum of 0.2ph/co were 102 cm^{-1}, 72cm^{-1} and 50 cm^{-1}. These shifts are considerable when compared to shifts observed in literature which are used as evidence for encapsulation (see discussion in Section

4.2.6.). The spectrum of $Co_2(CO)_7(PPh_2Et)$ shown in **Figure 3.6** resembles the IR spectrum of 0.2ph/co more closely because the fairly strong bands at 2079 cm^{-1}, 2024 cm^{-1} and 1994 cm^{-1} of the unbridged cobalt-phosphine complex, [7], show smaller shifts (<10 cm^{-1}).

From these results, it was concluded that the cobalt species present in 0.2ph/co was the unbridged isomer of $Co_2(CO)_7(PPh_2Et)$, [7]. It is interesting to note that, although the conditions of impregnation were similar to those used for the formation of [1] in solution and in 4ph/co, the reduction in the cobalt loading of the zeolite (from about 4% to about 0.2%) resulted in the formation of [7] instead of [1].

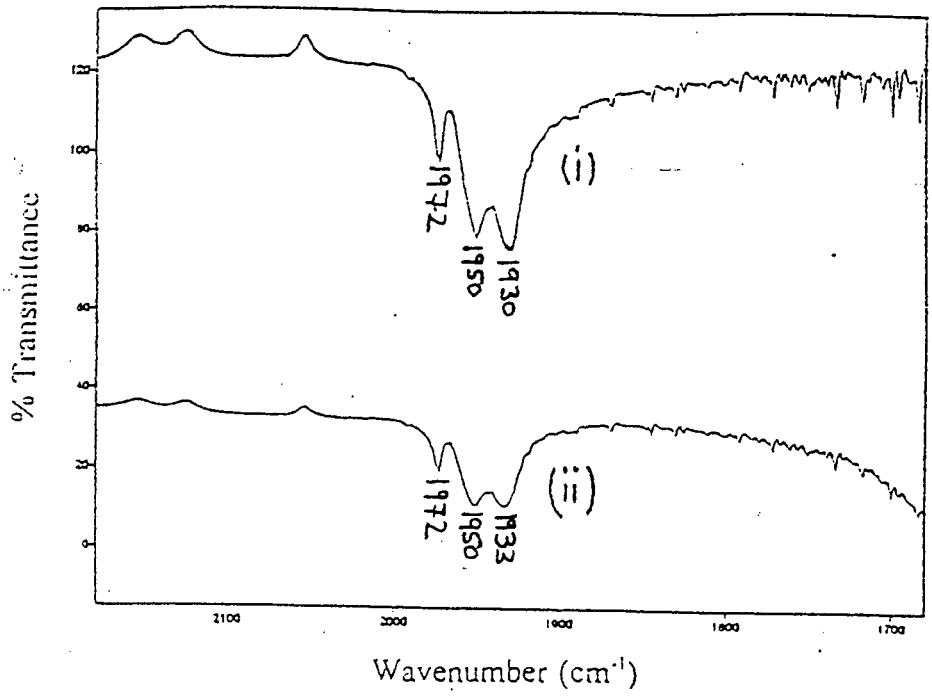

Figure 4.2 : IR spectra at 25°C in the ν(CO) region of $[Co(CO)_3(PPh_2Et)]_2$ mixed with (i) KBr and (ii) KBr and Na-Y

4.2.4. Na-Y zeolite impregnated with $Co_2(CO)_8$ followed by PPh_2Et (0.2co/ph)

The IR spectrum in the ν(CO) region of this impregnated zeolite is identical to that of the zeolite impregnated with PPh_2Et followed by $Co_2(CO)_8$ (see **Figure 3.12**). Thus, the cobalt species in 0.2ph/co and 0.2co/ph was the same, ie. **[7]**. This is interesting since it shows that reversal of the order of impregnation of $Co_2(CO)_8$ and PPh_2Et into zeolite Y under the conditions described in Section 2.6.2. does not affect the cobalt species formed in the zeolite. Furthermore, since $Co_2(CO)_8$ can easily enter the pores of the zeolite, this suggests that **[7]** was actually encapsulated in 0.2ph/co and 0.2co/ph.

4.2.5. Na-Y zeolite impregnated with DPPE followed by $Co_2(CO)_8$ (0.2pp/co)

The IR spectrum in the ν(CO) region of this impregnated zeolite is shown in **Figure 3.13**. Two peaks were observed at 2006 cm^{-1} and 1951 cm^{-1}. These two peaks were almost identical to two peaks shown in **Figure 3.11** (IR spectrum of $[Co_2(CO)_4(DPPE)_3]^{2+}\{[Co(CO)_4]^-\}_2$) corresponding to the cation. However, the band corresponding to the $[Co(CO)_4]^-$ anion (at 1885 cm^{-1}) was missing. It is possible that an ion exchange process had taken place: the $[Co_2(CO)_4(DPPE)_3]^{2+}$ ion replaced two Na^+ ions present in the Na-Y zeolite and the Na^+ ions reacted with $[Co(CO)_4]^-$ to form $Na^+[Co(CO)_4]^-$. The $Na^+[Co(CO)_4]^-$ remained in the impregnation solvent (benzene in this case) and therefore did not give rise to a ν(CO) band at 1885 cm^{-1} in the IR spectrum of 0.2pp/co. From these results, it was concluded that the species present in 0.2pp/co was the cation, $[Co_2(CO)_4(DPPE)_3]^{2+}$.

4.2.6. Location of the cobalt complexes from impregnation data

An important question arises concerning the location of the cobalt-phosphine complexes present on/in the zeolite support: were they attached to the outside of the zeolite crystals or were they encapsulated within the supercages of the zeolite crystals?

It has been reported that the ν(CO) bands of encapsulated transition metal carbonyl complexes are shifted compared to the bands observed for the same species present in solution (*11,25,29,32,33,80*). This is because the zeolite acts as a "solid solvent"; the high electrostatic

fields present in the zeolite Y supercages give the zeolite its solvent properties and affect the IR spectra of encapsulated carbonyl complexes (*25*). Large shifts (> 10 cm^{-1}) (*11,32,80*) as well as smaller shifts (< 10 cm^{-1}) (*29,33*) have been reported for encapsulated species. However, large shifts (*11,25,33*) and small shifts (*33*) have also been reported for species merely deposited on the outside of the zeolite crystals. The large shifts in ν(CO) bands were attributed to strong interactions with the zeolite surface (either inside the cages or on the zeolite crystal surfaces) while smaller shifts were attributed to weak interactions with the zeolite surface. "Ship-in-a-bottle" complexes should ideally show the weaker shifts because this means that immobilisation on the zeolite support is due to the size of the immobilised complex as opposed to some electronic interaction with the surface of the zeolite.

Purely from the shifts observed in the IR spectra of the impregnated zeolites in Sections 4.2.1.-4.2.5., it was not apparent which of the impregnated zeolites definitely contained encapsulated cobalt complexes. Further experiments involving washing of the zeolites with solvents and reactions with the zeolites as catalysts were carried out to try to discover the location of the complexes.

4.3. WASHING OF IMPREGNATED ZEOLITES WITH SOLVENTS

The impregnated zeolites described in Sections 3.4.1. and 3.4.2. were washed with a number of solvents to see the effect on the zeolites after the impregnation procedure (see washing procedure in Section 2.4.5.). If the complexes were inside the supercages of the zeolites, their sizes would prevent them being washed out by any solvents; if they were on the zeolite surface, they would wash off fairly easily.

4.3.1. High-cobalt catalysts (~4.5% cobalt)

This section describes the effects of washing 4ph/co and 4pp/co with a variety of solvents. The results of the AA analyses of the zeolites before and after washing are summarised in **Table 3.5**, Section 3.5.

IR spectra of the two zeolites (**Figure 3.10** and **Figure 3.11**) showed that the ionic species,

[1] and **[12]**, were present in 4ph/co and 4pp/co respectively (see Section 4.2.).

Dichloromethane was the only solvent that washed off much of the cobalt complexes from 4ph/co and 4pp/co (see **Table 3.5**). This makes sense: the initial species present on the zeolites were ionic and ionic complexes are not soluble in any of the other nonpolar solvents. Furthermore, dichloromethane washed off large amounts of the cobalt species from both 4ph/co and 4pp/co (as shown in **Figure 3.14** and **Figure 3.15**), lending support to the supposition that most of the cobalt species were not encapsulated within the zeolite but merely deposited upon the zeolite surface. This was expected in the case of impregnation with $Co_2(CO)_8$ and DPPE (4pp/co) since calculations of the size of DPPE molecules suggested that they could not enter the pores of Na-Y zeolite (see **Table 3.1**). However, PPh_2Et should have been able to enter the zeolite pores to react with $Co_2(CO)_8$ within the zeolite supercages.

The fact that **[1]** was predominantly deposited on the zeolite exterior surface in 4ph/co can be explained in terms of the adsorption characteristics of phosphines on zeolite surfaces together with the level of loading of cobalt and phosphine on the zeolite samples. Tertiary phosphines adsorb very strongly to the surface of zeolite Y, eg. PMe_3 cannot be entirely removed from the zeolite by evacuation of a zeolite-PMe_3 sample at room temperature (*80* and personal communication with A.J. Poë). Furthermore, the loading of 4ph/co with 10 cobalt atoms per supercage equates to about 20 phosphine molecules per zeolite supercage (see **Table 3.4**, Section 3.4. and the fact that P:Co = 2 in the impregnation procedure in Section 2.5.2.1.). Therefore, it is very likely that some of the PPh_2Et entered the zeolite pores and supercages, filling them and ultimately blocking the pores so that a large proportion of the PPh_2Et adsorbed to the outside surface of the zeolites. When the cobalt carbonyl was introduced, most of the reaction with PPh_2Et occurred on the outside surface of the zeolite.

After exhaustive washing with CH_2Cl_2, 4ph/co had a cobalt loading of 0.61% which was of the same order achieved in 0.2ph/co (0.2%, **Table 3.4**). This suggests that some cobalt carbonyl did actually manage to enter the cages of the zeolite, remaining on 4ph/co as encapsulated species within the zeolite supercages. Nevertheless, most of the cobalt was washed off the zeolite.

4pp/co ultimately had a cobalt loading of 0.17%, which is almost identical to the 0.13% cobalt loading achieved in 0.2pp/co. It appears that a small amount of DPPE managed to diffuse into the cages of the zeolite due to flexibility in its ethyl bridge and reacted with $Co_2(CO)_8$ inside the zeolite cages.

The washing experiments indicate that most of the cobalt complexes in both 4ph/co and 4pp/co were present predominantly on the exterior surface of the zeolite support and that only small amounts of the complexes were encapsulated within the zeolite cages.

4.3.2. Low-cobalt catalysts (~0.2% cobalt)

Washing 0.2ph/co, 0.2co/ph and 0.2pp/co with hexane, dichloromethane and 1-decene did not remove any of the cobalt complexes present on the zeolites. None of the aliquots of solvents filtered through the catalysts showed any ν(CO) bands and AA analyses showed that 100% of the cobalt was retained in the zeolite supports in all cases. These results indicate that the cobalt-phosphine complexes present in these samples was encapsulated within the supercages of the zeolite.

4.4. USE OF HIGH-COBALT CATALYSTS UNDER HYDROFORMYLATION REACTION CONDITIONS

It should be noted that Section 4.4.1. and Section 4.4.2. are general discussions, applicable to the low-cobalt catalysts (~0.2% cobalt) as well.

4.4.1. Some important equilibria between phosphines and cobalt carbonyl species

As mentioned in Section 1.5.2. and Section 1.5.3., the active cobalt catalysts under hydroformylation conditions are hydride species. If no tertiary or bidentate phosphine is present, the hydride is $HCo(CO)_4$. When a tertiary phosphine is present in the system, there is actually an equilibrium between the substituted hydride, $HCo(CO)_3(PR_3)$ (R = alkyl or aryl group), and the unsubstituted hydride, shown in equation (1) in Section 1.5.3. and repeated below:

$$HCo(CO)_4 + PR_3 \rightleftharpoons HCo(CO)_3(PR_3) + CO \quad \text{.....(1)}$$

Both the substituted and unsubstituted hydrides are not stable at room temperature and atmospheric pressure and decompose to $[Co(CO)_3(PR_3)]_2$ and $Co_2(CO)_8$ respectively (*81,82*). Although the equilibrium has been reported for the system containing $Co_2(CO)_8$ and monodentate tertiary phosphines (*40* and Section 1.5.3.), no reports have discussed the equilibrium involved when DPPE, a bidentate, chelating phosphine, has been used. Reactions have been carried out using $Co_2(CO)_8$ and DPPE for catalysis of the hydroformylation reaction (*3,83*), but no mechanistic studies were carried out. Since no information was forthcoming in the literature, it was assumed that the equilibria shown in equation (9) and equation (10) occur under hydroformylation conditions (by analogy with the tertiary phosphines):

$$HCo(CO)_4 + DPPE \rightleftharpoons HCo(CO)_3(DPPE) + CO \quad \text{... (9)}$$

$$HCo(CO)_3(DPPE) \rightleftharpoons HCo(CO)_2(DPPE) + CO \quad \text{... (10)}$$

The equilibrium in equation (9) involves the substitution of one carbonyl ligand on the cobalt hydride by one of the phosphorus atoms present in the DPPE molecule. The proposed substituted hydride is shown in **Figure 4.3**. This is analogous to monosubstitution observed with monodentate tertiary phosphines, although no evidence for this species has been found in the literature. The equilibrium in equation (10) involves the replacement of a second carbonyl ligand to form a chelate complex; the resultant hydride is shown in **Figure 4.4**.

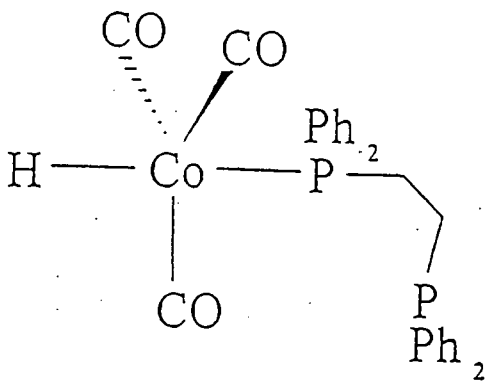

Figure 4.3 : The proposed monosubstituted hydride, $HCo(CO)_3(DPPE)$

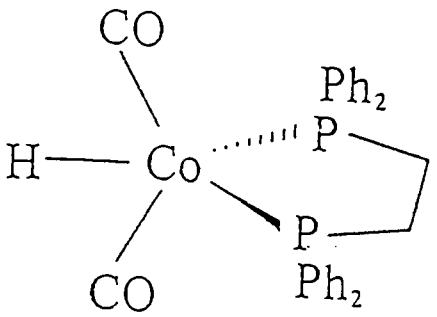

Figure 4.4 : The disubstituted hydride, $HCo(CO)_2(DPPE)$

Although there is no hydroformylation *in situ* IR data to support this in the literature or in the experiments carried out in this project, the disubstituted hydride shown in **Figure 4.4** has been reported in the literature (*84*). Furthermore, the hydride appeared to be stable (unlike the hydrides of the tertiary phosphines) since it was recrystallised and characterised by melting

point, IR and elemental analysis (*84*). This stability is due to the chelate effect by complexation of DPPE to the cobalt carbonyl hydride.

In the case of the monosubstituted DPPE-hydride, the coordinatively unsaturated 16e⁻ species which would take part in the catalytic cycle would be $HCo(CO)_2(DPPE)$, by analogy with the monodentate tertiary phosphine complexes. In the case of the disubstituted hydride, the coordinatively unsaturated 16e⁻ species which would take part in the catalytic cycle would be HCo(CO)(DPPE). The extra electron density on the cobalt centre due to donation by two phosphorus atoms would strengthen the bonds of the cobalt centre to the remaining carbonyl ligands by pi back-bonding. Thus, the chelate effect of DPPE resulting in the disubstituted hydride would be expected to reduce the activity of this hydride when compared to the tertiary phosphine hydrides because it would be more difficult for loss of a carbonyl ligand to occur to form the coordinatively unsaturated 16e⁻ species, HCo(CO)(DPPE).

From the equilibria given in equations (1), (9) and (10), it would appear that increasing the concentration of tertiary or bidentate phosphine in solution should shift the equilibria further to the right, ie. increasing the equilibrium concentration of the substituted hydride. However, this is only true for phosphines with weak basicities (low pK_a values). A strongly basic phosphine (such as PBu_3) shifts the equilibrium shown in equation (1) far to the right even at stoichiometric ratios of $HCo(CO)_4$ and PR_3 (ie. P:Co = 1) and an increase in concentration of phosphine does not affect the equilibrium much. For weaker bases, such as PPh_2Et, the equilibrium lies far to the left at P:Co < 2 (*40*). In this case, increasing the phosphine concentration shifts the equilibrium further and further to the right, increasing the equilibrium concentration of the substituted hydride. The effect is shown in **Figure 4.5** in a graph (note: log k_r = rate of hydroformylation reaction) and a table of pK_a values, reproduced from page 56 of a review on hydroformylation by F.E. Paulik (*40*).

The DPPE ligand is different to the monodentate tertiary phosphines in that it has two phosphorus atoms per molecule capable of bonding to cobalt. The pK_a values of the two phosphorus atoms have been reported as 3.86 and 0.99 (determined by successive protonation of the two atoms) (*85*). With reference to **Figure 4.5**, this means that DPPE is even less basic than PPh_2Et. For low P:Co ratios (< 2), the equilibria in equation (9) and equation (10)

should be shifted far to the left and the predominant species in solution should be the unsubstituted hydride. If a large amount of phosphine is present in solution, the equilibria should be shifted to the right and the predominant species present should be the disubstituted hydride.

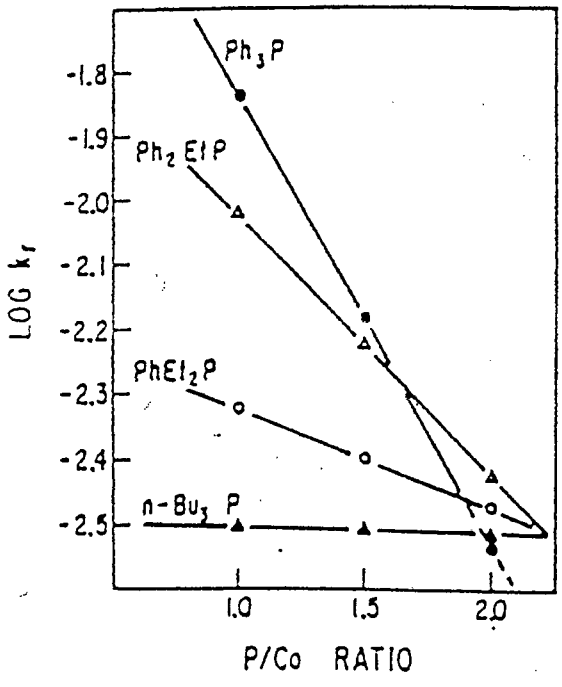

Organo-phosphine ligand	pKa value
i-Pr_3P	9.4
Et_3P	8.7
n-Pr_3P	8.6
n-Bu_3P	8.4
n-Oct_3P	8.4
Et_2PhP	6.3
$EtPh_2P$	4.9
Ph_3P	2.7

k_r : rate constant of hydroformylation reaction

Figure 4.5 : The effect of basicity of organophosphine ligands together with the P:Co ratio on the rate of hydroformylation

4.4.2. Catalyst colour : a qualitative indicator of catalyst activity

During the reactions using the various impregnated zeolites as catalysts, it was observed that the colour of the zeolites was a good, qualitative indicator of their activity. The catalysts tended to remain active if they were yellow or orange; this was not surprising since the cobalt carbonyl phosphine complexes were all yellow, orange or brown. If a catalyst turned purple, it had usually lost most of its activity. The species which gave this colour to the zeolite was not identified but a few possibilities are suggested. The purple colour was exactly the same as the following samples, all prepared in the laboratory :

(i) dehydrated CoNa-Y zeolite, ie. Na-Y zeolite partially ion-exchanged with cobalt ions; the cobalt was present as Co^{2+} ions
(ii) Na-Y impregnated with $Co_2(CO)_8$ and exposed to air
(iii) $Co_2(CO)_8$ exposed to air. The cobalt is most likely present as some oxide of cobalt (most probably CoO in which the cobalt is in the 2+ state).

Case (ii) has also been reported in literature but the species on the zeolite has only been referred to as "$Co_2(CO)_8$" (*86*). It is suspected that the species is either an oxide of cobalt (case (iii)) or a "subcarbonyl" species with formula $Co_x(CO)_y$ in which x is not necessarily 2 and y is not necessarily 8 (this term was coined by Schneider *et al* (*33*)).

Thus, the purple colour of the inactive catalysts could have been due to Co^{2+} ions, cobalt oxide (cobalt also in the 2+ state) or cobalt "subcarbonyls".

4.4.3. Reactions under hydroformylation conditions in decane (no alkene reagent)

Experiments were carried out using 4ph/co and 4pp/co. These reactions were performed to see the effect of the reaction temperature and pressure on the hybrid zeolite catalyst in the absence of alkene reagent.

4.4.3.1. 4ph/co

The IR spectrum of the solution after the experiment was completed (see **Figure 3.16**) showed one main ν(CO) band at 1960 cm^{-1}, indicating the presence of a cobalt carbonyl species in solution. The infrared spectrum of 4ph/co after reaction (see **Figure 3.16**) showed two ν(CO) bands at 1956 cm^{-1} and 1933 cm^{-1}, indicating the presence of a cobalt carbonyl species on the zeolite support.

The cobalt carbonyl species in the zeolite appeared to be $[Co(CO)_3(PPh_2Et)]_2$. The bands at 1956 cm^{-1} and 1933 cm^{-1} are similar to the bands at 1950 cm^{-1} and 1933 cm^{-1} observed for $[Co(CO)_3(PPh_2Et)]_2$ mixed with Na-Y and KBr (see **Figure 4.2**). The band at 1956 cm^{-1} is very broad, probably hiding another band at 1970 cm^{-1}. The ν(CO) band at 1960 cm^{-1} in the IR spectrum of the solution (see **Figure 3.16**) indicates that the species in solution was also $[Co(CO)_3(PPh_2Et)]_2$ (cf. the strong band at 1951 cm^{-1} shown in **Figure 3.4**). These IR spectra show that, under reaction conditions, some cobalt was retained on the zeolite and some leached out of the zeolite into solution. It could not be deduced where the cobalt remaining on the zeolite was situated.

4.4.3.2. 4pp/co

The infrared spectrum of the solution after the experiment was completed (see **Figure 3.17**) showed a large number of ν(CO) bands, indicating the presence of at least one, but very likely more than one, cobalt carbonyl species in solution. This IR spectrum was not similar to any of the cobalt-DPPE complexes synthesized and thus the species present in solution could not be identified. The infrared spectrum of 4pp/co after reaction (see **Figure 3.17**) showed a single weak ν(CO) band at 1936 cm^{-1}, indicating the presence of a cobalt carbonyl species on the zeolite support. The band was very badly resolved indicating a very low concentration of a carbonyl complex; the identity of the species could not be determined. These IR spectra show that, under hydroformylation conditions, some of the cobalt was retained on the zeolite while the rest leached out of the zeolite into solution. It could not be deduced where the cobalt remaining on the zeolite was situated.

4.4.3.3. General comments

The fact that cobalt carbonyl complexes were observed in solution when 4ph/co and 4pp/co were placed under hydroformylation reaction conditions correlated well with the washing experiments, supporting the supposition that most, if not all, of the cobalt carbonyl-phosphine complexes were present on the outside surface of the zeolites. The fact that cobalt carbonyl complexes were observed on the zeolites after the experiments were complete suggested that some cobalt was still retained on the zeolite, but it was not obvious whether this was due to encapsulation or merely interaction with the exterior surface of the zeolite crystals.

4.4.4. Hydroformylation reactions : impregnated zeolites vs homogeneous catalysts

4.4.4.1. $(Co_2(CO)_8 + PPh_2Et)$ vs 4ph/co

The experiments to be compared are PJV123 (homogeneous) and PJV116 (4ph/co).

Surprisingly, the conversion for the reaction with 4ph/co (63%) was higher than that achieved using the homogeneous catalyst (48%), especially considering that the cobalt concentration in the homogenously catalysed reaction was slightly higher than with 4ph/co. Also, if the cobalt complex was truly encapsulated within the zeolite supercages, there should have been mass transfer restrictions on movement of the reagents into and out of the zeolite cage and pore network. This would have reduced the activity of the impregnated zeolite catalyst compared to the homogeneous catalyst.

In the homogeneous case, it was observed that there was particulate matter at the bottom of the autoclave after the reaction was completed. This indicated that part of the cobalt carbonyl had been decomposed under reaction conditions, eliminating this cobalt from the catalytic cycle. In the reaction using 4ph/co, the same residue was not observed. Possibly the zeolite affected the cobalt complex in solution and prevented decomposition in solution. It should be noted that the zeolite was a light grey/purple colour indicating that, although the cobalt carbonyl complex in solution was stable, the complex on the zeolite itself had undergone a deactivating transformation (see Section 4.4.2.).

The solutions of both experiments after completion showed a very strong ν(CO) band at about 1957 cm^{-1}, characteristic of the covalent disubstituted dimer, $[Co(CO)_3(PPh_2Et)]_2$ (cf. **Figure 3.4**). The colour of the solutions was also identical to solutions of $[Co(CO)_3(PPh_2Et)]_2$; a deep red-brown. This shows that the cobalt on the zeolite leached off extensively into solution, supporting the observations made in the washing experiments. Most, if not all, the catalysis occurring in this system (PJV116) would therefore be due to homogeneous catalysis.

The decomposition of cobalt carbonyl in the homogeneously-catalysed system not only helps to explain the lower apparent activity of the homogeneous catalyst but also explains the higher linearity of the products and the higher selectivity to alcohols obtained in that reaction. Converting soluble cobalt carbonyl to insoluble residue would effectively increase the P:Co ratio in solution, increasing the equilibrium concentration of the substituted hydride. This hydride is less active and more selective for formation of linear products and of alcohols than the unsubstituted hydride.

4.4.4.2. $(Co_2(CO)_8$ + DPPE) vs 4pp/co

The conversions, product linearities and product selectivities for homogeneous vs impregnated zeolite catalytic systems were basically the same: conversion 87% vs 83%, n:iso 1 vs 0.8 and product selectivities within 2% of each other (see **Table 3.6**, reactions PJV109 and PJV122).

Unlike the previous case (Section 4.4.4.1.), no residue was observed in the homogeneously-catalysed system after the experiment was completed. This is probably because the complex formed between DPPE and cobalt carbonyl is much more stable than the complex formed between PPh_2Et and cobalt carbonyl, which prevented decomposition to metallic cobalt.

The same cobalt carbonyl species were present in the solutions of both the homogeneous catalyst and the impregnated-zeolite catalyst systems (observed in IR spectra of the solutions). Thus, cobalt did leach out of the zeolite into solution under hydroformylation conditions. In light of the similar conversions achieved in both reactions, it is very likely that almost all catalysis with the impregnated-zeolite system occurred due to homogeneous catalysis. The

zeolite had turned a light grey/purple colour after the reaction had been carried out, indicating that some cobalt species was still present on the zeolite but not as an active hydroformylation catalyst (as per the discussion in Section 4.4.2).

These results are in agreement with the observation made in the washing experiments that most of the cobalt carbonyl-DPPE complex was deposited on the exterior surface of the zeolite and only a small amount was encapsulated within the supercages of the zeolite.

4.4.5. Hydroformylation reactions : recycling of impregnated zeolite catalysts

All previous experiments with the high-cobalt catalysts showed that at least some of the cobalt on the zeolites leached into solution. However, this only showed that some of the cobalt was deposited upon the outside of the zeolite and did not show whether any cobalt remained on the zeolite, encapsulated as an active hydroformylation catalyst. It was decided to recycle the zeolite catalysts to see if catalysts could be obtained in which some of the cobalt was retained as an encapsulated complex for repeated use without further leaching of the cobalt.

4.4.5.1. 4ph/co

Recycling of 4ph/co led to decreasing conversions (63% to 3%), decrease in the linearity of the products (1.6 to 0.9) and a decrease in the alcohol:aldehyde ratio (2.44 to 0.03) (see **Table 3.7**).

As mentioned in Section 4.4.4.1., the IR spectrum of the solution after the first reaction (PJV116) showed that cobalt had leached from the zeolite and was present in solution as $[Co(CO)_3(PPh_2Et)]_2$. In the IR spectra of the solutions from the subsequent reactions (PJV117 and PJV118), no ν(CO) bands were observed, ie. there were no cobalt carbonyl complexes present in solution. After each reaction, the zeolite was removed from the reactant solution by centrifuging and washed with an alkane solvent. If the only active catalytic species was present in solution due to leaching from the zeolite support (as suggested by previous experiments), then this procedure was the cause of the decreasing activity of the catalyst due

to removal of cobalt from the system. However, the decrease in activity could also have been caused by removal of the phosphine during the centrifuge and washing procedure. This would decrease the P:Co ratio in the system and without excess phosphine present, the cobalt carbonyl catalyst would be less stable under the reaction conditions employed and would *decom*pose quicker. In fact, the results suggest that a combination of the two processes were occurring. Cobalt was definitely present in solution after the first reaction and was subsequently removed from the system. Also observed was a decrease in the linearity of products and a decrease in the selectivity to alcohols from reaction to reaction, characteristic of a decreasing P:Co ratio. The IR spectrum of the zeolite after the third reaction showed no ν(CO) bands indicating the absence of cobalt carbonyl species on the zeolite after the third reaction. The zeolite was observed to turn purple during PJV116 and remained this colour during subsequent reactions; this in agreement with the observation that a purple colour to the zeolite indicated a loss of activity for catalysis of the hydroformylation reaction (see Section 4.4.2).

4.4.5.2. 4ph/co with extra PPh_2Et added

This set of reactions was identical to those mentioned in the previous section 4.4.5.1. except that extra PPh_2Et was added to the solution before the first reaction, PJV119. Recycling of 4ph/co with extra phosphine, similar to the previous case, led to decreasing conversions (59% to 4%). In reactions PJV120 and PJV121, no aldehydes or alcohols were detected, so no trends could be observed for product distribution.

The reduction in conversion from reaction to reaction was much more extreme in this case than in the previous case in which no extra phosphine was added to solution. This was probably because adding extra PPh_2Et stabilised most of the cobalt in solution as $HCo(CO)_3(PPh_2Et)$. This species is too large to enter the pores of the zeolite and thus would stay outside the zeolite in solution rather than diffusing into the zeolite as the small, unsubstituted cobalt carbonyl hydride or decomposing/converting to some inactive species. After the first reaction (PJV119), the reaction solution was removed together with this large proportion of cobalt, leaving only a small portion of the cobalt present on the zeolite.

The IR spectrum of the solution after reaction PJV119 showed a ν(CO) band at 1956 cm^{-1}, similar to that observed for PJV116, indicating that cobalt had leached from the zeolite and was present in solution as $[Co(CO)_3(PPh_2Et)]_2$ (see **Figure 3.4**). The IR spectra of the solutions from PJV120 and PJV121 (after reaction) showed no carbonyl bands, ie. there were apparently no cobalt carbonyl complexes present in solution. There were also no ν(CO) bands observed in the IR spectrum of the zeolite after PJV121 and the zeolite had turned a purple colour. This agrees with the observation that a purple colour to the zeolite correlates with a decrease in activity (ie. a decomposition of the active cobalt carbonyl species).

It is interesting to compare the first reaction of the previous set (PJV116, Section 4.4.5.1.) to the first reaction of this set (PJV119) to see the effect of the addition of extra phosphine to solution. The conversion remained approximately the same, although an increase in the P:Co in a system should reduce the conversion (described in detail in Sections 4.4.1. and 4.5.1.). This was probably because the extra phosphine stabilised more of the cobalt outside of the zeolite as the active phosphine-substituted hydride, thereby increasing the cobalt concentration in solution for carrying out catalysis. The higher cobalt concentration in solution would offset the higher P:Co ratio, allowing the conversions to be similar for the two systems. The n:iso ratio and the alcohol to aldehyde ratio were both higher for the system containing extra phosphine. This trend agrees with what is reported in the literature when the P:Co of a system is increased (*40*).

4.4.5.3. 4pp/co

Recycling of 4pp/co led to decreasing conversions (83% to 10%) (see **Table 3.7**). The linearity of the products remained constant for two of the three reactions and there was a sharp decrease in the selectivity in the alcohol:aldehyde ratio (16.9 to 0.04) after the second reaction. As mentioned in Section 3.6.3.4., the IR spectrum of the solution after the first reaction (PJV109) showed that cobalt had leached from the zeolite and was present in solution as a cobalt carbonyl complex, although this complex could not be identified. In the IR spectra of the solutions from PJV110 and PJV111 after reaction, no carbonyl bands were observed, ie. there were apparently no cobalt carbonyl complexes present in solution. The IR spectrum of the zeolite after the third reaction did not show any ν(CO) bands, indicating

that any cobalt remaining on the zeolite was not in the form of a cobalt carbonyl complex. The zeolite had turned purple during the reactions, in agreement with the observed loss of activity of the catalyst.

The explanation for the trends is identical to that given in Section 4.4.5.1., the reactions using 4ph/co as catalyst.

4.4.5.4. 4pp/co with extra DPPE added

This set of reactions was identical to those mentioned in Section 4.4.5.3. except that extra DPPE was added to the solution before the first reaction, PJV112. Recycling of 4pp/co, unlike any previous experiments, led to an initial increase in conversion from 12% in reaction PJV112 to 31% in reaction PJV113. This conversion was maintained in reaction PJV114 and instigated the carrying out of a fourth reaction. The conversion in this fourth reaction dropped dramatically to 7%. The linearity of the products for all four reactions remained roughly the same (n:iso of 0.74-0.91) but the selectivity to aldehydes compared to alcohols increased sharply after the first reaction and in the final reaction, PJV115, no alcohol was detected by GC analysis.

The IR spectrum of the solution in the ν(CO) region after reaction PJV112 showed ν(CO) bands indicating that cobalt had leached from the zeolite and was present in solution as a cobalt carbonyl complex; the complex could not be identified. In the IR spectra of the solutions from PJV113-115 after reaction, no carbonyl bands were observed, ie. there were apparently no cobalt carbonyl complexes present in solution. The IR spectrum of the zeolite after the fourth reaction showed no ν(CO) bands and the zeolite was a purple colour.

No acceptable and logical explanation has been found for these anomalous results. The selectivity to decane is far higher than expected for the conversion achieved in the first reaction. In fact, this selectivity to decane is far higher than all other experiments with high-cobalt catalysts. The second and third reactions produce exactly the same conversion (and product selectivities for that matter) which is higher than observed in the first reaction; all previous experiments show a decreasing trend in conversion. Furthermore, this is only

possible if no cobalt is removed from the system in the washing procedure between reactions. This does agree with the infrared spectrum of the reaction solution after the second reaction had been completed: no ν(CO) bands were visible, ie. no carbonyl complex was in solution. However, this does **not** fit in with the fourth and final reaction carried out. In this reaction, the conversion suddenly decreased dramatically from 33% to 7%, even though no carbonyl bands were observed in the IR spectrum of the reaction solutions after the third or the fourth reactions.

4.5. USE OF LOW-COBALT CATALYSTS UNDER HYDROFORMYLATION REACTION CONDITIONS

It was suspected and ultimately confirmed in Sections 4.2.-4.4. that most of the cobalt in the high-cobalt catalysts (4ph/co and 4pp/co) was present on the exterior surface of the zeolite crystals rather than in the supercages. It was suspected that the high loading of phosphine combined with the fact that the phosphine was impregnated into the zeolite first, resulted in pore blocking. When the $Co_2(CO)_8$ was subsequently added, the $Co_2(CO)_8$ was prevented from entering the pores of the zeolite and only reacted with the phosphine on the surface of the zeolite. It was therefore decided to impregnate Na-Y zeolite with a much smaller amount of $Co_2(CO)_8$ and PPh_2Et or DPPE to try and ensure that all the $Co_2(CO)_8$ reacted with the phosphines within the supercages of the zeolite. It was also decided to reverse the order of impregnation of $Co_2(CO)_8$ and PPh_2Et to see if it made any difference to the effectiveness of encapsulation or the performance of the catalyst. According to infrared analysis and washing experiments, it did appear that the lower cobalt loadings had resulted in encapsulation of the cobalt species on the zeolite (see Section 3.5.2. and Section 4.3.2.). Interestingly, the impregnation with DPPE also appeared to have encapsulated the cobalt-dppe complex since no cobalt was removed by washing the zeolite with various solvents. It was hoped that reactions using the impregnated zeolites as catalysts would prove more conclusive.

4.5.1. Hydroformylation reactions : homogeneous catalysts

The homogeneously catalysed reactions described in this section were essentially carried out for comparison of catalyst activity and product distribution with reactions using 0.2ph/co,

0.2co/ph and 0.2pp/co as catalysts. However, it was also decided to test the reproducibility of the experiments as well as testing the effect of varying the P:Co ratio on catalyst activity and product distribution. All the results are summarised in **Table 3.8**, Section 3.7. The reproducibility of the experiments was shown to be satisfactory in Section 3.7.1.1. and requires no further comment. The effect of varying the P:Co ratio is discussed below.

4.5.1.1. Effect of varying P:Co ratio

(i) $Co_2(CO)_8$ and PPh_2Et

As the P:Co ratio was increased, the conversion decreased and the linearity of products increased. The alcohol to aldehyde ratio does not show a definite trend but the increase in proportion of decane indicates a change to a more hydrogenating environment.

$HCo(CO)_3(PR_3)$ (R = tertiary phosphine) is less active than $HCo(CO)_4$ and an increase in the equilibrium concentration of $HCo(CO)_3(PR_3)$ should decreases conversion. Furthermore, $HCo(CO)_3(PR_3)$ is known to produce a higher proportion of linear products than $HCo(CO)_4$ (*3*). Finally, $HCo(CO)_3(PR_3)$ is known to be a better hydrogenation catalyst than $HCo(CO)_4$ (Section 1.5.3.) resulting in a higher proportion of alcohols and hydrogenated alkene as products. Since PPh_2Et is a weak Lewis base, increasing its concentration in the reaction solution was expected to increase the equilibrium concentration of the catalytically active species, $HCo(CO)_3(PPh_2Et)$, as shown in equation (1). The trends for conversion and product distribution indicated that the equilibrium concentration of $HCo(CO)_3(PPh_2Et)$ did increase with an increase in P:Co ratio in the system.

The IR spectra of all the solutions after reaction for two hours under hydroformylation conditions showed a strong band at 1957 cm^{-1}, indicating the presence of the dimer, $[Co(CO)_3(PPh_2Et)]_2$, in solution (see **Figure 3.4**). The presence of $[Co(CO)_3(PPh_2Et)]_2$ as opposed to $HCo(CO)_3(PPh_2Et)$ was expected since the IR spectra were obtained at atmospheric pressure and room temperature, conditions under which the hydride would convert to the dimer very quickly (*81*,*82*).

(ii) $Co_2(CO)_8$ and DPPE

As the P:Co ratio was increased, the conversion decreased dramatically (about 14-fold) while the linearity of the products increased. The alcohol to aldehyde ratio decreased sharply together with a large increase in the relative amounts of decane (hydrogenation product of 1-decene).

The trends can be explained according to the postulated equilibria in equations (9) and (10) and the low basicities of the DPPE phosphorus atoms. At P:Co = 2, the low basicity of DPPE allowed the equilibria to be shifted to the left resulting in a high equilibrium concentration of $HCo(CO)_4$. As the concentration of DPPE was increased, the equilibrium was shifted to the right increasing the concentration of the monosubstituted and disubstituted hydrides. By analogy with monodentate tertiary phosphine systems, the substituted hydrides were expected to be less active catalysts than $HCo(CO)_4$; this was in agreement with the observed decrease in conversion which accompanied an increase in DPPE concentration (see **Table 3.8**). The increase in the linearity of the products was expected for the same reason: an increase in the concentration of the phosphine-substituted hydrides.

The trend in product selectivity appears at first to be anomalous. Since the phosphine-substituted hydrides are more active hydrogenating catalysts, the proportion of aldehyde as products should have decreased while the proportion of both alcohol and decane should have increased as DPPE concentration was increased. Aldehyde percentage did decrease and decane percentage did increase; however, the alcohol percentage decreased, exactly opposite to what was expected. This was probably due to the low conversions achieved for higher concentrations of DPPE (P:Co = 5 and 10). Production of decane is a function of alkene concentration while alcohol formation is a function of aldehyde concentration, ie. decane is a primary product while alcohol is a secondary product. At low conversions, the concentration of aldehyde as a primary product will always be low, suppressing the rate of conversion to alcohol. Conversion to decane, on the other hand, is reliant on the alkene which is always present in relatively high concentration at low conversions. This trend is reported in the literature for reactions using DPPE and $Co_2(CO)_8$ for the hydroformylation of dodecene (*83*) and is in agreement with the trend observed in the

experiments.

The IR spectra of the reaction solutions in which P:Co = 2 gave four peaks in the ν(CO) region : 2078 cm^{-1}, 2024 cm^{-1}, 1991 cm^{-1} and 1956 cm^{-1}. Interestingly, these spectra appeared very similar to the spectra obtained for the monosubstituted complex $Co_2(CO)_7(PPh_2Et)$ (see **Figure 3.6**). This suggested that at this lower P:Co ratio, the predominant substituted complex present is the monosubstituted complex $Co_2(CO)_7$(DPPE). However, no IR data for such a complex was found in the literature and the complex could not be isolated for further characterisation. When P:Co was increased (5:1 and 10:1), the IR spectra of the solutions gave two very strong ν(CO) bands at 1992 cm^{-1} and 1937 cm^{-1}. These bands were shifted considerably compared to the bands observed for $[Co(CO)_2(DPPE)]_2$ in CH_2Cl_2 at 1951 cm^{-1} and 1920 cm^{-1} (see **Figure 3.9**) and could not be attributed merely to differences in solvent. It was thought that the species present was possibly the stable disubstituted hydride, $HCo(CO)_2$(DPPE) (see **Figure 4.4**) but only one report on this complex was found in the literature (*84*) and the spectrum was given in KBr with bands at 1978 cm^{-1} and 1917 cm^{-1}. Unfortunately, the complex obtained in our reactions was not isolated for further characterisation. Nevertheless, since the IR analyses were carried out at room temperature and atmospheric pressure in a solvent (as opposed to KBr), this does not disprove the presence of the disubstituted hydride under hydroformylation conditions.

(iii) ($Co_2(CO)_8$ + PPh_2Et) vs ($Co_2(CO)_8$ + DPPE)

The most striking difference between the two systems was the dramatic reduction in conversion observed when DPPE was used compared to when PPh_2Et was used, as the P:Co ratio was increased. Again referring to the postulated equations (9) and (10), this sharp decrease in conversion correlated with a shift in the equilibria far to the right, ie. an increase in the concentration of the disubstituted hydride, $HCo(CO)_2$(DPPE), which was expected to be much more stable to loss of carbonyl ligands (ie. less catalytically active) than $HCo(CO)_3(PPh_2Et)$.

4.5.2. Hydroformylation reactions : recycle of impregnated zeolites

4.5.2.1. 0.2ph/co

The conversion, n:iso ratio and alcohol:aldehyde ratio for the first reaction (PJV171) were all lower than for the homogeneous catalyst (see **Table 3.9**). The lower conversion was expected if the cobalt was encapsulated within the zeolite supercages since mass transfer resistances to transfer of reactants and products into and out of the zeolite pore structure would be expected to reduce the global rate of hydroformylation. However, the product distribution is closer to that of unsubstituted cobalt carbonyl (lower linearity, less hydrogenation). Recycling of 0.2ph/co resulted in a decrease in conversion (24% to 4.5%) while the linearity of the products remained constant (n:iso of 0.8). Selectivity to decane increased slowly while selectivity to aldehydes and alcohols decreased (see **Table 3.10**). The increase in selectivity to decane with concurrent decreases in selectivity to alcohol and aldehyde is characteristic of low conversions, as previously described. After each reaction, the reaction solution was analysed by IR and no ν(CO) bands were detected. At the end of the three reactions, 90% of the initial cobalt had been retained in or on the zeolite but was not in the form of carbonyl species, as shown by IR. This was qualitatively supported by the purple colour of the zeolite after the third reaction was complete.

There are two possible explanations for the decrease in conversion as well as the trends in the product distribution. Both explanations involve the formation of the unsubstituted hydride, $HCo(CO)_4$. The first possibility is that the cobalt complexes remained inside the zeolite cages, acting catalytically but nevertheless decomposing over a period of time to inactive cobalt species. The second possibility is that the cobalt complexes exited the zeolite cages via the pores, carried out catalysis outside of the zeolite crystals and were decomposed and deposited back onto the zeolite support. It should be noted here that the species initially present on the zeolite was postulated to be the monosubstituted cobalt complex, $Co_2(CO)_7(PPh_2Et)$. If the rest of the phosphine added during impregnation was removed with the supernatant solution after the impregnation was completed (see Section 2.6.2.1. for impregnation procedure), then the effective P:Co ratio at the start of reaction PJV171 (first reaction) would be 0.5. Thus, the equilibrium shown in equation (1) would lie to the left, ie. more $HCo(CO)_4$, according to

Figure 4.5. $HCo(CO)_4$ would not be stable under the relatively low syngas pressure (80 bar) and high operating temperature (180°C) and would decompose to cobalt metal or some other inactive cobalt carbonyl species. This supports both the first and second possibilities, decomposition either within or outside the zeolite cages. The second possibility not only involves decomposition of the cobalt complex, but also diffusion of the complex from within the cages to the exterior of the zeolite crystals. Formation of the $HCo(CO)_4$ explains the possibility of diffusion since formation of $HCo(CO)_4$ would defeat the technique used to encapsulate the cobalt complex within the zeolite, *viz.* the substitution of one of the carbonyl ligands of $HCo(CO)_4$ to form $HCo(CO)_3(PPh_2Et)$ within the zeolite supercages which is too large to exit the cages via the pores.

At this stage it was not clear where the catalysis was occurring since most of the cobalt had been retained on the zeolite and cobalt carbonyl complexes were never detected in solution.

4.5.2.2. 0.2ph/co with extra PPh_2Et added

Reaction conditions for these two duplicate sets of reactions (PJV191-PJV193 and PJV197-PJV199) were similar to those for the set of reactions PJV171-PJV173 (see Section 4.5.2.1.) except that extra PPh_2Et was added to the system before each reaction. As mentioned in Section 2.6.4., the amount of phosphine added was equivalent to a 2:1 P:Co ratio based on the moles of cobalt present on the zeolite in the first reaction and assuming that no cobalt was lost from reaction to reaction. The reason for doing this was to try to shift the equilibrium shown in equation (1) (see Section 1.5.3.) to the right, hopefully stabilising and maintaining the substituted hydride species under hydroformylation conditions.

The first reaction in these sets gave very similar results to the first reaction using 0.2ph/co with no extra phosphine, except that the conversion was lower (16% as opposed to 24%). Again the conversion and product distributions were more characteristic of catalysis by the unsubstituted hydride complex than of the substituted hydride complex (low n:iso ratios and less hydrogenation).

The subsequent reactions, however, were considerably different. As the zeolite was recycled

from reaction to reaction, the conversion remained constant (~16%) while the n:iso ratio of the products steadily increased (0.9 to 1.8). Selectivities to both decane and alcohols increased while selectivity to aldehydes decreased. IR analysis of the solutions after reaction showed weak ν(CO) bands (cobalt in solution was in the form of unidentified carbonyl species) and only about 50% of the initial cobalt was retained on the zeolite by the time the third reaction had been completed. This means that the cobalt was actually leaching out of the zeolite support and probably carrying out catalysis in solution rather than within the cages of the zeolite. The constant conversion confirmed that catalysis occurred in solution. Since the liquid reagent containing cobalt carbonyl species was removed after every reaction, the cobalt content of the system was decreasing from reaction to reaction. If catalysis was occurring predominantly within the zeolite cages, a decrease in conversion should have resulted since the zeolite cages were the source of cobalt in the system. Since conversion was being maintained, most of the catalysis must have occurred in solution.

The removal of cobalt dissolved in the reaction solution between each reaction resulted in the increase in the P:Co ratio of the system for each subsequent reaction since the same amount of phosphine was added to each reaction. The increase in product linearity and increase in selectivity to decane and alcohols from reaction to reaction was in agreement with a steadily increasing P:Co ratio in the system.

The colour of the zeolite remained yellow throughout all three reactions in a set and also remained catalytically active. This agreed with the observation that a yellow colour equated to an active catalyst as opposed to a purple colour which indicated deactivation.

These results show that the extra PPh_2Et added to the system stabilised an active hydroformylation catalyst and allowed the activity of the catalyst to be maintained. However, the results also show that the cobalt leached out of the zeolite and carried out catalysis as a homogeneous catalyst.

4.5.2.3. 0.2co/ph

The important difference between 0.2co/ph and 0.2ph/co was that 0.2co/ph was impregnated

with $Co_2(CO)_8$ before PPh_2Et. The reason for reversing the impregnation order was to see if it made any difference to the performance of the catalyst. Since phosphines adsorb fairly strongly to the surface of zeolites, there was the possibility that impregnation with phosphine first could result in blocking of the zeolite pores either at the surface or at various places throughout the zeolite crystals. If this was the case, then impregnating with smaller, less strongly adsorbed $Co_2(CO)_8$ molecules first should allow the final cobalt complex to be distributed more evenly throughout the zeolite crystals.

Basically, the results were similar to those obtained for 0.2ph/co without extra phosphine added, ie. lower conversion than in the homogeneously-catalysed system (P:Co = 2), lower product linearity and a predominance of aldehyde in the products. This product distribution resembled the reaction catalysed by $HCo(CO)_4$ rather than by $HCo(CO)_3(PPh_2Et)$. Recycling of 0.2co/ph resulted in a decrease in conversion (16% to 1.6%) while the linearity of the products appeared to increase slightly (0.8 to 1.25). Selectivity to decane increased sharply while selectivity to aldehydes decreased sharply; alcohols did not appear to be formed in any of the reactions.

The discussion in Section 4.5.2.1. can be applied to this catalytic system as well. The only difference is that the amount of initial cobalt retained on the zeolite is 95% (not as a carbonyl complex).

Although conversions for 0.2co/ph (cobalt impregnated first) were all lower than those obtained for the analogous reactions with 0.2ph/co, it was not clear at this stage whether reversing the impregnation procedure was the cause of the difference in catalyst performance.

4.5.2.4. 0.2co/ph with extra PPh_2Et added

These two duplicate sets of reactions (PJV180-PJV182 and PJV194-PJV196) were similar to the set of reactions PJV177-PJV179 (see Section 4.5.2.3.) except that extra PPh_2Et was added to the system before each reaction.

The results were identical to those obtained with 0.2ph/co and extra phosphine (see Section

4.5.2.2.) except for the first reaction; the very low conversions in the first reactions explain the apparently odd results for product distributions. In the second and third reactions, the conversions and product distributions were similar to those obtained with 0.2ph/co and extra phosphine. The discussion in Section 4.5.2.2. is applicable to these second and third reactions.

The low conversion in the first reaction in a set appears to be reproducible since both duplicate reactions gave this result. Furthermore, no carbonyl bands were detected in the IR spectra of the solution after the first reaction which suggests that the catalysis was occurring mainly in the zeolite cages rather than in solution. The lower conversions of about 2%, dramatically different from the conversions of 16% in the first reactions described in Section 4.5.2.2., also suggest that reaction was occurring predominantly within the zeolite cages. However, considering that it was previously observed for other reactions that catalysis occurred mainly in solution, it was more likely that a very small amount of cobalt carbonyl complex leached out of the zeolite, resulting in a low concentration of cobalt in solution and giving a very low conversion. This was supported by the fact that no ν(CO) bands were observed in the IR spectrum of the solution, even though extra PPh_2Et was added to the system. At this stage, it was not clear where catalysis was occurring.

After the initial reaction, however, the performances of the two catalysts (0.2ph/co and 0.2co/ph) were very similar. Since the only difference between 0.2ph/co and 0.2co/ph was the order in which the zeolite supports were impregnated with $Co_2(CO)_8$ and PPh_2Et, it appeared that the order of impregnation only made a difference to the initial performance of the catalyst. It is possible that impregnating the zeolite with $Co_2(CO)_8$ before PPh_2Et distributed the cobalt deeper and more evenly throughout the zeolite support. This would have affected the time required for cobalt species to migrate out of the zeolite cages. Thus, the low conversion in the first reaction resulted simply because the two hour reaction time was not enough for a significant amount of cobalt to reach the exterior surface of the zeolite support to carry out catalysis.

ν(CO) bands were observed in the IR spectrum of the zeolite indicating the presence of cobalt carbonyl species on the zeolite (the species were unidentified). The zeolite retained a yellow

colour throughout all of the reactions in a set, similar to reactions with 0.2ph/co and extra PPh_2Et. This agreed with the observation that a yellow colour equates to an active catalyst.

4.5.2.5. 0.2pp/co

Essentially, the results obtained with this catalyst were the same as those obtained for 0.2ph/co with no extra phosphine (see Section 4.5.2.4.). Recycling of 0.2pp/co resulted in a decrease in conversion (24% to 1%) while the linearity of the products appeared to increase slightly (0.7 to 0.9). Selectivities to decane increased while selectivity to aldehydes decreased sharply; selectivity to alcohol appeared to be increase slightly but was not conclusive since the very low conversion in the third reaction resulted in negligible alcohols and aldehydes being formed.

The amount of cobalt retained on the zeolite after the third reaction, PJV185, was 100%; however, this cobalt was not in the form of a carbonyl complex because no ν(CO) bands were observed in the IR spectrum of the zeolite. This observation was qualitatively supported by the purple colour of the zeolite after the third reaction.

The retention of the cobalt on the zeolite is interesting. The catalysis appeared to be homogeneous (relatively high conversion in the first reaction), yet all the cobalt was retained on the zeolite. This could be explained by the equilibria shown in equations (9) and (10). In the absence of extra DPPE in solution, the equilibria were shifted very far to the left, resulting in a high equilibrium concentration of $HCo(CO)_4$ which diffused through the pores of Na-Y zeolite. The $HCo(CO)_4$ would then decompose within the zeolite thereby being retained within the zeolite at the end of reaction. This explains how 100% of the cobalt can be retained, even though catalysis was most likely homogeneous.

4.5.2.6. 0.2pp/co with extra DPPE added

The reaction conditions of this set of reactions (PJV186-PJV188) were similar to those of the set of reactions PJV183-PJV185 (see Section 4.5.2.5.) except that extra DPPE was added to the system before each reaction. The conversion for all three reactions is negligible (<1%)

and only some decane (no alcohols or aldehydes) was detected by GC analysis.

Interestingly, the amount of cobalt retained on the zeolite after all three reactions was 100% and the cobalt was in the form of some unidentified carbonyl complex because ν(CO) bands were observed in the IR spectrum of the final zeolite. Since the cobalt carbonyl complex on the zeolite was fairly stable, it must have been a cobalt carbonyl-DPPE complex because the previous set of reactions with no extra DPPE (see Section 4.5.2.5.) resulted in decomposition of the cobalt carbonyl complex. The colour of the zeolite remained yellow throughout all three runs in the set and, although the catalyst was not active, this still supports the observation that the species on the zeolite was a cobalt carbonyl-DPPE complex.

A few qualitative washings of this catalyst (after reaction) were carried out in air with undried solvents. The catalyst was washed consecutively with hexane, dichloromethane, THF and acetone, yet still retained its bright yellow colour and left the supernatant solutions colourless. This strongly suggests that the cobalt-DPPE complex was in fact encapsulated within the cages of Na-Y, even though it was the least expected result. Unfortunately, these washings were carried out as an afterthought and time restrictions did not allow any further quantitative experiments to be carried out on this system.

CHAPTER 5

Conclusions

5. CONCLUSIONS

The following new cobalt complexes were synthesized and characterised by IR, ^{31}P NMR, melting point, colour and elemental analysis: $[Co(CO)_3(PPh_2Et)_2]^+[Co(CO)_4]^-$ and $[Co(CO)_3(PPh_2Et)]_2$.

The following cobalt complexes were synthesized and characterized by IR, melting point and colour: $[Co_2(CO)_4(DPPE)_3]^{2+}\{[Co(CO)_4]^-\}_2$ and $[Co(CO)_2(DPPE)]_2$.

The monosubstituted dimer, $Co_2(CO)_7(PPh_2Et)$, appeared to have been formed as a mixture of a carbonyl-bridged isomer and a non-bridged isomer from analysis by infrared spectroscopy. However, the ^{31}P NMR and elemental analysis did not give very good results because the complex was not very stable.

Impregnation of zeolite with $Co_2(CO)_8$ and PPh_2Et resulted in different cobalt species present on the zeolite depending on the cobalt loading of the zeolite. $[Co(CO)_3(PPh_2Et)_2]^+[Co(CO)_4]^-$ was formed on the zeolite when the zeolite was loaded with 4.4% cobalt. $Co_2(CO)_7(PPh_2Et)$ appeared to have been formed on the zeolite when the zeolite was loaded with 0.2% cobalt. Reversing the order of impregnation of the cobalt carbonyl and PPh_2Et in the case of 0.2% cobalt loading also resulted in formation of $Co_2(CO)_7(PPh_2Et)$ on the zeolite.

Impregnation of zeolite with $Co_2(CO)_8$ and DPPE resulted in different cobalt species present on the zeolite depending on the cobalt loading of the zeolite. $[Co_2(CO)_4(DPPE)_3]^{2+}\{[Co(CO)_4]^-\}_2$ was formed on the zeolite when the zeolite was loaded with 4.7% cobalt. Only the cation, $[Co_2(CO)_4(DPPE)_3]^{2+}$, appeared to be present after impregnation when the zeolite was loaded with 0.13% cobalt.

Washing the zeolites loaded with 4% cobalt (and either of the phosphines) with dichloromethane washed off a large percentage of the cobalt initially present on the zeolites (>86%). It was concluded that most of the cobalt complexes present on the zeolite were on the surface of the zeolites and were not encapsulated.

Washing of the zeolites loaded with 0.2% cobalt with hexane, 1-decene or dichloromethane did not remove any of the cobalt initially present on the zeolites. From this it was concluded that the cobalt complexes present on the zeolites were encapsulated within the cages of the zeolite crystals.

Reactions using the zeolites loaded with 4% cobalt resulted in leaching of the cobalt into solution. Catalysis observed in the first reaction in a set of three consecutive reactions resulted in product selectivities characteristic of homogeneous catalysis with $Co_2(CO)_8$ and PPh_2Et or DPPE. Subsequent reactions in a set showed catalysis characteristic of homogeneous catalysis with $Co_2(CO)_8$ and no phosphine. It was concluded that the cobalt was washed off the zeolite and carrying out catalysis in solution rather than in the cages of the zeolite support.

Reactions using zeolites loaded with 0.2% cobalt also resulted in leaching of the cobalt into solution. If no extra phosphine was added to the system, the results were similar to those obtained with the 4% cobalt-loaded catalysts. When extra PPh_2Et was added to the reactions using zeolites impregnated with $Co_2(CO)_8$ and PPh_2Et, leaching of the cobalt into solution was observed for all three reactions in a set; conversions from reaction to reaction in a set were constant. It was concluded that cobalt was leaching out of the zeolite cages and carrying out catalysis in solution rather than within the cages of the zeolite. Since washing experiments suggested that the cobalt was initially residing within the zeolite cages, the leaching was explained according to the equilibrium:

$$HCo(CO)_4 + PPh_2Et \rightleftharpoons HCo(CO)_3(PPh_2Et) + CO$$

Formation of the smaller $HCo(CO)_4$ from $HCo(CO)_3(PPh_2Et)$ under hydroformylation conditions would allow the cobalt to diffuse out of the zeolite cages and to then perform catalysis in the bulk solution.

If extra DPPE was added to the system containing zeolite impregnated with DPPE and

0.2% cobalt, 100% of the cobalt was retained on the zeolite in the form of a cobalt-DPPE complex. It was not clear whether this retention was due to encapsulation or attachment to the exterior surface of the zeolite support, although certain qualitative experiments actually suggested encapsulation.

From these results, it appears that encapsulation of a cobalt hydroformylation catalyst within zeolite Y was not successful. Leaching of the cobalt from the zeolite or deactivation of the cobalt species on the zeolite occurred in every case except one (and in this exception, the catalyst was inactive). However, loading of Na-Y with small amounts of cobalt and DPPE gave a surprising and encouraging result in terms of encapsulation and bears further investigation.

REFERENCES

REFERENCES

1. M. Beller, B. Cornils, C.D. Frohning and C.W. Kohlpaintner, *Journal of Molecular Catalysis A*, 1995, **104**, pp 17-85

2. C. Masters; "Homogeneous Transition-metal catalysis: a gentle art", Chapman and Hall Ltd., London, 1981, pp 102-120

3. L.H. Slaugh and R.D. Mullineaux, *Journal of Organometallic Chemistry*, 1968, **13**, pp 469-477

4. D.C. Bailey and S.H. Langer, *Chemical Reviews*, 1981, **81**(2), pp 109-148

5. N. Herron, G.D. Stucky and C.A. Tolman, *Inorganica Chimica Acta*, 1985, **100**, pp 135-140

6. K.J. Balkus Jr. and A.G. Gabrielov, *Journal of Inclusion Phenomena and Molecular Recognition in Chemistry*, 1995, **21**, pp 159-184

7. N. Herron, *Inorganic Chemistry*, 1986, **25**, pp 4714-4717

8. R.S. Dickson; "Homogeneous Catalysis with Compounds of Rhodium and Iridium", D. Riedel Publishing Company, The Netherlands, 1985, pp 2-3

9. T.H. Maugh II, *Science*, 1983, **220**, 3 June, pp 1032-1035

10. F.R. Hartley; "Supported Metal Complexes", D. Riedel Publishing Company, The Netherlands, 1985, pg 6

11. M.C. Connaway and B.E. Hanson, *Inorganic Chemistry*, 1986, **25**, pp 1445-1451

12. S. Kowalak, R.C. Weiss and K.J. Balkus Jr., *Journal of the Chemical Society, Chemical Communications*, 1991, pp 57-58

13. B.C. Gates; "Catalytic Chemistry", John Wiley and Sons, New York, 1992, pp 254-305

14. R. Szostak;"Handbook of Molecular Sieves", Van Nostrand Reinhold, United States of America, 1992

15. J.H. Lunsford, *Reviews in Inorganic Chemistry*, 1987, **9**(1), pp 2-35

16. J.W. Ward, *Journal of Catalysis*, 1971, **22**, pp 237-244

17. S.M. Csicsery, *Zeolites*, 1984, **4**, July, pp 202-213

18. M.E. Davis, *Accounts of Chemical Research*, 1993, **26**, pp 111-115

19. J. Weitkamp, *Proceedings of the 9th International Zeolite Conference, Montreal 1992*, Eds. R. von Balmoos et al, Butterworth-Heinemann, 1993, pp 13-45

20. W.M.H. Sachtler, *Accounts of Chemical Research*, 1993, **26**, pp 383-387

21. C.V. McDaniel and P.K. Maher, *Molecular Sieves, Papers read at the Conference, School of Pharmacy, University of London, London, April 4-6, 1967*, 1968, pp 186-195

22. C. Naccache and Y.B. Taarit, *Pure and Applied Chemistry*, 1980, **52**, pp 2175-2189

23. S. Yoshida, M. Nakajima, K. Naito, Y. Koshimidzu and K. Tarama, *Bulletin of the Institute for Chemical Research, Kyoto University*, 1974, **52**(4), pp 567-578

24. T. Maschmeyer, F. Rey, G. Sankar and J.M. Thomas, *Nature*, 1995, **378**, 9 November, pp 159-162

25. G.A. Ozin and C. Gil, *Chemical Reviews*, 1989, **89**, pp 1749-1764

26. D.E. de Vos, P.P. Knops-Gerrits, R.F. Parton, B.M. Weckhuysen, P.A. Jacobs and R.A. Schoonheydt, *Journal of Inclusion Phenomena and Molecular Recognition in Chemistry*, 1995, **21**, pp 185-213

27. K.J. Balkus Jr. and K. Nowinska, *Microporous Materials*, 1995, **3**, pp 665-686

28. T. Beutel, S. Kawi, S.K. Purnell, H. Knözinger and B.C. Gates, *Journal of Physical Chemistry*, 1993, **97**, pp 7284-7289

29. W. Ross-Hastings, C.J. Cameron, M.J. Thomas and M.C. Baird, *Inorganic Chemistry*, 1988, **27**, pp 3024-3028

30. E. Pàez-Mozo, N. Gabriunas, F. Lucaccioni, D.D. Acosta, P. Patrono, A. La Ginestra, P. Ruiz and B. Delmon, *Journal of Physical Chemistry*, 1993, **97**, pp 12819-12827

31. G.Q. Li and R. Govind, *Inorganica Chimica Acta*, 1994, **217**, pp 135-140

32. T. Bein, S.J. McLain, D.R. Corbin, R.D. Farlee, K. Moller, G.D. Stucky, G. Woolery and D. Sayers, *Journal of the American Chemical Society*, 1988, **110**, pp 1801-1810

33. R.L. Schneider, R.F. Howe and K.L. Watters, *Inorganic Chemistry*, 1984, **23**, pp 4600-4607

34. M.R. Steele, P.M. MacDonald and G.A. Ozin, *Journal of the American Chemical Society*, 1993, **115**, pp 7285-7292

35. R.A. Schoonheydt, D. Van Wouwe, M. Van Hove, E.F. Vansant and J.H. Lunsford, *Journal of the Chemical Society, Chemical Communications*, 1980, pp 33-34

36. R. Jelinek, S. Öskar, H.O. Pastore, A. Malek and G.A. Ozin, *Journal of the American Chemical Society*, 1993, **115**, pp 563-568

37. M.J. Sabater, A. Corma, A. Domonech, V. Fornés and H. Garcia , *Chemical Communications*, 1997, pp 1285-1286

38. D.R. Corbin, W.C. Siedel, L. Abrams, N. Herron, G.D. Stucky and C.A. Tolman, *Inorganic Chemistry*, 1985, **24**, pp 1800-1803

39. M. Iwamoto, S. Nakamura, H. Kusano and S. Kagawa, *Journal of Physical Chemistry*, 1986, **90**, pp 5244-5249

40. F.E. Paulik, *Catalysis Reviews*, 1972, **6**(1), pp 49-84

41. O. Roelen, *Angewandte Chemie*, 1948, **60**, pg 62

42. "Kirk-Othmer: Encyclopedia of Chemical Technology"; eds J.I. Kroschwitz and M. Howe-Grant, John Wiley & Sons, United States of America, 1996, Vol. 17, pp 902-919

43. R.F. Heck and D.S. Breslow, *Journal of the American Chemical Society*, 1961, **83**, pp 4023-4027

44. G. Henrici-Olivé and S. Olivé, *Transition Metal Chemistry*, 1976, **1**, pp 77-93

45. "Kirk-Othmer: Encyclopedia of Chemical Technology"; eds M. Grayson and D. Eckroth, John Wiley & Sons, United States of America, 1981, Vol. 16, pp 637-653

46. J. Haggin, *Chemical and Engineering News*, 1995, 17 April, pp 25-26

47. G.W. Parshall; "Homogeneous Catalysis: The applications and chemistry of catalysis by soluble transition metal complexes"; John Wiley & Sons, United States of America, 1980

48. F.A. Cotton and G. Wilkinson; "Advanced Inorganic Chemistry"; 5th ed., John Wiley & Sons, United States of America, 1988

49. "Comprehensive Organometallic Chemistry: The synthesis, reactions and structures of organometallic compounds"; 1st ed., eds G. Wilkinson, F.G.A. Stone and E.W. Abel, Pergamon Press, Great Britain, 1982, Vol. 5, pp 1-276

50. S.L.T. Andersson and R.F. Howe, *Journal of Physical Chemistry*, 1989, **93**, pp 4913-4920

51. P. Szabó, L. Fekete, G. Bor, Z. Nagy-Magos and L. Markó, *Journal of Organometallic Chemistry*, 1968, **12**, pp 245-248

52. P. Braunstein, I. Pruskil, G. Predieri and A. Tiripicchio, *Journal of Organometallic Chemistry*, 1983, **247**, pp 227-237

53. D.J. Thornhill and A.R. Manning, *Journal of the Chemical Society, Dalton Transactions*, 1973, pp 2086-2090

54. A.R. Manning, *Journal of the Chemical Society (A)*, 1968, pp 1135-1137

55. R.L. Petersen and K.L. Watters, *Inorganic Chemistry*, 1973, **12**(12), pp 3009-3010

56. J.A. McCleverty, A. Davison and G. Wilkinson, *Journal of the Chemical Society*, 1965, pp 3890-3891

57. D. de Montauzon and R. Poilblanc, *Journal of Organometallic Chemistry*, 1975, **93**, pp 397-404

58. P. Rigo, M. Bressan and A. Morvillo, *Journal of Organometallic Chemistry*, 1976, **105**, pp 263-269

59. A. Misono, Y. Uchida, M. Hidai and T. Kuse, *Chemical Communications*, 1968, pg 981

60. G.F. Pregaglia, A. Andreetta and G.F. Ferrari, *Journal of Organometallic Chemistry*, 1971, **30**, pp 387-405

61. T. Bartik, T. Krümmling, B. Happ, A. Sieker, L. Markó, R. Boese, R. Ugo, C. Zucchi and G. Pályi, *Catalysis Letters*, 1993, **19**, pp 383-389

62. L.M. Bower and M.H.B. Stiddard, *Journal of Organometallic Chemistry*, 1968, **13**, pp 235-239

63. A.R. Manning and J.R. Miller, *Journal of the Chemical Society (A)*, 1970, pp 3352-3356

64. G. Capron-Cotigny and R. Poilblanc, *Bulletin de la Société Chimique de France*, 1967, **4**, pg 1440

65. S.E. Pedersen and W.R. Robinson, *Inorganic Chemistry*, 1975, **14**(10), pp 2360-2365

66. N. Takahashi and M. Kobayashi, *Journal of Catalysis*, 1984, **85**, pp 89-97

67. H. Arai and H. Tominaga, *Journal of Catalysis*, 1982, **75**, pp 188-189

68. M.E. Davis, E. Rode, D. Taylor and B.E. Hanson, *Journal of Catalysis*, 1984, **86**, pp 67-74

69. R.J. Davis, J.A. Rossin and M.E. Davis, *Journal of Catalysis*, 1986, **98**, pp 477-486

70. E. Mantovani, N. Palladino and A. Zanobi, *Journal of Molecular Catalysis*, 1977/78, **3**, pp 285-291

71. J.M. Andersen, *Platinum Metal Reviews*, 1997, July, **41**(3), pp 132-141

72. D.F. Taylor, B.E. Hanson and M.E. Davis, *Inorganica Chimica Acta*, 1987, **128**, pp 55-60

73. J.P. Arhancet, M.E. Davis, J.S. Merola and B.E. Hanson, *Nature*, 1989, **339**, 8 June, pp 454-455

74. M.E. Davis, *CHEMTECH*, 1992, August, pp 498-502

75. J. Haggin, *Chemical and Engineering News*, 1994, 10 October, pp 28-36

76. B. Cornils and E. Wiebus, *CHEMTECH*, 1995, January, pp 33-38

77. *Mining Journal*, The Mining Journal Ltd., London, 1997, **328**(8410), January 3, pg 11

78. O. Vohler, *Chemische Berichte*, 1958, **91**, pp 1235-1238

79. G. Bor and L. Markó, *Chemistry and Industry*, 1963, June 1, pp 912-913

80. H.O. Pastore, G.A. Ozin and A.J. Poë, *Journal of the American Chemical Society*, 1993, **115**, pp 1215-1230

81. M.F. Mirbach, *Journal of Organometallic Chemistry*, 1984, **265**, pp 205-213

82. R. Whyman, *Journal of Organometallic Chemistry*, 1974, **81**, pp 97-106

83. W. Cornely and B. Fell, *Journal of Molecular Catalysis*, 1982, **16**, pp 89-94

84. T. Ikariya and A. Yamamoto, *Journal of Organometallic Chemistry*, 1976, **116**, pp 231-237

85. J.R. Sowa Jr. and R.J. Angelici, *Inorganic Chemistry*, 1991, **30**, pp 3534-3537

86. B. Coughlan and C. Ó Domhnaill, *Topics in Catalysis*, 1994, **1**, pp 163-167

87. W.A. Dietz, *Journal of Gas Chromatography*, 1967, **5**, pp 68-71

APPENDICES

APPENDIX A

Calculation of cobalt loadings of impregnated zeolites

CALCULATION OF COBALT LOADINGS OF IMPREGNATED ZEOLITES

There are two different ways in which cobalt loading on the zeolite support can be measured. The first is the mass of cobalt per unit mass of zeolite support (excluding cobalt mass) as a percentage; this is represented below as "X". The second is the mass of cobalt per unit mass of zeolite support (including the mass of any cobalt complex on the zeolite) as a percentage; this is represented below as "Y".

$$X = \frac{Mass\ of\ cobalt}{Mass\ of\ zeolite\ support} \times 100\% = \frac{M_{Co}}{M_z} \times 100\% \quad \text{..... (1)}$$

$$Y = \frac{Mass\ of\ cobalt}{Total\ mass\ of\ sample} \times 100\% = \frac{M_{Co}}{M_T} \times 100\% \quad \text{..... (2)}$$

Both X and Y were used in this project. The value X is more useful for comparison of cobalt loadings of samples containing different cobalt complexes. The value Y is useful for calculating the amount of cobalt present in a given mass of impregnated zeolite sample; this was important for calculating the amount of cobalt added to a system with a given amount of impregnated zeolite.

Determination of X and Y for a given impregnated zeolite was carried out as follows. The impregnated zeolite was heated in a furnace to about 400°C and maintained at this temperature for 12 hours. This was done to oxidise the cobalt complex present on the zeolite to a cobalt oxide species. The necessity of oxidising the cobalt complexes was due to the method used for dissolving the zeolite support for subsequent AA analysis. The zeolite could only be dissolved using a solution of hydrofluoric acid (HF). Unfortunately, the supported cobalt-phosphine complexes formed insoluble material and therefore were

not present in solution when AA analysis was carried out. It was found that initial treatment in a furnace allowed the cobalt to form water-soluble species when the zeolite was subsequently treated with HF.

Calculation of X

The following symbols are used in the derivation of X:

M : total mass of sample used in an AA analysis in grams
Co_{ppm} : ppm of cobalt from AA analysis of sample
V : volume of solution used in AA analysis in cm^3
Co_aO_b : cobalt oxide species; a=1-3, b=1,3,4
Co : cobalt
M_A : mass of substance A in grams
MM_A : molar mass of substance A in grams
m_A : moles of substance A in grams

$$M_{Co_aO_b} = m_{Co_aO_b} MM_{Co_aO_b}$$

$$= (\frac{1}{a} m_{Co}) MM_{Co_aO_b}$$

$$= \frac{1}{a} \frac{M_{Co}}{MM_{Co}} MM_{Co_aO_b} \quad \text{..... (3)}$$

$$\textit{Now}: \quad M = M_z + M_{Co_aO_b}$$

$$\Rightarrow M_z = M - M_{Co_aO_b} \quad \text{..... (4)}$$

$$\text{(3) } \textit{into} \text{ (4)} \quad = M - \frac{MM_{Co_aO_b}}{a\ MM_{Co}} M_{Co} \quad \text{..... (5)}$$

From AA analysis : $M_{Co} = Co_{ppm} \; x \; V \; x \; 10^{-6}$ ..... (6)

(5) *into* (1) : $$X = \frac{M_{Co}}{\left(M - \frac{MM_{Co_aO_b}}{a\ (MM_{Co})} M_{Co} \right)} \; x \; 100\%$$

$$= \left(\frac{M}{M_{Co}} - \frac{MM_{Co_aO_b}}{a\ (MM_{Co})} \right)^{-1} x \; 100\% \quad \text{..... (7)}$$

(6) *into* (7) $$= \left(\frac{M}{Co_{ppm} \; x \; V \; x \; 10^{-6}} - \frac{MM_{Co_aO_b}}{a\ (MM_{Co})} \right)^{-1} x \; 100\% \quad \text{..... (8)}$$

Calculation of Y

All the symbols used in the derivation of X retain their meanings for the derivation of Y. The following are extra symbols used:

M_T : total mass of sample, ie. zeolite mass + cobalt complex mass

Co-P : cobalt-phosphine complex

P : moles of cobalt in 1 mole of Co-P

$$M_T = M_z + M_{Co\text{-}P} \quad \text{..... (9)}$$

$$M_{Co\text{-}P} = m_{Co\text{-}P} \, MM_{Co\text{-}P}$$

$$= \frac{1}{P} m_{Co} \, MM_{Co\text{-}P}$$

$$= \frac{1}{P} \left(\frac{M_{Co}}{MM_{Co}} \right) MM_{Co\text{-}P}$$

$$= \frac{MM_{Co\text{-}P}}{P\ (MM_{Co})} M_{Co} \quad \text{..... (10)}$$

(5) *and* (10) *into* (9) :

$$M_T = M + \left(\frac{MM_{Co\text{-}P}}{P} - \frac{MM_{Co_aO_b}}{a} \right) \frac{M_{Co}}{MM_{Co}}$$

$$\Rightarrow \quad \frac{M_{Co}}{M_T} = \frac{M}{M_{Co}} + \left(\frac{MM_{Co\text{-}P}}{P} - \frac{MM_{Co_aO_b}}{a} \right) \frac{1}{MM_{Co}}$$

$$\Rightarrow \quad \frac{M_T}{M_{Co}} = \left[\frac{M}{M_{Co}} + \left(\frac{MM_{Co\text{-}P}}{P} - \frac{MM_{Co_aO_b}}{a} \right) \frac{1}{MM_{Co}} \right]^{-1} \quad \text{..... (11)}$$

(11) *into* (2) :

$$Y = \left[\frac{M}{M_{Co}} + \left(\frac{MM_{Co\text{-}P}}{P} - \frac{MM_{Co_aO_b}}{a} \right) \frac{1}{MM_{Co}} \right]^{-1} x \ 100\% \quad \text{..... (12)}$$

(6) *into* (12) :

$$Y = \left[\frac{M}{Co_{ppm} \ x \ V \ x \ 10^{-6}} + \left(\frac{MM_{Co\text{-}P}}{P} - \frac{MM_{Co_aO_b}}{a} \right) \frac{1}{MM_{Co}} \right]^{-1} x \ 100\% \quad \text{..... (13)}$$

The form of the cobalt oxide on the zeolite was not determined, therefore a cobalt oxide form had to be assumed to be able to calculate X and Y. The term affected by the form of the cobalt oxide is $\frac{MM_{Co_aO_b}}{a}$ in both (8) and (13). It was found that any form of the cobalt oxide on the zeolite can be assumed (CoO, Co_3O_4 or Co_2O_3) with only a small effect on X or Y (~0.5% absolute). It was decided to use CoO in calculations.

All cobalt mass% values reported in the body of this report are value X. Value Y was used during experimentation to make it easier to do calculations essential for carrying out some of the experiments.

Example of a calculation

As an example, the calculation of X and Y of one of the impregnated zeolites, 4pp/co, is given.

Calculation of X

Mass of zeolite used in AA analysis = 0.0162g = M

ppm of cobalt in sample by AA analysis = 7.16 = Co_{ppm}

Volume of solution used in AA analysis = 100 cm^{-3} = V

Assuming that the form of cobalt oxide on the zeolite after being placed in the furnace is CoO:

Molar Mass of cobalt oxide = 75 $g.mol^{-1}$

Number of cobalt atoms per atom of cobalt oxide = 1 = a

Molar mass of cobalt = 59 $g.mol^{-1}$ = MM_{Co}

Thus:
$$X = \left(\frac{0.0162}{7.16 \times 100 \times 10^{-6}} - \frac{75}{1 \times 59} \right)^{-1} \times 100\%$$

$$= 4.71\%$$

Calculation of Y

For the same sample as used in the calculation of X, the species initially present on the

zeolite was found (by IR) to be $[Co_2(CO)_4(DPPE)_3]^{2+}\{[Co(CO)_4]^-\}_2$. So, $MM_{Co\text{-}P}$ will be 1767.1 $g.mol^{-1}$ and P = 4.

Thus:
$$Y = \left[\frac{0.0162}{7.16 \; x \; 100 \; x \; 10^{-6}} + \left(\frac{1767.1}{4} - \frac{75}{1} \right) \frac{1}{59} \right]^{-1} \; x \; 100\%$$

$$= 3.48\%$$

APPENDIX B

Calculations of carbon balances, conversions and selectivities

Importantly, all peaks in a spectrum which were not identified were assumed to be by-products or impurities. These peaks were assigned as alkanes for the purposes of a mass balance and the carbons in these "alkanes" were arbitrarily determined according to their position relative to the C_{10}'s and the C_{16}. For example, the peaks at times of 40.735 and 42.578 shown in **Figure C.1** were assigned as C_{15}'s for the purposes of the mass balance. Acetone was always present because of the injection procedure used for samples (see Section 2.1.1.).

The calculations were entered into a spreadsheet to simplify the calculation procedure. The spreadsheet for experiment PJV123 is shown in **Figure C.2**. The response factors of the alkanes and alkenes were all assumed to be 1 while the response factors of the undecanals and undecanols were assumed to be 0.8. These values were considered to be good approximations when compared to literature (*87*). The function of the internal standard, hexadecane, was to enable calculation of the "g/unit area", ie. the mass represented by each unit of area under any peak. The "g/unit area" value (4.35e-5) in **Figure C.2**, was obtained by dividing the mass of hexadecane added to the system (5.298g) by the area under the hexadecane peak, peak 8 in **Figure C.1** (area = 116859).

The calculation steps for the branched C_{11} alcohols follows. It should be noted that the values reported here are rounded off whereas the values used in the spreadsheet are not rounded off during calculation. The answers to calculations are reported as the values given in the spreadsheet, not as the answers strictly from the rounded-off numbers shown. It is important to note that the carbons added to the system due to addition of CO across the alkene double-bond **were not included** in the mass balance. This means that, although the alcohol and aldehyde products contained 11 carbons per molecule, the calculations were done assuming that only 10 carbons were present per molecule.

AREA%

RT	AREA	TYPE	WIDTH	AREA%
4.436	1073	PB	.046	.18532
5.492	652	BB	.049	.11261
14.360	1127	BV	.102	.19464
15.165	2010	PV	.109	.34714
15.335	1455	VP	.113	.25129
16.031	112989	PV	.177	19.49686
16.224	60562	VV	.109	10.47603
16.352	12532	VV	.084	2.16438
16.641	34331	VV	.125	5.92925
16.817	37803	VB	.105	6.52889
17.547	15581	BB	.107	2.69097
33.502	3134	PV	.075	.54127
33.775	3129	VB	.075	.54040
34.383	3679	VV	.075	.63539
34.845	6555	PB	.076	1.13210
36.936	27451	PV	.089	4.74101
37.144	3786	VV	.075	.65387
37.379	3784	VB	.072	.65353
38.077	5317	PV	.079	.91829
38.335	17207	VB	.081	2.97179
40.235	91539	PV	.124	15.80955
40.735	2279	VB	.079	.39360
42.570	11444	BB	.072	1.97647
48.025	537	BB	.068	.09274
49.534	116059	PB	.110	20.10252
52.051	2196	BV	.085	.37927

TOTAL AREA= 579011
MUL FACTOR=1.0000E+00

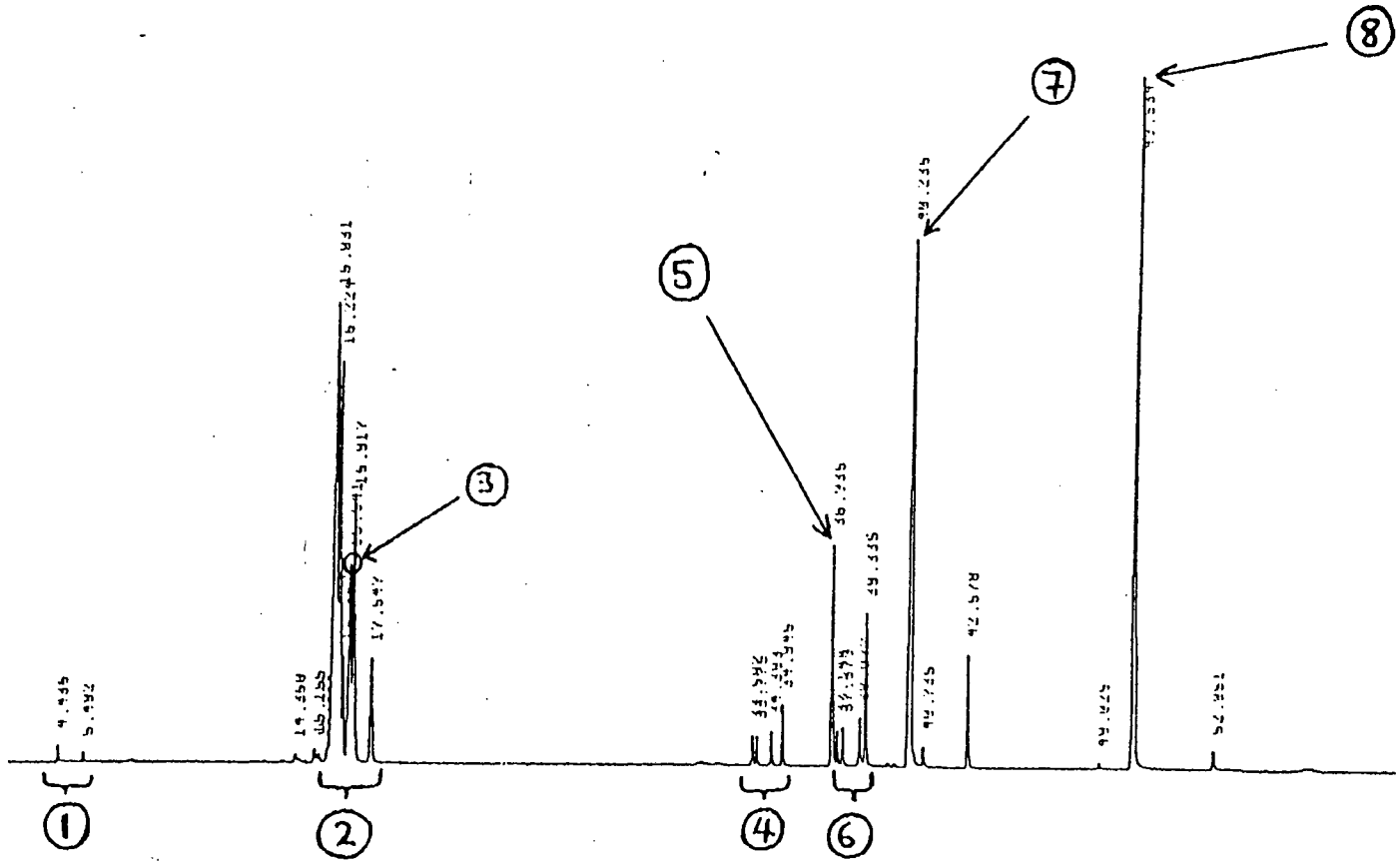

Figure C.1 : GC trace for final reaction solution of Experiment PJV123

Compound	Molar mass	Rf
Hexadecane	226	1
1-Decene	140	1
Decane	142	1
C11 alcohols	172	0.8
C11 aldehydes	170	0.8

* Mass 1-decene	20.223
Moles 1-decene	0.144
* Mass hexadecane	5.298
Moles hexadecane	0.023
* Area count of hexadecane	116859
g/unit area	4.53E-05
Total moles added	0.168
Moles C (total)	1.820
Moles C (1-decene)	1.445
* Total area count	579011

Compound	Area count	Modified area count	Mass	Moles	Moles C
Hexadecane	116859	116859	5.2980	0.0234	0.3751
1-Decene + isomers	242932	242932	11.0137	0.0787	0.7867
Decane	34331	34331	1.5565	0.0110	0.1098
Linear C11 alcohol	91539	114423.75	5.1876	0.0302	0.3018
Branched C11 alcohols	30094	37617.5	1.7055	0.0099	0.0992
Linear C11 aldehyde	27451	34313.75	1.5557	0.0092	0.0915
Branched C11 aldehydes	16497	20621.25	0.9349	0.0055	0.0550
Acetone	1725				
phosphine	0				
Other (un-ID'd)					
C10	1127	1127	0.0511	0.0004	0.0036
C11		0	0.0000	0.0000	0.0000
C12		0	0.0000	0.0000	0.0000
C13		0	0.0000	0.0000	0.0000
C14	13723	13723	0.6222	0.0031	0.0440
C15		0	0.0000	0.0000	0.0000
C16	2733	2733	0.1239	0.0005	0.0088
C17		0	0.0000	0.0000	0.0000
C18		0	0.0000	0.0000	0.0000
C19		0	0.0000	0.0000	0.0000
C20		0	0.0000	0.0000	0.0000
TOTALS	579011	618681.25	28.0490	0.1718	1.8750
	0				

Carbon balance	103.05		
Conversion of 1-decene (%)	48.28		
n/iso	2.55	% linearity	71.83
Alcohol/aldehydes	2.74	Alcohols %	73.23
		Aldehydes %	26.77
Selectivity to decane (%)	15.72		
Selectivity to alcohols (%)	57.47		
Selectivity to aldehydes (%)	21.01		
Sum of selectivities (%)	94.19		

Figure C.2 : Spreadsheet showing data used to calculate the carbon balance, conversion and selectivities obtained in Experiment PJV123

Calculations involving the branched C_{11} alcohols:

$$Area\ count = 17207 + 5317 + 3784 + 3786$$

$$= 30094$$

$$Modified\ area\ count\ (MAC) = \frac{Area\ count}{Response\ factor}$$

$$= \frac{30094}{0.8}$$

$$= 37617.5$$

$$Equivalent\ mass\ (g) = MAC\ x\ \frac{g}{Unit\ area}$$

$$= 37617.5\ x\ 4.53e{-}5$$

$$= 1.7055g$$

$$Moles = \frac{Mass}{Molar\ mass}$$

$$= \frac{1.7055}{172}$$

$$= 0.0099$$

$$Moles\ of\ carbon = Number\ of\ carbon\ atoms\ per\ molecule\ x\ Moles$$

$$= 10\ x\ 0.0099$$

$$= 0.0992$$

The carbon balance was calculated by summing the "Moles C" column and dividing it by the total moles of carbon added to the system as 1-decene and hexadecane. The calculation follows:

Total of "Moles C" column = 1.875

Total moles of carbon added = 1.820

$$\therefore \textit{ Carbon balance } = \frac{1.875}{1.820} \times 100\%$$

$$= 103.05\%$$

In the calculation of the conversion of 1-decene, it was assumed that one mole of 1-decene forms one mole of product. Thus, the moles of 1-decene converted must equal the moles of products formed which is equal to the total of the column titled "Moles" (excluding the moles of hexadecane and 1-decene). The calculation of the conversion follows.

Total of "Moles" column = 0.0697

Initial moles of 1-decene present = 0.1445

$$\therefore \textit{ Conversion } = \frac{0.0697}{0.1445} \times 100\%$$

$$= 48.28\%$$

The calculation of the selectivity to alcohols follows. This calculation holds for any product. In the body of this report, the selectivities to decane, alcohols and aldehydes are reported for the various reactions and it might have been noticed that the selectivities of the products do not always add up to 100%. In fact, the summation sometimes adds up to considerably less than 100%. Calculating the selectivities to decane, alcohols and

aldehydes using the following method will produce this result if these products only make up a small percentage of the converted 1-decene.

Total moles of 1*-decene converted* = 0.0697 (*previous calculation*)

Moles of alcohols formed = 0.0302 + 0.0099

= 0.0401

$\therefore$ *Selectivity to alcohols* = $\frac{0.0401}{0.0697}$

= 57.47%